



**HAL**  
open science

## OSSOS. XII. Variability Studies of 65 Trans-Neptunian Objects Using the Hyper Suprime-Cam

Mike Alexandersen, Susan Benecchi, Ying-Tung Chen, Marielle Eduardo, Audrey Thirouin, Megan Schwamb, Matthew Lehner, Shiang-Yu Wang, Michele Bannister, Brett Gladman, et al.

► **To cite this version:**

Mike Alexandersen, Susan Benecchi, Ying-Tung Chen, Marielle Eduardo, Audrey Thirouin, et al.. OSSOS. XII. Variability Studies of 65 Trans-Neptunian Objects Using the Hyper Suprime-Cam. The Astrophysical Journal Supplement, 2019, 244 (1), pp.19. 10.3847/1538-4365/ab2fe4 . hal-02372345

**HAL Id: hal-02372345**

**<https://hal.science/hal-02372345>**

Submitted on 17 Dec 2020

**HAL** is a multi-disciplinary open access archive for the deposit and dissemination of scientific research documents, whether they are published or not. The documents may come from teaching and research institutions in France or abroad, or from public or private research centers.

L'archive ouverte pluridisciplinaire **HAL**, est destinée au dépôt et à la diffusion de documents scientifiques de niveau recherche, publiés ou non, émanant des établissements d'enseignement et de recherche français ou étrangers, des laboratoires publics ou privés.

## OSSOS XII: Variability studies of 65 Trans-Neptunian Objects using the Hyper Suprime-Cam\*

MIKE ALEXANDERSEN,<sup>1</sup> SUSAN D. BENECCHI,<sup>2</sup> YING-TUNG CHEN,<sup>1</sup> MARIELLE R. EDUARDO,<sup>3</sup> AUDREY THIROUIN,<sup>4</sup>  
MEGAN E. SCHWAMB,<sup>5</sup> MATTHEW J. LEHNER,<sup>1,6,7</sup> SHIANG-YU WANG,<sup>1</sup> MICHELE T. BANNISTER,<sup>8</sup> BRETT J. GLADMAN,<sup>9</sup>  
STEPHEN D. J. GWYN,<sup>10</sup> JJ. KAVELAARS,<sup>10,11</sup> JEAN-MARC PETIT,<sup>12</sup> AND KATHRYN VOLK<sup>13</sup>

<sup>1</sup>*Institute of Astronomy and Astrophysics, Academia Sinica; 11F of AS/NTU Astronomy-Mathematics Building, No. 1 Roosevelt Rd., Sec. 4, Taipei 10617, Taiwan*

<sup>2</sup>*Planetary Science Institute, 1700 East Fort Lowell, Suite 106, Tucson, AZ 85719, USA*

<sup>3</sup>*Department of Physical Sciences, University of the Philippines Baguio, Gov. Pack Rd., Baguio City, Benguet, Philippines 2600*

<sup>4</sup>*Lowell Observatory, 1400 W Mars Hill Rd, Flagstaff, Arizona, 86001, USA*

<sup>5</sup>*Gemini Observatory, Northern Operations Center, 670 North A'ohoku Place, Hilo, HI 96720, USA*

<sup>6</sup>*Department of Physics and Astronomy, University of Pennsylvania, 209 S. 33rd St., Philadelphia, PA 19104, USA*

<sup>7</sup>*Harvard-Smithsonian Center for Astrophysics, 60 Garden St., Cambridge, MA 02138, USA*

<sup>8</sup>*Astrophysics Research Centre, School of Mathematics and Physics, Queen's University Belfast, Belfast BT7 1NN, United Kingdom*

<sup>9</sup>*Department of Physics and Astronomy, University of British Columbia, Vancouver, BC V6T 1Z1, Canada*

<sup>10</sup>*Herzberg Astronomy and Astrophysics Research Centre, National Research Council of Canada, 5071 West Saanich Rd, Victoria, British Columbia V9E 2E7, Canada*

<sup>11</sup>*Department of Physics and Astronomy, University of Victoria, Elliott Building, 3800 Finnerty Rd, Victoria, BC V8P 5C2, Canada*

<sup>12</sup>*Institut UTINAM UMR6213, CNRS, Univ. Bourgogne Franche-Comté, OSU Theta F25000 Besançon, France*

<sup>13</sup>*Lunar and Planetary Laboratory, University of Arizona, 1629 E University Blvd, Tucson, AZ 85721, USA*

### ABSTRACT

We present variability measurements and partial light curves of Trans-Neptunian Objects (TNOs) from a two-night pilot study using Hyper Suprime-Cam (HSC) on the Subaru Telescope (Maunakea, Hawai'i, USA). Subaru's large aperture (8-m) and HSC's large field of view (1.77 deg<sup>2</sup>) allow us to obtain measurements of multiple objects with a range of magnitudes in each telescope pointing. We observed 65 objects with  $m_r = 22.6$ – $25.5$  mag in just six pointings, allowing 20–24 visits of each pointing over the two nights. Our sample, all discovered in the recent Outer Solar System Origins Survey (OSSOS), span absolute magnitudes  $H_r = 6.2$ – $10.8$  mag and thus investigates smaller objects than previous light curve projects have typically studied. Our data supports the existence of a correlation between light curve amplitude and absolute magnitude seen in other works, but does not support a correlation between amplitude and orbital inclination. Our sample includes a number of objects from different dynamical populations within the trans-Neptunian region, but we do not find any relationship between variability and dynamical class. We were only able to estimate periods for 12 objects in the sample and found that a longer baseline of observations is required for reliable period analysis. We find that 31 objects (just under half of our sample) have variability  $\Delta_{\text{mag}}$  greater than 0.4 mag during all of the observations; in smaller 1.25 hr, 1.85 hr and 2.45 hr windows, the median  $\Delta_{\text{mag}}$  is 0.13, 0.16 and 0.19 mags, respectively. The fact that variability on this scale is common for small TNOs has important implications for discovery surveys (such as OSSOS or the Large Synoptic Survey Telescope) and color measurements.

*Keywords:* Kuiper belt: general — minor planets, asteroids: general — planets and satellites: surfaces

### 1. INTRODUCTION

Over the years, rotational light curves (the brightness variation versus time) from small bodies in our Solar System have been used to derive physical properties about the shape, surface, cohesion, internal structure, and density of objects, and to infer binarity (Sheppard et al. 2008; Thirouin et al. 2010; Benecchi & Sheppard 2013). Small light curve amplitudes can be caused by albedo variation across the surface of a spherical object, but moderate/large amplitude light curves (maximum minus minimum,

$\Delta_{\text{mag}} \geq 0.15$ - $0.2$  mag) are likely due to the shape of the object (Sheppard et al. 2008; Thirouin et al. 2010). Flat light curves can be explained by a nearly-spherical object with a homogeneous surface or an elongated object with a pole-on orientation. A flat light curve can also be due to an extremely slow rotational period undetectable during the observing window, and such a slow rotation may infer the presence of a companion (Thirouin et al. 2010; Benecchi & Sheppard 2013; Thirouin et al. 2014). Alternatively, very large amplitude light curves ( $\Delta_{\text{mag}} \geq 0.9$  mag) with a U-/V-shape at the maximum/minimum of brightness are due to close/contact binary systems (Sheppard & Jewitt 2004; Lacerda et al. 2014; Thirouin et al. 2017; Thirouin & Sheppard 2017, 2018; Ryan et al. 2017).

In the trans-Neptunian belt, four main dynamical populations - *classical*, *resonant*, *detached* and *scattering* objects - have been identified with additional sub-divisions inside some of these broad groupings. Resonant objects are trapped in mean-motion resonance with Neptune, such that the orbital period (or mean-motion) of the TNO and Neptune have a small integer ratio, which causes the TNO to experience stabilizing gravitational perturbations. Objects that are currently interacting strongly with Neptune in such a way that their orbits are unstable are called scattering (a semi-major axis change of at least 1.5 AU in 10 Myr is required for this classification in the nomenclature of Gladman et al. 2008). The detached objects are those objects with perihelia that are so distant that they are beyond significant gravitational influence from Neptune; how they got there is a subject of active research. The resonant, detached and scattering objects are all dynamically excited (“hot”) populations, with wide inclination and eccentricity distributions, thought to have been caused by significant interaction with the giant planets or other small bodies during the era of planetary migration (Kaula & Newman 1992; Malhotra 1993, 1995; Thommes et al. 2002; Kortenkamp et al. 2004; Hahn & Malhotra 2005; Murray-Clay & Chiang 2005; Tsiganis et al. 2005; Levison et al. 2008). The classical objects consists of non-resonant, non-scattering objects, primarily located at semi-major axes between 42 AU and 48 AU. The classical population has both a hot sub-population and a dynamically cold sub-population of object that have nearly circular orbits with low inclinations and eccentricities; the dynamically cold objects likely had only limited interactions with the giant planets. Due to their different formation mechanisms, it is possible that these dynamical populations have different light curve properties, just as they have different color distributions (Trujillo & Brown 2002; Peixinho et al. 2003; Fraser & Brown 2012; Sheppard 2012; Tegler et al. 2016; Pike et al. 2017).

Because light curves of TNOs have been studied by several surveys over the past decades, it is now possible to study the rotational properties of the different dynamical populations. Several studies have identified different correlations/anti-correlations between orbital and physical/rotational properties, allowing us to understand the different dynamical environments in the trans-Neptunian belt (Duffard et al. 2009; Benecchi & Sheppard 2013; Thirouin et al. 2016). However, most of the past surveys focused on bright objects, as they are the easiest ones to study with small/moderate aperture facilities. Therefore, we present a pilot study using the Subaru/HSC to study the rotational properties of the faint TNOs ( $H_r > 8.0$  mag). We aim to explore the rotational properties of TNOs in several size ranges, particularly for smaller objects around the break in each population’s size distribution (Shankman et al. 2013; Fraser et al. 2014; Alexandersen et al. 2016; Lawler et al. 2018); however, firm conclusions will require additional observations.

## 2. SAMPLE & OBSERVATIONS

Our sample consists entirely of objects discovered or detected in the Outer Solar System Origins Survey (OSSOS, Bannister et al. 2016, 2018). OSSOS was a large program on the Canada-France-Hawaii Telescope (CFHT), which ran from 2013 through 2017. OSSOS detected and tracked more than 800 trans-Neptunian objects (TNOs) with regular follow-up observations during at least two years to determine accurate orbits and secure dynamical classifications (Bannister et al. 2018). Due to the design and success of OSSOS, we have very complete information on the orbital characteristics and classification of these objects. Likewise, because these objects were discovered recently, they are still tightly clustered on the sky, having only slightly diffused apart due to Kepler shear. This allows us to observe up to 17 objects at once within the  $1.77 \text{ deg}^2$  field of view of Subaru Telescope’s Hyper Suprime-Cam (HSC, Miyazaki et al. 2018). The six fields used in this study (coordinates in Table 1) were chosen in order to maximize the number of objects within each field (see Figure 1), for a total of 63 TNOs (37 classical, 15 resonant, 5 detached, 6 scattering) and two Centaurs spanning apparent magnitudes  $m_r = 22.6$ – $25.5$  mag and absolute magnitudes  $H_r = 6.2$ – $10.8$  mag (as calculated from our light curve observations). This sample far outnumbers (by a factor of 2.5) previously reported variability studies for faint ( $H_r \geq 8$  mag) TNOs. Our sample thus much more thoroughly probes a smaller size regime than previous light curve studies have typically studied, thanks to the combined aperture size and field of view of Subaru/HSC. Information about the individual objects in our sample can be found in Table 2.

**Table 1.** Field centers used in this work. On the second night, each field lost one or two observations due to low transparency.

Field Identifier	Right Ascension (hrs)	Declination (deg)	Observations night 1 Useful/Total	Observations night 2 Useful/Total
LF07	00 <sup>h</sup> 31 <sup>m</sup> 33 <sup>s</sup>	+04°54′54″	12/12	10/12
LF08	00 <sup>h</sup> 41 <sup>m</sup> 41 <sup>s</sup>	+05°17′52″	12/12	10/12
LF09	00 <sup>h</sup> 42 <sup>m</sup> 34 <sup>s</sup>	+06°37′44″	12/12	10/12
LF10	00 <sup>h</sup> 45 <sup>m</sup> 37 <sup>s</sup>	+07°59′02″	12/12	10/12
LF11	01 <sup>h</sup> 10 <sup>m</sup> 00 <sup>s</sup>	+05°43′25″	10/10	9/10
LF12	01 <sup>h</sup> 21 <sup>m</sup> 51 <sup>s</sup>	+06°34′20″	10/10	9/10

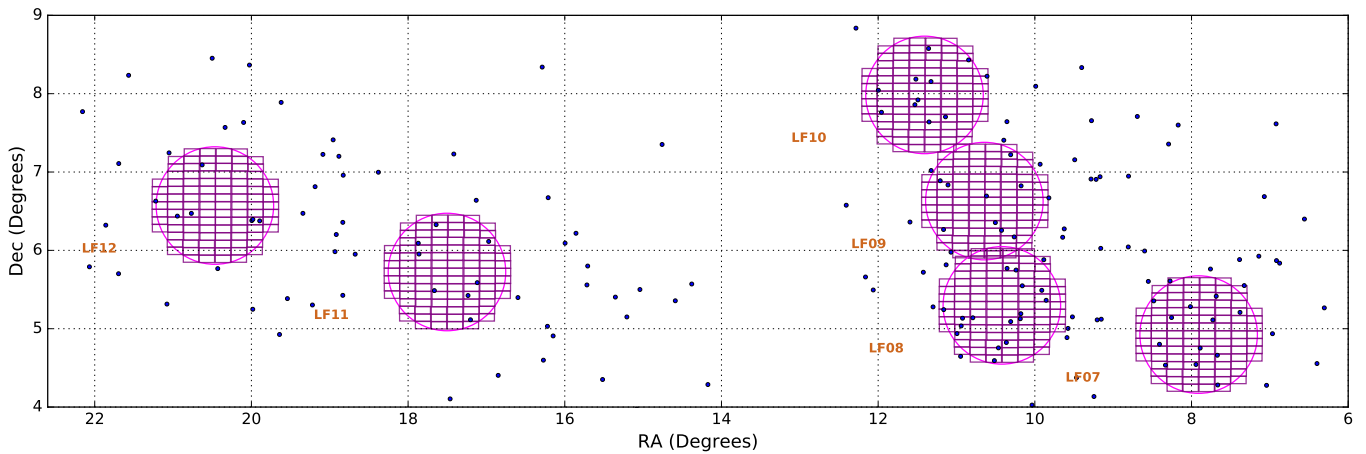


**Figure 1.** The location of our 2016 fields relative to TNOs discovered in the OSSOS L and S blocks (left and right, respectively). The large field of view of HSC (magenta) allowed us to observe many objects at once. The field centers used are listed in Table 1.

**Table 2.** Summary of information about the objects in our sample. *ID* refers to the internal OSSOS designation (as used in (Bannister et al. 2018)). *Field* is the field in which the target was observed (Table 1). *a*, *e* and *i* are the barycentric orbital parameters semi-major axis, eccentricity and inclination (uncertainties on eccentricity and inclination are always 0.001 or smaller and are therefore not listed here). *Class* is the dynamical classification of the object. *MPC* is the Minor Planet Center<sup>2</sup> designation (Note: all objects will have MPC designations before final publication.). *m<sub>r</sub>* and *H<sub>r</sub>* are the mean apparent and absolute magnitudes of the objects, as measured in this work (these are the magnitudes used everywhere in this paper, as they are more accurate than the discovery magnitudes from OSSOS); due to the quality of the OSSOS orbits, the uncertainty on *H<sub>r</sub>* is identical to that of *m<sub>r</sub>* to the given precision.  $\Delta_{\text{mag}}$  is the maximum magnitude variation measured for the object within this work.  $\sigma_{\text{mag}}$  is the standard deviation of the magnitudes measured in this work. This table is ordered in the same order as Figures 3 to 6: brightest object at the top to faintest object at the bottom.

ID	Field	<i>a</i> (au)	<i>e</i>	<i>i</i> (deg)	Class	MPC	<i>m<sub>r</sub></i> (mag)	<i>H<sub>r</sub></i> (mag)	$\Delta_{\text{mag}}$	$\sigma_{\text{mag}}$
o5t09PD	LF09	67.760 ± 0.009	0.459	3.575	det	2014 UA <sub>225</sub>	22.627 ± 0.002	7.033	0.110 <sup>+0.012</sup> <sub>-0.012</sub>	0.027 <sup>+0.002</sup> <sub>-0.002</sub>
o3l43	LF11	45.785 ± 0.004	0.097	2.025	cla	2013 UL <sub>15</sub>	22.989 ± 0.002	6.702	0.363 <sup>+0.012</sup> <sub>-0.011</sub>	0.109 <sup>+0.002</sup> <sub>-0.002</sub>
o5s21	LF10	43.851 ± 0.007	0.170	2.373	cla		23.225 ± 0.003	7.564	0.36 <sup>+0.02</sup> <sub>-0.02</sub>	0.106 <sup>+0.003</sup> <sub>-0.003</sub>
o3l57	LF12	45.044 ± 0.004	0.075	1.841	res 11:6	2013 UM <sub>15</sub>	23.297 ± 0.003	6.872	0.127 <sup>+0.015</sup> <sub>-0.014</sub>	0.034 <sup>+0.003</sup> <sub>-0.003</sub>
o5t03	LF09	25.967 ± 0.0014	0.288	18.849	cen		23.380 ± 0.003	10.825	0.15 <sup>+0.03</sup> <sub>-0.02</sub>	0.041 <sup>+0.004</sup> <sub>-0.004</sub>

Table 2 continued on next page

Table 2 (continued)

ID	Field	$a$ (au)	$e$	$i$ (deg)	Class	MPC	$m_r$ (mag)	$H_r$ (mag)	$\Delta_{\text{mag}}$	$\sigma_{\text{mag}}$
o5t34PD	LF07	45.959 ± 0.003	0.170	5.081	res 17:9	2003 SP <sub>317</sub>	23.511 ± 0.006	7.226	0.56 <sup>+0.05</sup> <sub>-0.04</sub>	0.177 <sup>+0.007</sup> <sub>-0.006</sub>
o5s07	LF08	39.332 ± 0.004	0.249	16.270	res 3:2		23.615 ± 0.004	8.957	0.22 <sup>+0.02</sup> <sub>-0.02</sub>	0.048 <sup>+0.004</sup> <sub>-0.003</sub>
o5s52	LF10	50.85 ± 0.03	0.247	27.196	res 11:5		23.616 ± 0.003	7.054	0.314 <sup>+0.014</sup> <sub>-0.014</sub>	0.094 <sup>+0.003</sup> <sub>-0.003</sub>
o5s36	LF09	43.258 ± 0.003	0.053	2.206	cla		23.638 ± 0.003	7.569	0.43 <sup>+0.02</sup> <sub>-0.02</sub>	0.128 <sup>+0.004</sup> <sub>-0.004</sub>
o5s05	LF10	21.981 ± 0.010	0.479	15.389	cen	2015 RV <sub>245</sub>	23.640 ± 0.004	10.767	0.10 <sup>+0.02</sup> <sub>-0.02</sub>	0.025 <sup>+0.004</sup> <sub>-0.004</sub>
o3l64	LF11	44.355 ± 0.003	0.073	1.972	cla	2013 UW <sub>16</sub>	23.729 ± 0.004	7.233	0.13 <sup>+0.02</sup> <sub>-0.02</sub>	0.038 <sup>+0.004</sup> <sub>-0.004</sub>
o3l46	LF12	46.612 ± 0.004	0.079	2.471	cla	2013 UP <sub>15</sub>	23.730 ± 0.004	7.404	0.29 <sup>+0.02</sup> <sub>-0.02</sub>	0.089 <sup>+0.004</sup> <sub>-0.004</sub>
o5t08	LF08	38.848 ± 0.003	0.057	1.097	cla		23.751 ± 0.004	8.164	0.21 <sup>+0.02</sup> <sub>-0.02</sub>	0.057 <sup>+0.004</sup> <sub>-0.004</sub>
o5t30	LF08	43.791 ± 0.008	0.073	2.170	cla		23.811 ± 0.004	7.648	0.55 <sup>+0.02</sup> <sub>-0.02</sub>	0.159 <sup>+0.005</sup> <sub>-0.005</sub>
o5t42	LF07	39.451 ± 0.011	0.204	1.587	res 3:2		23.833 ± 0.004	7.254	0.16 <sup>+0.02</sup> <sub>-0.02</sub>	0.045 <sup>+0.004</sup> <sub>-0.004</sub>
o5s14	LF07	34.841 ± 0.002	0.047	7.122	res 5:4		23.911 ± 0.004	8.488	0.22 <sup>+0.02</sup> <sub>-0.02</sub>	0.054 <sup>+0.004</sup> <sub>-0.004</sub>
o5t51	LF08	59.83 ± 0.10	0.425	13.851	res 14:5		23.936 ± 0.004	6.833	0.24 <sup>+0.03</sup> <sub>-0.02</sub>	0.057 <sup>+0.004</sup> <sub>-0.004</sub>
o3l82	LF11	43.657 ± 0.005	0.286	24.987	res 7:4	2013 UK <sub>17</sub>	23.936 ± 0.005	6.621	0.15 <sup>+0.02</sup> <sub>-0.02</sub>	0.044 <sup>+0.006</sup> <sub>-0.005</sub>
o3l63	LF12	45.132 ± 0.004	0.054	3.363	cla	2013 UN <sub>15</sub>	23.986 ± 0.005	7.493	0.56 <sup>+0.03</sup> <sub>-0.03</sub>	0.161 <sup>+0.005</sup> <sub>-0.004</sub>
o3l83	LF11	200.2 ± 0.5	0.781	10.652	det	2013 UT <sub>15</sub>	24.001 ± 0.005	6.168	0.33 <sup>+0.02</sup> <sub>-0.02</sub>	0.098 <sup>+0.005</sup> <sub>-0.005</sub>
o5s35	LF09	46.40 ± 0.02	0.161	24.307	cla		24.065 ± 0.005	8.023	0.37 <sup>+0.03</sup> <sub>-0.03</sub>	0.106 <sup>+0.005</sup> <sub>-0.005</sub>
o3l55	LF11	44.004 ± 0.004	0.096	2.358	cla	2013 UY <sub>16</sub>	24.086 ± 0.005	7.667	0.37 <sup>+0.02</sup> <sub>-0.02</sub>	0.121 <sup>+0.005</sup> <sub>-0.005</sub>
o5t16	LF08	44.79 ± 0.02	0.176	17.756	cla		24.158 ± 0.005	8.358	0.36 <sup>+0.04</sup> <sub>-0.03</sub>	0.093 <sup>+0.006</sup> <sub>-0.006</sub>
o5s30	LF07	41.477 ± 0.005	0.073	33.327	cla		24.164 ± 0.007	8.247	0.27 <sup>+0.03</sup> <sub>-0.03</sub>	0.063 <sup>+0.006</sup> <sub>-0.006</sub>
o3l71	LF12	45.319 ± 0.003	0.014	1.927	cla	2013 UW <sub>17</sub>	24.178 ± 0.006	7.612	0.42 <sup>+0.03</sup> <sub>-0.03</sub>	0.125 <sup>+0.006</sup> <sub>-0.005</sub>
o5t06	LF08	72.06 ± 0.03	0.535	12.327	sca		24.183 ± 0.006	8.941	0.25 <sup>+0.03</sup> <sub>-0.03</sub>	0.069 <sup>+0.006</sup> <sub>-0.006</sub>
o5s22	LF10	46.162 ± 0.010	0.222	8.482	res 19:10		24.207 ± 0.005	8.538	0.21 <sup>+0.02</sup> <sub>-0.02</sub>	0.059 <sup>+0.005</sup> <sub>-0.005</sub>
o5s15	LF07	45.439 ± 0.009	0.238	25.362	res 13:7		24.246 ± 0.006	8.809	0.31 <sup>+0.03</sup> <sub>-0.03</sub>	0.084 <sup>+0.006</sup> <sub>-0.006</sub>
o3l65	LF11	44.609 ± 0.007	0.278	11.207	sca	2013 UZ <sub>16</sub>	24.272 ± 0.006	7.775	0.36 <sup>+0.03</sup> <sub>-0.03</sub>	0.095 <sup>+0.007</sup> <sub>-0.007</sub>
o3l20	LF12	39.425 ± 0.010	0.181	2.085	res 3:2	2013 UV <sub>17</sub>	24.335 ± 0.008	8.354	0.69 <sup>+0.04</sup> <sub>-0.04</sub>	0.185 <sup>+0.008</sup> <sub>-0.008</sub>
o5s19	LF10	45.054 ± 0.006	0.194	17.960	res 11:6		24.357 ± 0.006	8.758	0.38 <sup>+0.03</sup> <sub>-0.03</sub>	0.105 <sup>+0.006</sup> <sub>-0.006</sub>
o5t10	LF07	37.844 ± 0.006	0.051	1.540	cla		24.375 ± 0.007	8.768	0.31 <sup>+0.05</sup> <sub>-0.04</sub>	0.081 <sup>+0.008</sup> <sub>-0.008</sub>
o5t44	LF08	43.560 ± 0.004	0.071	3.566	cla		24.383 ± 0.007	7.768	0.28 <sup>+0.03</sup> <sub>-0.03</sub>	0.085 <sup>+0.005</sup> <sub>-0.006</sub>
o3l62	LF11	39.230 ± 0.004	0.238	4.416	res 3:2	2013 UX <sub>16</sub>	24.415 ± 0.008	7.950	0.27 <sup>+0.05</sup> <sub>-0.04</sub>	0.076 <sup>+0.010</sup> <sub>-0.010</sub>
o5s24	LF10	50.376 ± 0.018	0.278	9.376	res 13:6		24.435 ± 0.007	8.657	0.58 <sup>+0.04</sup> <sub>-0.04</sub>	0.153 <sup>+0.007</sup> <sub>-0.007</sub>
o3l19	LF11	45.334 ± 0.003	0.126	1.480	cla	2013 SM <sub>100</sub>	24.447 ± 0.007	8.507	0.68 <sup>+0.04</sup> <sub>-0.04</sub>	0.174 <sup>+0.007</sup> <sub>-0.007</sub>
o5s42	LF10	39.323 ± 0.011	0.165	5.772	res 3:2		24.482 ± 0.007	8.284	0.38 <sup>+0.05</sup> <sub>-0.04</sub>	0.102 <sup>+0.009</sup> <sub>-0.010</sub>
o5t27	LF08	43.907 ± 0.011	0.079	1.498	cla		24.490 ± 0.007	8.348	0.42 <sup>+0.04</sup> <sub>-0.04</sub>	0.101 <sup>+0.006</sup> <sub>-0.006</sub>
o5t48	LF07	42.183 ± 0.003	0.156	5.209	res 5:3		24.526 ± 0.011	7.693	0.41 <sup>+0.04</sup> <sub>-0.04</sub>	0.107 <sup>+0.009</sup> <sub>-0.009</sub>
o5t13	LF08	79.06 ± 0.03	0.535	17.629	res 17:4		24.531 ± 0.007	8.849	0.41 <sup>+0.05</sup> <sub>-0.05</sub>	0.100 <sup>+0.008</sup> <sub>-0.008</sub>
o5t32	LF08	43.791 ± 0.005	0.035	2.209	cla		24.537 ± 0.008	8.292	0.48 <sup>+0.05</sup> <sub>-0.05</sub>	0.117 <sup>+0.010</sup> <sub>-0.010</sub>
uo3l84	LF11	44.012 ± 0.003	0.082	1.435	cla		24.547 ± 0.009	7.858	0.44 <sup>+0.06</sup> <sub>-0.06</sub>	0.117 <sup>+0.011</sup> <sub>-0.010</sub>
o3l44	LF12	42.793 ± 0.005	0.042	2.940	cla	2013 UC <sub>18</sub>	24.557 ± 0.008	8.261	0.47 <sup>+0.04</sup> <sub>-0.04</sub>	0.141 <sup>+0.010</sup> <sub>-0.009</sub>
uo3l88	LF11	43.935 ± 0.004	0.081	2.479	cla		24.558 ± 0.007	8.275	0.53 <sup>+0.04</sup> <sub>-0.05</sub>	0.169 <sup>+0.009</sup> <sub>-0.008</sub>
o5t07	LF07	39.513 ± 0.009	0.192	2.802	res 3:2		24.611 ± 0.014	9.159	0.48 <sup>+0.06</sup> <sub>-0.06</sub>	0.143 <sup>+0.015</sup> <sub>-0.014</sub>
o5t41	LF08	44.310 ± 0.004	0.043	0.997	cla		24.659 ± 0.011	8.085	0.23 <sup>+0.05</sup> <sub>-0.04</sub>	0.068 <sup>+0.012</sup> <sub>-0.009</sub>
o5t22	LF08	39.58 ± 0.02	0.176	5.457	res 3:2		24.664 ± 0.009	8.612	0.28 <sup>+0.05</sup> <sub>-0.03</sub>	0.076 <sup>+0.009</sup> <sub>-0.008</sub>
o5t49	LF08	44.851 ± 0.004	0.096	1.968	cla		24.672 ± 0.008	7.807	0.64 <sup>+0.04</sup> <sub>-0.04</sub>	0.204 <sup>+0.008</sup> <sub>-0.008</sub>
o5s61	LF10	44.942 ± 0.012	0.117	3.023	cla		24.696 ± 0.009	7.879	0.65 <sup>+0.05</sup> <sub>-0.04</sub>	0.177 <sup>+0.009</sup> <sub>-0.009</sub>
o5t23	LF08	46.215 ± 0.007	0.132	5.089	cla		24.813 ± 0.009	8.760	0.66 <sup>+0.08</sup> <sub>-0.06</sub>	0.174 <sup>+0.012</sup> <sub>-0.012</sub>
o5s40	LF09	44.310 ± 0.007	0.075	2.276	cla		24.965 ± 0.010	8.702	0.41 <sup>+0.05</sup> <sub>-0.04</sub>	0.117 <sup>+0.009</sup> <sub>-0.009</sub>
o5t26	LF09	43.173 ± 0.004	0.043	16.024	cla		24.973 ± 0.013	8.855	0.41 <sup>+0.07</sup> <sub>-0.05</sub>	0.115 <sup>+0.014</sup> <sub>-0.014</sub>

Table 2 continued on next page

Table 2 (continued)

ID	Field	$a$ (au)	$e$	$i$ (deg)	Class	MPC	$m_r$ (mag)	$H_r$ (mag)	$\Delta_{\text{mag}}$	$\sigma_{\text{mag}}$
uo5t55	LF08	44.25 ± 0.02	0.073	1.544	cla		25.015 ± 0.011	8.702	0.54 <sup>+0.08</sup> <sub>-0.07</sub>	0.129 <sup>+0.013</sup> <sub>-0.013</sub>
o5s29	LF07	41.396 ± 0.003	0.045	34.929	cla		25.023 ± 0.012	9.111	0.33 <sup>+0.05</sup> <sub>-0.04</sub>	0.097 <sup>+0.011</sup> <sub>-0.011</sub>
o5s43	LF07	70.84 ± 0.07	0.465	10.192	det		25.044 ± 0.011	8.837	0.49 <sup>+0.07</sup> <sub>-0.08</sub>	0.120 <sup>+0.014</sup> <sub>-0.015</sub>
o5t25	LF08	43.288 ± 0.006	0.047	0.461	cla		25.084 ± 0.012	8.971	0.40 <sup>+0.06</sup> <sub>-0.06</sub>	0.099 <sup>+0.011</sup> <sub>-0.011</sub>
o5t21	LF08	43.633 ± 0.003	0.074	6.872	res 7:4		25.104 ± 0.014	9.082	0.59 <sup>+0.07</sup> <sub>-0.06</sub>	0.165 <sup>+0.013</sup> <sub>-0.013</sub>
o5s55	LF09	46.93 ± 0.02	0.173	4.812	cla		25.107 ± 0.010	8.528	0.59 <sup>+0.07</sup> <sub>-0.06</sub>	0.148 <sup>+0.011</sup> <sub>-0.010</sub>
o5s26	LF09	41.344 ± 0.007	0.112	17.483	cla		25.111 ± 0.014	9.299	0.54 <sup>+0.05</sup> <sub>-0.05</sub>	0.152 <sup>+0.012</sup> <sub>-0.012</sub>
o5s12	LF10	34.791 ± 0.005	0.100	2.668	res 5:4		25.118 ± 0.015	9.798	0.40 <sup>+0.08</sup> <sub>-0.06</sub>	0.13 <sup>+0.02</sup> <sub>-0.02</sub>
o5s49	LF07	44.017 ± 0.007	0.044	2.088	cla		25.178 ± 0.012	8.889	1.01 <sup>+0.10</sup> <sub>-0.09</sub>	0.22 <sup>+0.02</sup> <sub>-0.02</sub>
o5s60	LF10	42.530 ± 0.007	0.128	40.362	cla		25.180 ± 0.012	8.510	0.51 <sup>+0.07</sup> <sub>-0.06</sub>	0.127 <sup>+0.012</sup> <sub>-0.012</sub>
o5t24	LF09	44.953 ± 0.006	0.107	2.398	cla		25.257 ± 0.014	9.199	0.80 <sup>+0.08</sup> <sub>-0.08</sub>	0.20 <sup>+0.02</sup> <sub>-0.02</sub>
o5s57	LF07	41.356 ± 0.011	0.140	32.358	cla		25.276 ± 0.016	8.649	0.84 <sup>+0.10</sup> <sub>-0.09</sub>	0.227 <sup>+0.016</sup> <sub>-0.015</sub>
uo5s77	LF09	65.95 ± 0.11	0.413	38.607	res 13:4		25.604 ± 0.018	9.477	0.98 <sup>+0.09</sup> <sub>-0.09</sub>	0.295 <sup>+0.02</sup> <sub>-0.02</sub>

Data were collected by M. Alexandersen and S.-Y. Wang on the nights of 2016 August 25 and 26, using HSC on Subaru Telescope, located on Maunakea, Hawai'i, USA<sup>3</sup>. Figure 1 shows our field locations in relation to the swarm of OSSOS TNOs. As TNOs are typically brightest in r-band, this filter was used. The six fields were observed in a repeated sequence with one 300 second exposure of each field, resulting in about 36 minutes between repeat observations of the same field. Because the observing nights were approximately 1.5 months from opposition, we were unable to observe our fields for the entire night; the four fields closer to opposition thus were observed 12 times each night, while two other fields were observed 10 times each night. Observations were taken at airmasses ranging from 1.02 to 2.04. The conditions were generally good (transparency near 1.0, seeing mostly between 0.65'' and 1.0''), apart from about one hour of clouds and very low transparency on the second night. One or two observations of each field were therefore unusable for this project.

### 3. PHOTOMETRY & CALIBRATION

Images were processed using `hscPipe`<sup>4</sup>, the official HSC data reduction software package, which includes calibration of astrometry/photometry and basic image processing (bias, darks, and flats) (Bosch et al. 2018). `hscPipe` was developed as a prototype pipeline for the Large Synoptic Survey Telescope (LSST) project (Ivezic et al. 2008). The algorithms and conceptions of `hscPipe` were inherited from the Sloan Digital Sky Survey (SDSS) Photo Pipeline (Lupton et al. 2001). The standard outputs of the `hscPipe` process include detection catalogs and calibrated images. We used the Pan-STARRS1 PV2 catalog (PS1, Tonry et al. 2012; Schlafly et al. 2012; Magnier et al. 2013) as the reference catalog for photometry and astrometry.

Photometry of bright point sources revealed systematic variability (of order 0.01 magnitudes), caused by the fact that `hscPipe` calibrates images individually; images of the same field can thus have slight discrepancies relative to each other due to uncertainties in the zero-point determinations. To mitigate for this effect, background stars were inspected to find a set of 10-15 non-variable stars, defined as those that exhibit similar systematic variability, to reveal the systematic variability of the zero-point error. A secondary correction was then applied to the zero points, such that the average magnitude of the non-variable stars is constant across the set of images. This adjustment was typically smaller than 0.02 magnitudes, but is important for obtaining the most accurate TNO photometry possible.

In order to get the best possible photometric measurements of our TNOs, we used the Python package `TRIPPY` (Fraser et al. 2016). TNOs move at typical rates of 3–6''/hr at opposition, thus moving up to 0.5'' during our 300-second exposures, causing slight trailing. `TRIPPY` uses knowledge of the rate and angle of motion to accurately measure photometry for moving objects using an elongated aperture and appropriate aperture correction.

We obtained 9–23 useful measurements for each object over two nights; the median number of measurements per object is 19. One or two images per field were discarded due to low transparency during one hour on the second night; while some reduced transparency can be corrected for in calibration, we found that images with transparency < 50% consistently produced anomalous results, so we chose to exclude those images. Many objects lost one or more measurement due to being too close to a background source for reliable photometry. Three objects (o5t41, o5t07 and o5s12) only have data on one night because they fell into chip

<sup>3</sup> All data obtained as part of this project can be downloaded from <https://smoka.nao.ac.jp/fssearch> or <http://www.cadc-ccda.hia-ihp.nrc-cnrc.gc.ca/en/search/>

<sup>4</sup> [https://hscdata.mtk.nao.ac.jp:4443/hsc\\_bin\\_dist/index.html](https://hscdata.mtk.nao.ac.jp:4443/hsc_bin_dist/index.html)

gaps on one of the two nights; this was difficult to avoid when optimizing field location for up to 17 objects moving at different rates. One object (o5t44) was on a different chip on the two nights; however, we are confident that our zero point calibration is accurate such that there is not an offset between the two nights. The final calibrated photometric measurements as well as the calibrated zero points can be found in [Table 3](#).

[tbp]

**Table 3.** Photometric measurements from this HSC data set.  $\sigma_{\text{Rand}}$  is the random uncertainty of the  $m_r$  magnitude measurement.  $Zp$  is the zero-point used.  $\sigma_{\text{Sys}}$  is the systematic uncertainty on the zero-point (and thus also on the measurement). This is an example for a single object; all measurements from all 65 objects are available in machine readable format in the on-line supplements.

MJD-57620	$m_r \pm \sigma_{\text{Rand}}$	$Zp \pm \sigma_{\text{Sys}}$
o3119		
6.3913125	$24.09 \pm 0.03$	$26.995 \pm 0.005$
6.4154337	$24.21 \pm 0.02$	$27.012 \pm 0.005$
6.4393438	$24.45 \pm 0.02$	$27.022 \pm 0.005$
6.4634385	$24.69 \pm 0.04$	$27.058 \pm 0.005$
6.4876346	$24.78 \pm 0.03$	$27.047 \pm 0.005$
6.5123402	$24.56 \pm 0.03$	$27.039 \pm 0.005$
6.5375195	$24.41 \pm 0.03$	$27.043 \pm 0.005$
6.5628085	$24.29 \pm 0.03$	$27.045 \pm 0.005$
6.5875091	$24.28 \pm 0.02$	$27.038 \pm 0.005$
7.3876072	$24.55 \pm 0.03$	$26.978 \pm 0.005$
7.4114040	$24.67 \pm 0.03$	$27.002 \pm 0.005$
7.4353624	$24.45 \pm 0.02$	$26.885 \pm 0.005$
7.4595078	$24.47 \pm 0.02$	$26.869 \pm 0.005$
7.5081300	$24.36 \pm 0.03$	$26.497 \pm 0.005$
7.5584662	$24.35 \pm 0.02$	$27.019 \pm 0.005$
7.5830743	$24.42 \pm 0.02$	$27.004 \pm 0.005$
7.6079518	$24.58 \pm 0.02$	$26.994 \pm 0.005$

#### 4. RESULTS

We have measured partial light curves for 63 TNOs and two Centaurs. The measurements can be found in graphical form in [Figures 2 to 6](#); the photometric data can be found in [Table 3](#). Several objects (such as 2013 UL<sub>15</sub>, o5s21, 2003 SP<sub>317</sub>, o5t30 and 2013 UN<sub>15</sub>) feature clear, high-amplitude variability. We have investigated the relationships between our measured light curve variability and other properties such as absolute magnitude, dynamical class, and other orbital parameters ([Section 4.1](#)). For the best quality light curves, estimates of the rotation periods were also made ([Section 4.2](#)).

In order to estimate the uncertainty on parameters such as the magnitude variation, period, correlation coefficient and so on, a resampling method was used. One thousand resampled datasets were generated by resampling each magnitude measurement of each object. This resampling was drawn from a normal distribution centered on the measured value with a width equal to the measurement uncertainty. The analysis was then performed on each resampled dataset independently to find the distribution of

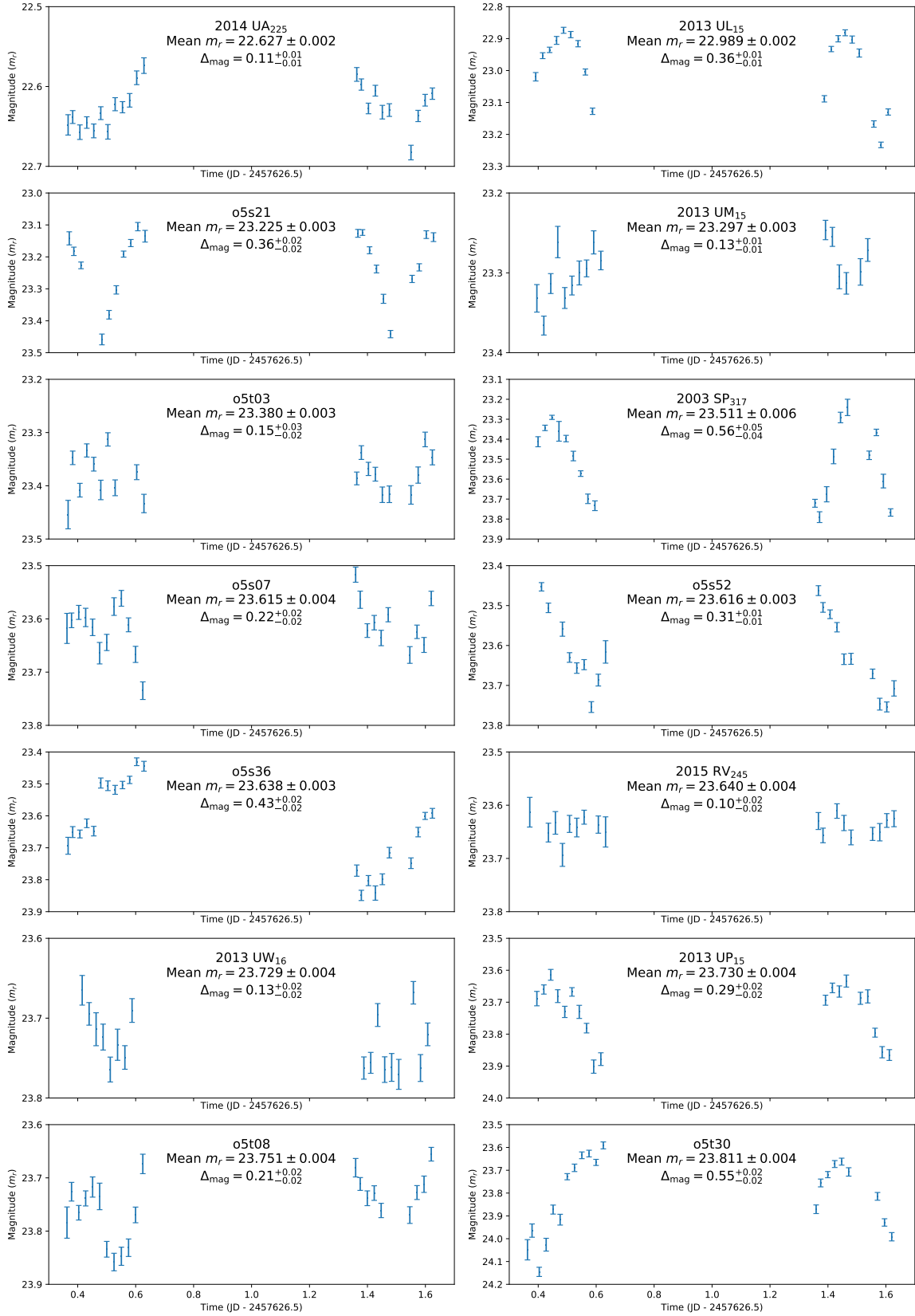
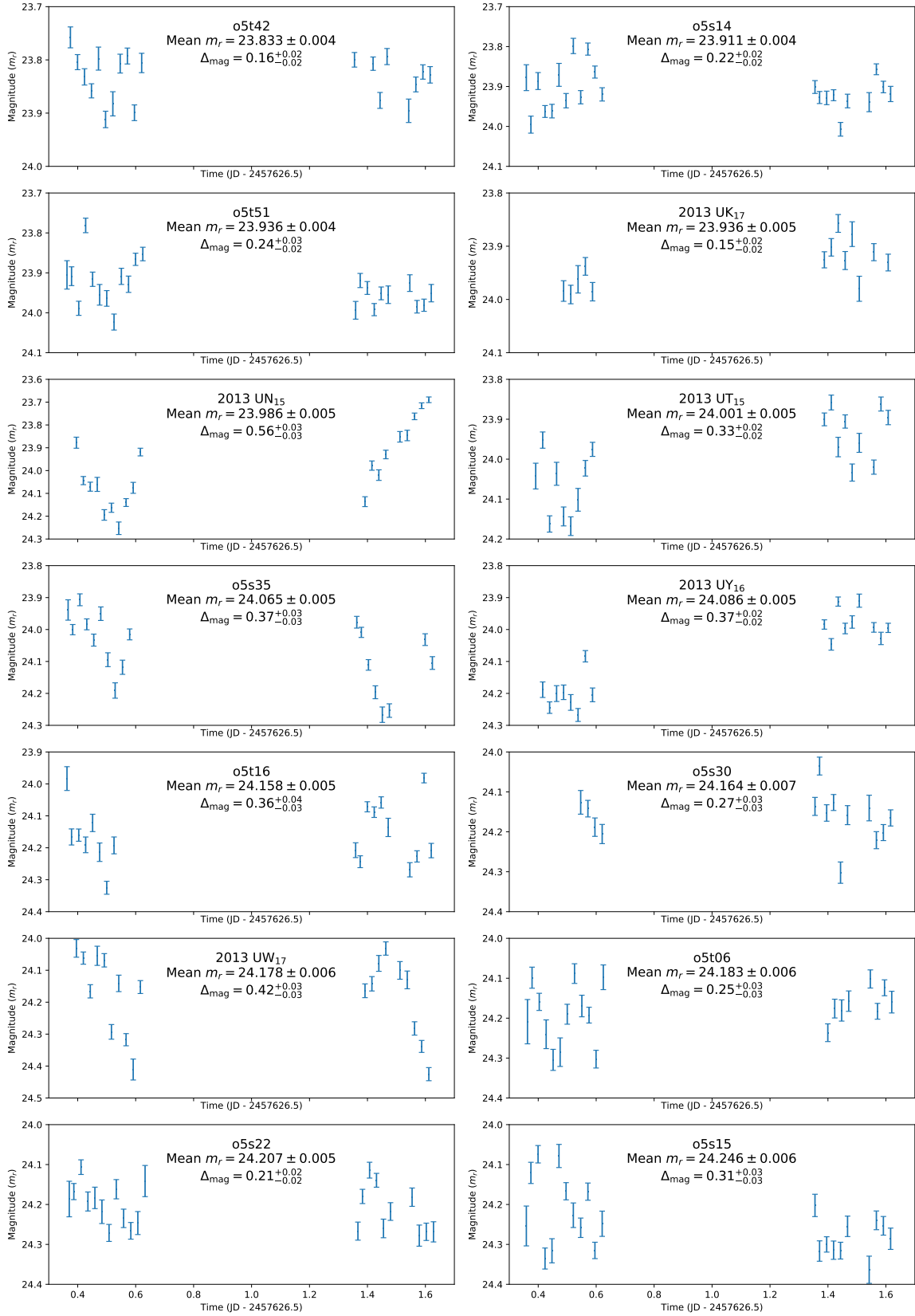


Figure 2. Absolutely calibrated photometry of our TNO sample. Objects 0–13, ordered by average magnitude.



**Figure 3.** Absolutely calibrated photometry of our TNO sample. Objects 14–27, ordered by average magnitude.

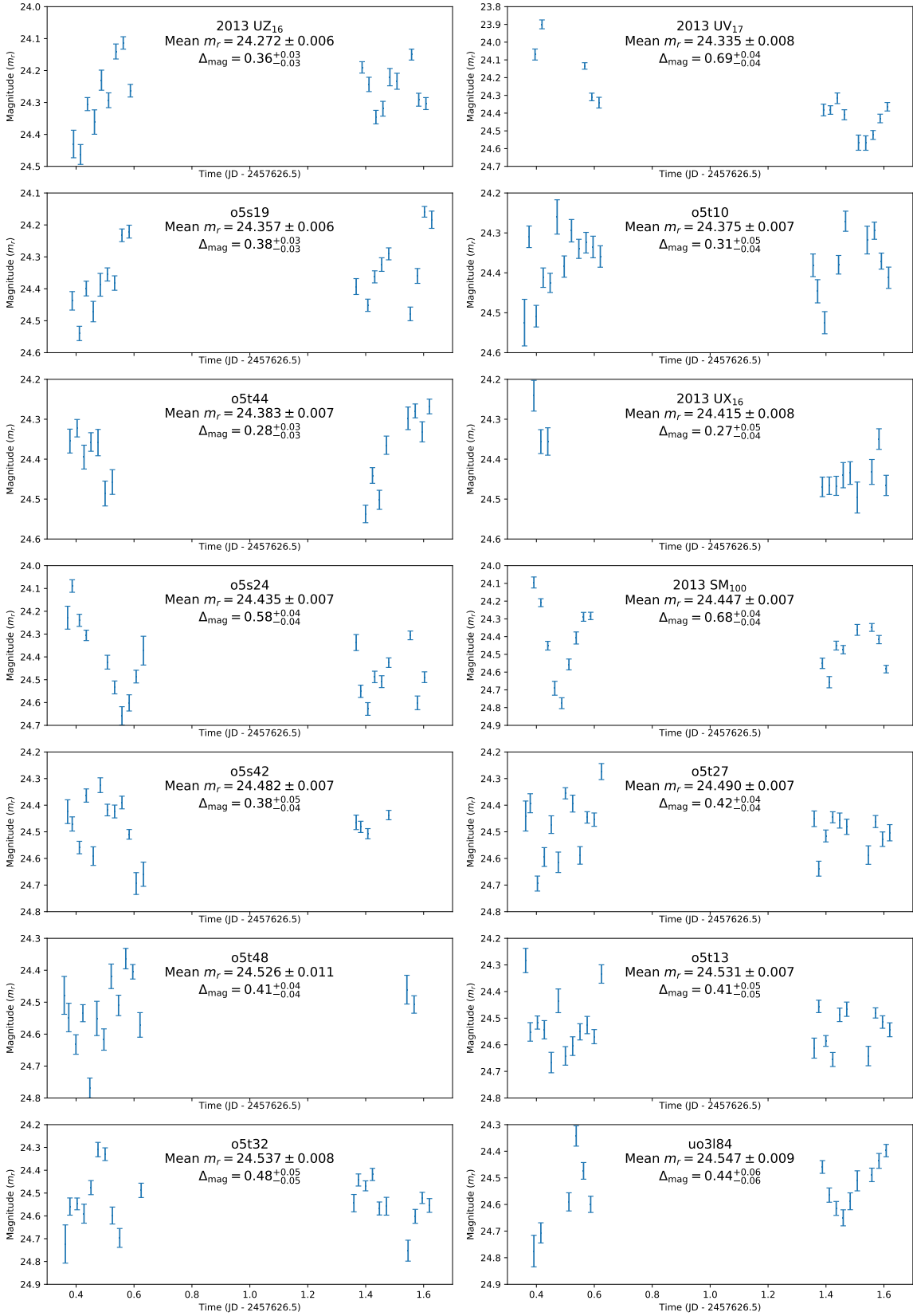
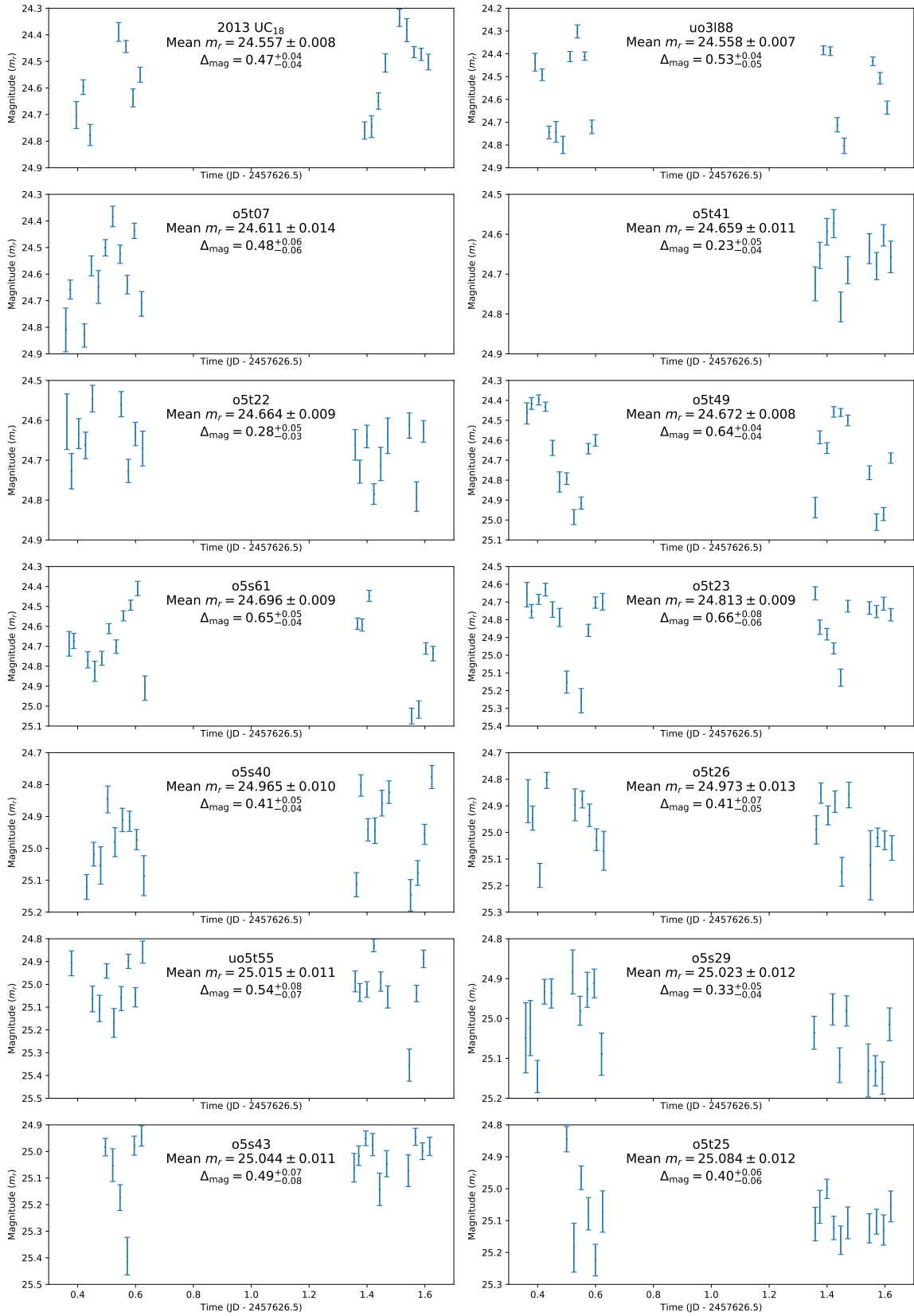
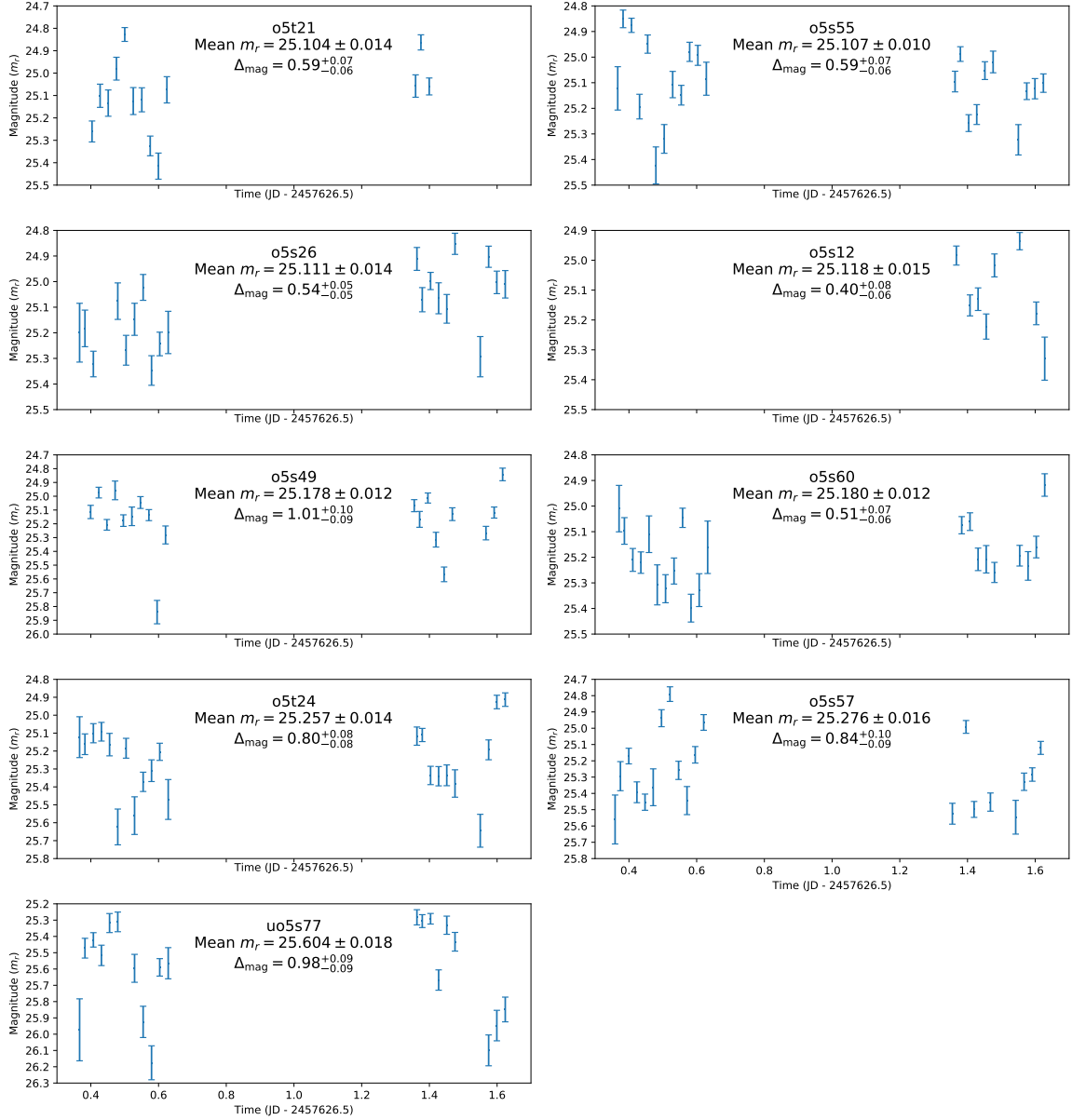


Figure 4. Absolutely calibrated photometry of our TNO sample. Objects 28–41, ordered by average magnitude.



**Figure 5.** Absolutely calibrated photometry of our TNO sample. Objects 42–55, ordered by average magnitude.



**Figure 6.** Absolutely calibrated photometry of our TNO sample. Objects 56–64, ordered by average magnitude.

resultant values. The  $2\sigma$  uncertainty on a value is then taken to be the range that spans the central 95% of values (ie. 2.5% in each tail).

#### 4.1. Amplitude analysis

The mean rotational period of TNOs has been found to be 7–9 hours (Duffard et al. 2009; Benecchi & Sheppard 2013; Thirouin et al. 2016), although periods range from 3.9 hours (Haumea) to 154 hours (Pluto). While we don’t have full light curves for all of our target objects, the mean period of 7–9 hours means that we likely observed a near-maximum and near-minimum of most of our target objects. Simple simulations of our observations confirm that for objects of a given period between 3 and 40 hours, we observe more than 80% of the variability on average (averaged over random starting phase); for periods between 3 and 22 hours, we observe more than 88% of the variability on average. It is thus reasonable to assume that our measurements of  $\Delta_{\text{mag}}$  (maximum minus minimum magnitude) are close to the full light curve amplitudes and that the slight underestimation will not affect our results (such as whether or not correlations exist). In this subsection, we have removed the two Centaurs (2015 RV<sub>245</sub> and o5t03) from the sample, because the surface and rotation of these objects might have been altered by close approaches to the

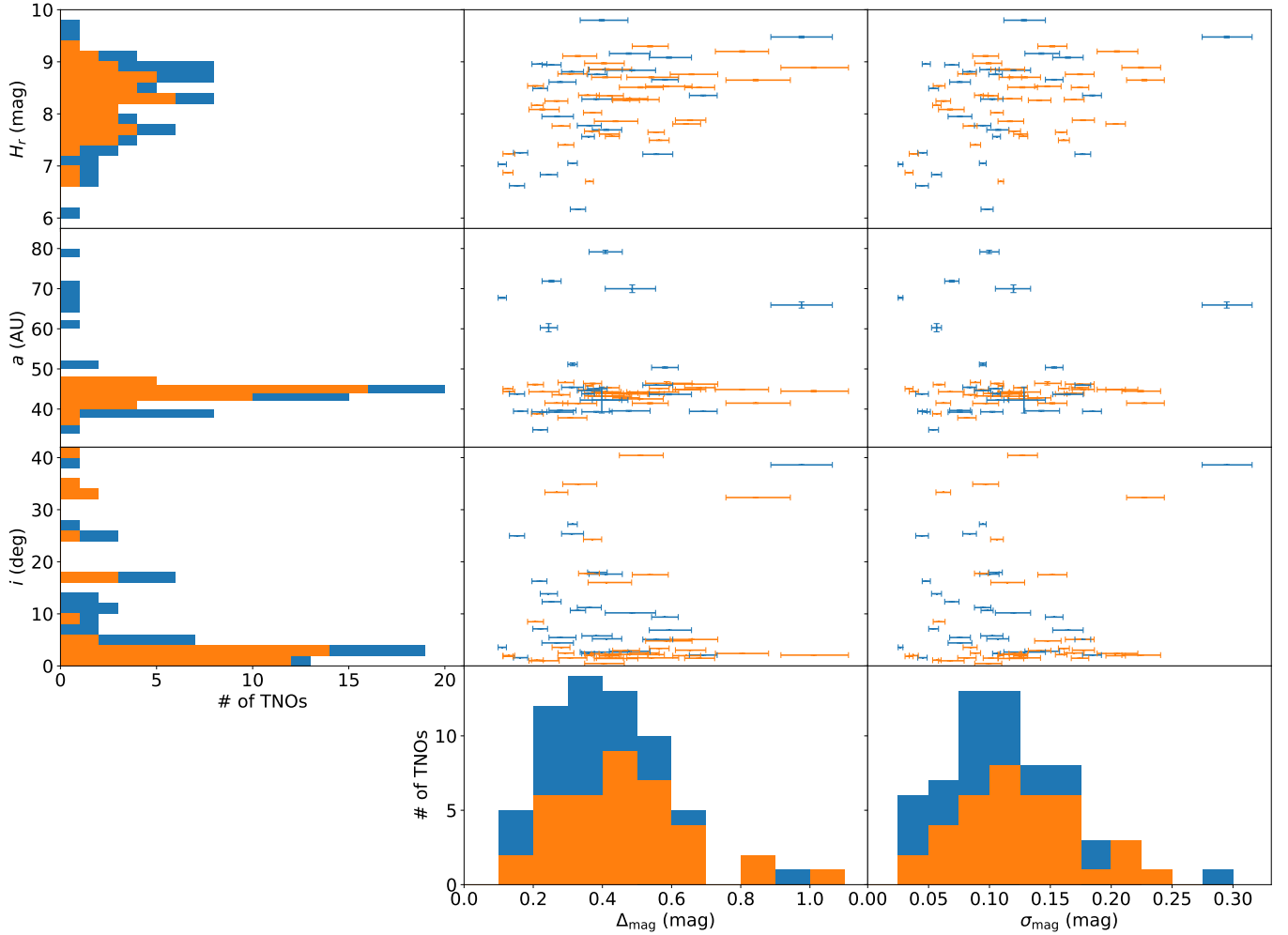


**Figure 7.** Left and bottom sides: histograms of  $H_r$  magnitude, semi-major axis  $a$ , inclination  $i$ ,  $\Delta_{\text{mag}}$  and  $\sigma_{\text{mag}}$  of our data. Center and top right: scatter plots of these parameters. Classical TNOs are shown in orange, and non-classical objects are shown in blue.

Sun or planets (Thirouin et al. 2010; Duffard et al. 2009). As an alternative to the difference between the brightest and faintest observation ( $\Delta_{\text{mag}}$ ), we also examine the standard deviation ( $\sigma_{\text{mag}}$ ) of all the observations of each object, because the standard deviation is a measure of overall variation that is less influenced by individual anomalous measurements.

In Figure 7, we plot both  $\Delta_{\text{mag}}$  and  $\sigma_{\text{mag}}$  versus object  $H_r$ , semi-major axis  $a$ , and inclination  $i$  to illustrate possible relations between these parameters. In a sample of 128 objects, Benecchi & Sheppard (2013) found a statistically significant correlation ( $\rho = 0.288$ ,  $P = 0.001$ ) between light curve amplitude and absolute magnitude. Their sample spanned absolute magnitudes from 0 to 12 mag, although most were between 4 and 7 mag; very few had absolute magnitude fainter than 8 mag. Our sample of 63 TNOs span  $H_r = 6.2\text{--}10.8$  mag<sup>5</sup>, with more than half the sample at  $H_r > 8.0$  mag; our sample thus represents variability properties for fainter TNOs than the bulk of the Benecchi & Sheppard (2013) sample. Using the Spearman Rank correlation test (Spearman 1904) and our independent sample of 63 TNOs, we find  $\rho = 0.37$ ,  $P = 0.003$  for  $\Delta_{\text{mag}}$  versus  $H_r$  and  $\rho = 0.31$ ,  $P = 0.013$  for  $\sigma_{\text{mag}}$  versus  $H_r$ . Our data thus strongly support the existence of a weak relationship where intrinsically fainter (likely smaller) bodies on average have larger light curve amplitudes. This is likely due to increasingly elongated shapes. Benecchi & Sheppard (2013) also found a borderline significant anti-correlation ( $\rho = -0.170$ ,  $P = 0.056$ ) between light curve amplitude and inclination ( $i$ ), however, our data do not support the existence of such an anti-correlation.

Because the cold classicals are thought to have formed in place while all the hot populations (hot classicals, resonant, detached and scattering) are thought to have been scattered outwards to some extent after having formed closer to the Sun (e.g. Li et al.

<sup>5</sup> Whenever we discuss apparent and absolute magnitudes for our sample objects, those magnitudes are measured/calculated from our light curves observations, as these are more accurate than the discovery magnitudes reported by OSSOS.

**Table 4.** Spearman Rank correlation test results. Tests for correlation between the measured light curve variation  $\Delta_{\text{mag}}$  and  $\sigma_{\text{mag}}$  and the parameter listed in the first column.

Parameter	$\rho_{\Delta_{\text{mag}}}$	$P_{\Delta_{\text{mag}}}$	$\rho_{\sigma_{\text{mag}}}$	$P_{\sigma_{\text{mag}}}$
All objects				
$H_r$	$0.37^{+0.03}_{-0.03}$	0.003	$0.31^{+0.03}_{-0.02}$	0.013
$a$	$0.10^{+0.03}_{-0.03}$	0.43	$0.11^{+0.02}_{-0.02}$	0.41
$i$	$-0.05^{+0.03}_{-0.03}$	0.7	$-0.07^{+0.02}_{-0.02}$	0.60
Cold classicals				
$H_r$	$0.43^{+0.04}_{-0.05}$	0.029	$0.30^{+0.03}_{-0.04}$	0.14
$i$	$0.25^{+0.05}_{-0.05}$	0.21	$0.38^{+0.03}_{-0.04}$	0.06
Hot populations				
$H_r$	$0.42^{+0.04}_{-0.05}$	0.013	$0.41^{+0.03}_{-0.04}$	0.015
$a$	$0.04^{+0.05}_{-0.05}$	0.79	$0.04^{+0.04}_{-0.04}$	0.79
$i$	$0.08^{+0.05}_{-0.04}$	0.6	$0.03^{+0.03}_{-0.03}$	0.85

2008; Levison et al. 2008; Batygin et al. 2011), we also test the dynamically cold and hot samples separately to identify whether a trend might be present in one population and not in the other. In this work, we use the term “hot population” to refer to all of the dynamically excited populations combined (as done in Fraser et al. 2014, and others); specifically our hot population sample contains everything non-classical plus classical objects with  $i \geq 6^\circ$ . Our “cold classicals” sample consists only of classicals with  $i \leq 4^\circ$ . Classicals with  $4^\circ < i < 6^\circ$  (two objects in our sample) are excluded from either sample to minimize contamination. The correlation values as well as their significance levels can be found in Table 4 and are simply summarized here. For our samples of 26 cold classical TNOs and 35 hot TNOs, we find that both have similar correlation coefficients to the full sample for amplitude versus  $H_r$ , but with a lower significance than in the full sample (likely due mostly to the now smaller sample sizes). For amplitude versus inclination, we find that neither population has a statistically significant correlation, just as in the overall sample. Because the semi-major axis ( $a$ ) is possibly related to where objects formed, we also tested for correlations between the light curve variation and  $a$  for the full sample and the hot population (the cold population was not tested due to its narrow  $a$  range). We find that the semi-major axis is not at all correlated with the variability in the full sample nor in the hot population.

To further test the notion that different populations may have different amplitude distributions, the 2-sample Anderson-Darling test was used to compare subsamples. The subsamples used were the classical, resonant, hot and cold populations. We did not look at the scattering and detached objects in this analysis because the sample sizes are too small for any meaningful results. In every case, the subsample was tested against the remainder of the sample (ie. classicals versus everything non-classical, etc). See Table 5 for the resultant  $P$  values. No subsample was found to be significantly different from the rest of the sample.

#### 4.2. Period analysis

The rotation periods of TNOs range from 3.9 hours (Haumea) to 154 hours (Pluto), with a mean of 7–9 hours (Duffard et al. 2009; Benecchi & Sheppard 2013; Thirouin et al. 2016); there are clearly a number of assumptions and biases that go into this mean, not the least of which is the aliasing effects from observations on consecutive nights and the fact that tracking low amplitude and slowly varying objects requires a lot of telescope time. Both of these biases exist in our dataset; nevertheless, we seek to use the data we present here to at least place limits on the rotation periods and amplitudes of the objects in our sample. In the few cases where our data allow for more extensive interpretation, we proceed as appropriate for each object. We attempt to fit periods to our light curve data using two methods: a Phase Dispersion Minimization (PDM) method and a Power Spectral Density (PSD) method. Because our TNOs are all small enough that we do not expect them to be spherical, they should all have double peaked periods. The two light curve peaks of an elongated TNO are often difficult to distinguish (for a perfectly symmetrical ellipsoid, the two peaks would be identical). These methods therefore simply identify the period of the light curve,

**Table 5.** 2-sample Anderson-Darling test results. Tests for whether two samples are likely to have been drawn from the same source population. Here we test whether the light curve variability (measured by  $\Delta_{\text{mag}}$  and  $\sigma_{\text{mag}}$ ) distribution is different for different dynamical sub-populations. In every case here, a sub-sample is tested against the remainder of our sample (eg. the resonant objects against everything that is not resonant).

sub-population	$N_{\text{obj}}$	$P_{\Delta_{\text{mag}}}$	$P_{\sigma_{\text{mag}}}$
classicals	37	$0.15^{+0.10}_{-0.07}$	$0.11^{+0.06}_{-0.05}$
resonant	15	$0.8 \pm 0.2$	$0.76^{+0.12}_{-0.14}$
hot	35	$0.13^{+0.09}_{-0.06}$	$0.09^{+0.06}_{-0.03}$
cold	26	$0.4 \pm 0.2$	$0.29^{+0.12}_{-0.09}$

not the TNO. We double the single-peaked periods found by our two period methods to get the most likely rotation period of the TNO.

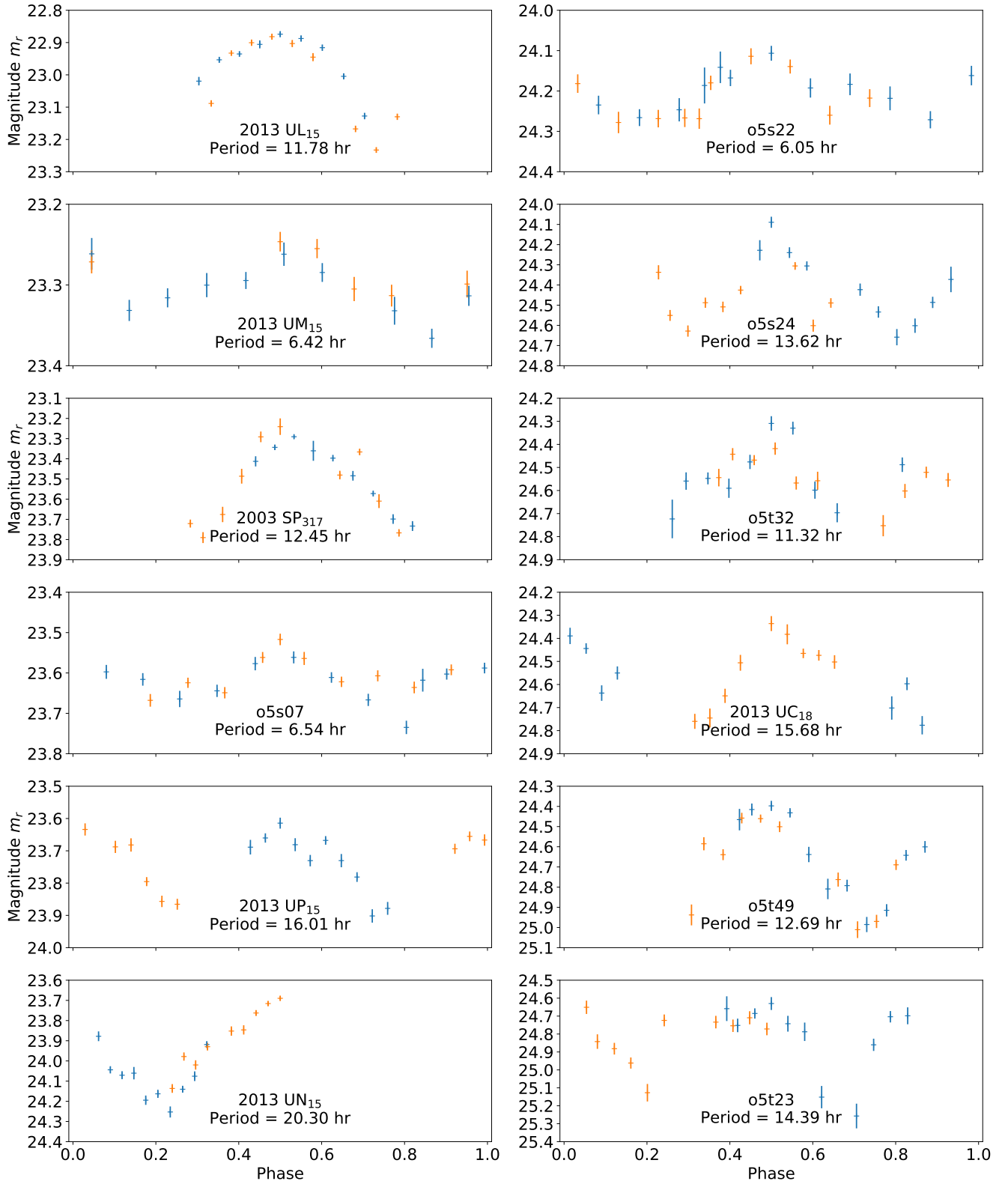
Because our observing window is about 30 hours (from the start of night one to the end of night two) we are able to sample rotation periods from the rotational break-up-limit of 3.3 hours (Romanishin & Tegler 1999) to about 60 hours (where we are sampling half a rotation, which is a full peak-to-peak cycle for a double-peaked light curve). For the PSD method, we therefore fold the light curves using every period from 1.0 hours to 30.0 hours in 0.1 hour intervals. The Fourier coefficients are calculated from each folded light curve; the sum of the squares of the Fourier coefficients as a function of period is the PSD. The period that has the highest PSD value is selected as the most likely period of the TNO. In the PDM method, we fit the data points for each object using a modified PDM (Stellingwerf 1978; Buie et al. 2018). This method goes through every possible period, folds the data and fits a second-order Fourier series to each folded light curve. The quality of each fit is captured from the residuals; the fits are ranked and the fit with the highest quality is selected.

Table 6 lists the periods found from these two methods (converted into double-peak periods) for objects where the two methods agree; Figure 8 shows the light curves folded at those periods. When the two methods do not agree, it is likely evidence that we do not have enough data to determine the period with confidence. The PDM curves from our period analysis is available in the supplementary materials, Figures 10 to 14. Although the mean period from our dataset analysis is somewhat greater than that given in the literature ( $\sim 12.3$  hours compared with 7-9 hours, Duffard et al. (2009); Benecchi & Sheppard (2013); Thirouin et al. (2010)) it is important to recognize that the periods we are reporting are based on single epoch measurements without the same fidelity of many of the light curves in the literature. The literature contains both single and double-peaked light curves and light curves of binary objects. We cannot distinguish among these interpretations and have assumed a double-peaked light curve for all objects, so one should not over-interpret this apparent result from our dataset. This sample of 12 periods is insufficient to draw any conclusions, other than the fact that we would need a larger baseline than two consecutive 6-hour nights to determine the period of a larger fraction of objects. Adding a third night and observing closer to opposition (when the targets are visible for 8 hours) would allow determination of periods for a much larger fraction of light curves. We therefore leave discussion of the period distribution for future work.

## 5. DISCUSSION AND CONCLUSIONS

### 5.1. Implications for large surveys

Large variability can have an influence on whether or not an object is discovered in a magnitude limited survey. Most large surveys use an automated moving object pipeline to find TNO candidates. For the Canada-France Ecliptic Plane Survey (Kavelaars et al. 2009; Petit et al. 2011), OSSOS and the Alexandersen et al. (2016) survey, TNOs were identified using three discovery images with one hour between each. Non-stationary sources within three images of a field are linked together as a candidate TNO detection; various constraints on the rate, angle and linearity of motion are imposed, as well as a requirement of similar magnitudes, in order to limit the number of false candidates. If a TNO's magnitude is highly variable, this might leave it undetected,



**Figure 8.** Folded light curves for the 12 objects for which we have a period estimate. Blue and orange points show data from the first and second nights, respectively. The arbitrary phase=0 point was chosen such that the brightest measured magnitude falls at phase=0.5. The exact values of MJD, magnitude and uncertainty of all observations can be found in [Table 3](#).

**Table 6.** Best periods from two methods, in hours. Numbers in parentheses are the percentage of resampled light curves that had a “best” period within  $5\sigma$  of the reported value. Only objects where the two methods agree on the best period are included. As these objects are small, their variability is most likely shape-dominated; shape dominated light curves have two peaks per rotation of the object.

Object	Period <sub>PDM</sub> (hour)	Period <sub>PDS</sub> (hour)
2013 UL <sub>15</sub>	11.76 ± 0.02 (41.3%)	11.80 ± 0.03 (100.0%)
2013 UC <sub>18</sub>	15.66 ± 0.23 (80.7%)	15.70 ± 0.08 (68.8%)
2013 UP <sub>15</sub>	16.02 ± 0.09 (37.7%)	16.00 ± 0.07 (100.0%)
2013 UM <sub>15</sub>	6.44 ± 0.03 (81.0%)	6.40 ± 0.04 (49.0%)
2013 UN <sub>15</sub>	20.30 ± 0.08 (79.2%)	20.30 ± 0.09 (43.6%)
o5s07	6.58 ± 0.05 (84.4%)	6.50 ± 0.03 (99.3%)
o5s22	6.03 ± 0.02 (98.2%)	6.07 ± 0.04 (54.3%)
o5s24	13.54 ± 0.04 (94.8%)	13.70 ± 0.14 (74.9%)
o5t23	14.38 ± 0.08 (74.0%)	14.40 ± 0.09 (41.3%)
o5t32	11.34 ± 0.11 (30.3%)	11.30 ± 0.09 (71.9%)
o5t34	12.45 ± 0.04 (100.0%)	12.45 ± 0.04 (100.0%)
o5t49	12.66 ± 0.05 (99.7%)	12.72 ± 0.04 (100.0%)

either because it might be too faint to be detected in one of the three images or, if the constraints in the detection pipeline are too tight, because the pipeline might not consider the three points to be the same object due to having different magnitudes.

In our sample of 63 TNO light curves (most having observation on both nights), we find that only  $6 \pm 1$  have a  $\Delta_{\text{mag}} < 0.2$  magnitudes, while  $31 \pm 2$  (just under half the sample) have a  $\Delta_{\text{mag}} > 0.4$  magnitudes and  $11 \pm 1$  have  $\Delta_{\text{mag}} > 0.6$  magnitudes<sup>6</sup>. However, those variations are usually over many hours. In order to evaluate the impact that light curve variation could have on shorter timescales, we measured the typical variation on 1–2 hour timescales. Since our images for these light curves are typically spaced 36 minutes apart, we calculated the  $\Delta_{\text{mag}}$  for all 1.25 hr (3 images), 1.85 hr (4 images) and 2.45 hr (5 images) subsets of our light curves. We find that in 1.25 hr, the median value of the  $\Delta_{\text{mag}}$  is 0.13 magnitudes and the standard deviation of the  $\Delta_{\text{mag}}$  distribution is 0.12 magnitudes. For 1.85 hr, the median and standard deviation are 0.16 and 0.13, respectively, while for 2.45 hr they are 0.19 and 0.14 magnitudes, respectively. Figure 9 shows the  $\Delta_{\text{mag}}$  distribution within these three time spans. The moving object pipeline used for the [Alexandersen et al. \(2016\)](#) survey and for OSSOS only had the weak constraint that the faintest and brightest points within the three discovery images (spaced about 1 hour apart) had to have a flux-ratio of less than 4, which corresponds to a magnitude difference of about 1.5 mag. In our data from this work, we never see variability greater than 1.2 mag within a 2-hour window; it therefore seems highly unlikely that a real objects was rejected by the detection pipeline due to natural variability. Because the overall average variability seen within our data is much larger than the average variability measured within 1.25-2.45 hours, this demonstrates the perhaps obvious point that the average magnitude measured within a few hours is not an accurate measurement of the true average magnitude of the TNO. Discovery images from surveys like CFEPs, OSSOS and the [Alexandersen et al. \(2016\)](#) survey all depend on having measured the magnitude in three discovery images; the fact that these measured magnitudes are potentially several tenths of a magnitude from the true average magnitude should be included when performing survey simulation and model analysis.

Variability is important to consider when measuring photometric colors of TNOs as well. Because most facilities do not have the ability to observe in multiple band-passes simultaneously, the images in different filters must be taken in sequence. If the object is faint and thus requires a long exposure time in some/each filter, its variability could cause an erroneous measurement of the color if the brightness varies significantly within the timespan of the observations. For accurate photometric colors, it

<sup>6</sup> The uncertainties quoted in this sentence on the number of objects come from resampling the light curve photometry 1000 times and calculating the values for each resampled set.

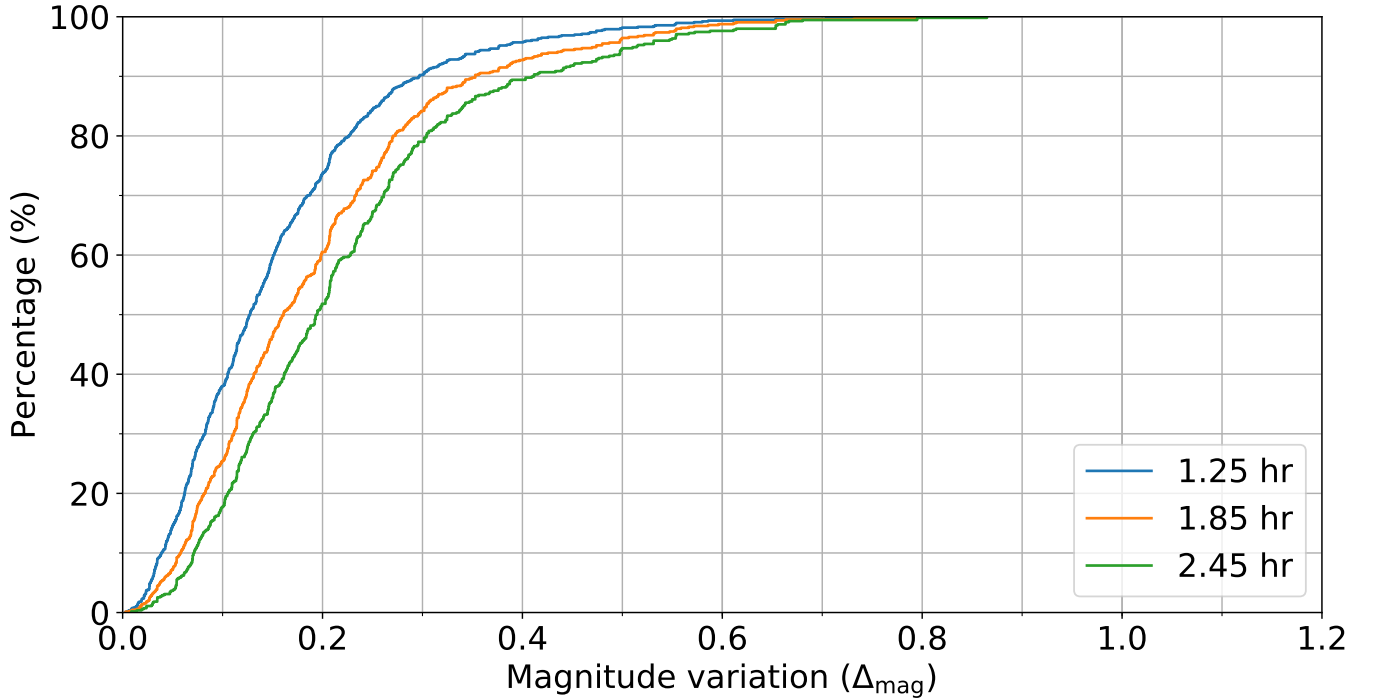


**Figure 9.** Cumulative distribution of the magnitude variation (maximum minus minimum,  $\Delta_{\text{mag}}$ ) within 1.25 hr (blue, top), 1.85 hr (orange, middle) and 2.45 hr (green, bottom) sections of light curves.

is therefore important to account for light curve variability, except in cases of very short (thus nearly simultaneous) exposure sequences for bright objects. This can be done by repeating observations of the filter that requires least exposure time several times during a sequence (for example *r-g-r-J-r*), as has become common practice, to get a rough idea of the light curve variation during the sequence. Alternatively, if some of the filters require enough exposure time to warrant multiple exposures, those exposures should be spread out in the sequence (for example the *r-g-J-g-r* sequence used by [Bannister et al. \(2017\)](#)). Of course, this relies on having fast filter changes and can therefore not be done with Hyper Suprime-Cam, which has a filter exchange time of about 30 minutes. It should be obvious that photometry acquired on different days cannot be used to calculate reliable colors unless the light curve is known, so TNO colors reported from surveys like the Hyper Suprime-Cam Subaru Strategic Program (HSC SSP [Aihara et al. 2018](#); [Terai et al. 2018](#)) or the LSST survey should be seen as very rough color estimates with a likely uncertainty of  $\sim 0.2$  magnitude.

Expected to start science operations in 2022, LSST will provide an inventory of the trans-Neptunian region down to a  $5\text{-}\sigma$  limiting magnitude of approximately 24.6 in *r* and 24.8 in *g* ([Ivezic et al. 2008](#); [LSST Science Collaboration et al. 2009](#)). LSST is expected to discover over 40,000 TNOs during its planned ten years of science operations ([LSST Science Collaboration et al. 2009](#)). During this period, TNOs within the survey footprint will be imaged hundreds of times by LSST in multiple filters (*ugrizy*), producing sparsely sampled light curves. Our HSC variability study overlaps the size and magnitude range that LSST will be sensitive to. Thus, the variability we observe can be taken as a minimum value for the variability LSST will see for its TNO sample. Over a few hour baseline, 90% of our HSC sample vary in brightness up to 0.4 magnitudes. This is more variability than shallower past wide-field Solar System surveys had to deal with. As detailed above, OSSOS, which our sample is derived from, had no significant brightness/variability constraints when identifying moving objects ([Bannister et al. 2018](#)). This may be important in the development of the LSST moving object detection pipeline and for consideration when assessing the TNO detection completeness for LSST. Additionally, in the sparse light curves LSST will produce, objects with more than 0.5 magnitudes variation can potentially be flagged as extreme shapes in need of further higher-cadence follow-up observations.

Finally, we note that objects in this size range do not have enough mass to ensure hydrostatic equilibrium, so the variability seen is therefore most likely caused by the objects being highly non-spherical. Given the correlation between absolute  $H_r$  magnitude and variability shown above, it is unreasonable to expect that even smaller object can be modeled as roughly spherical shapes. A number of surveys have searched for serendipitous stellar occultations by small (diameters  $\sim 1$  km, roughly corresponding to  $H_r \sim 16\text{--}19$  depending on albedo) TNOs in order to measure the size distribution of such objects ([Lehner et al. 2016](#); [Zhang](#)

et al. 2013; Schlichting et al. 2012; Bianco et al. 2009; Liu et al. 2008; Bickerton et al. 2008; Roques et al. 2003). TNOs in this size range are in the Fresnel regime when measuring from the ground at visible wavelengths, and their occultation shadows thus exhibit significant diffraction features (Nihei et al. 2007; Roques et al. 1987). Most survey teams use the approximation of spherical occulting objects in order to simplify the calculation of the occultation event parameters, but when non-spherical shapes are considered there may be significant effects on the resulting occultation shadows (Roques et al. 1987; Castro-Chacón 2018). Obviously, we did not measure light curves of such small objects in this survey; however, based on our observations of larger ( $8 > H_r > 10$ ) TNOs, we propose that these surveys need to consider the expectation of non-spherical objects when defining event detection criteria, characterizing any occultation events or estimating any survey detection efficiencies.

### 5.2. Contact binaries

To date, in the trans-Neptunian belt, only 2001 QG<sub>298</sub> has been confirmed as a contact binary (Sheppard & Jewitt 2004; Lacerda et al. 2014). This confirmation is based on the large light curve amplitude  $\Delta_{\text{mag}} \geq 0.9$  mag, and the V-/U-shape at the minimum/maximum of brightness. However, such a large amplitude is only observed if the two components are seen equator-on (or almost equator-on). If the two components are not aligned with the viewer’s line of sight, the amplitude will be smaller (simple geometry, Lacerda 2011; Lacerda et al. 2014; Thirouin et al. 2017; Thirouin & Sheppard 2017, 2018).

Our sparse light curves reveals no obvious contact binaries, although do contain candidates that should be observed further. None of the light curves reported here present a definite full peak-to-peak amplitude larger than 0.9 mag. 05s49, uo5s77 and 05s57 have a  $\Delta_{\text{mag}}$  around 1 mag, but the light curves are too noisy for drawing conclusions. Several objects like 2003 SP<sub>317</sub>, o5t30, 2013 UN<sub>15</sub> and 2013 SM<sub>100</sub> display a  $\Delta_{\text{mag}} > 0.5$  mag. Unfortunately, because we do not have a full maximum and minimum showing a clear U- and V-shape, it is difficult to classify them as likely contact binaries. More observations are required in order to confirm whether these objects are contact binaries or simply highly elongated bodies.

### 5.3. Conclusions

We have obtained a large sample of sparse partial light curves 65 TNOs, most of which are small ( $H_r > 7$ ) and therefore fainter than have typically been studied before, with up to 22 observations in acceptable conditions over two nights. While the variability for many of these objects might only be a lower limit due to not having observed the full rotation of the object, we can draw some tentative conclusions. As seen by Benecchi & Sheppard (2013), we confirm that the amplitude of the light curve correlates with the absolute magnitude. However, in contrast, we do not see a statistically significant correlation with inclination.

We find that a large fraction of our observed TNOs have large brightness variations, even on 1-2 hour timescales. 31 objects (just under half the sample) have a  $\Delta_{\text{mag}} > 0.4$  mag over the course of our observations, while the median variability within a 1.85 hour timespan was 0.16 mag. TNO variability must be accounted for when simulating/modeling discovery surveys like OSSOS and LSST, as well as when observing non-simultaneous TNO colors.

In this pilot study we did not find any significant difference in amplitude distribution between different dynamical classes. However, our sample included very few objects in the scattering and detached classes. Future work should therefore target more of these objects in order to have similar sample sizes for each population.

We were able to estimate periods for 12 of the 65 TNOs. However, these periods are not certain due to aliasing. In order to estimate periods for a larger fraction of the sample and reduce aliasing effects, a longer baseline of observations is needed.

## ACKNOWLEDGEMENTS

This paper is based on data collected at the Subaru Telescope and retrieved from the Hyper Suprime-Cam data archive system, which is operated by Subaru Telescope and Astronomy Data Center at National Astronomical Observatory of Japan. The access to Subaru telescope from Taiwan is supported by the Academia Sinica Institute of Astronomy and Astrophysics. The authors wish to recognize and acknowledge the very significant cultural role and reverence that the summit of Maunakea has always had within the indigenous Hawaiian community. We are most fortunate to have the opportunity to conduct observations from this mountain. We would also like to acknowledge the maintenance, cleaning, administrative and support staff at academic and telescope facilities, whose labor maintains the spaces where astrophysical inquiry can flourish.

This work is based on TNO discoveries obtained with MegaPrime/MegaCam, a joint project of the Canada France Hawaii Telescope (CFHT) and CEA/DAPNIA, at CFHT which is operated by the National Research Council (NRC) of Canada, the Institut National des Sciences de l’Univers of the Centre National de la Recherche Scientifique (CNRS) of France, and the University of Hawaii. A portion of the access to the CFHT was made possible by the Academia Sinica Institute of Astronomy and Astrophysics, Taiwan. This research used the facilities of the Canadian Astronomy Data Centre operated by the National Research Council of Canada with the support of the Canadian Space Agency.

MES was supported by Gemini Observatory, which is operated by the Association of Universities for Research in Astronomy, Inc., on behalf of the international Gemini partnership of Argentina, Brazil, Canada, Chile, and the United States of America. MB acknowledges support from UK STFC grant ST/L000709/1. KV acknowledges support from NASA grants NNX14AG93G and NNX15AH59G. SBD acknowledges support by the National Aeronautics and Space Administration under Grant/Contract/Agreement No. NNX15AE04G issued through the SSO Planetary Astronomy Program.

This paper makes use of software developed for the Large Synoptic Survey Telescope. We thank the LSST Project for making their code available as free software at <http://dm.lsst.org>. This research has made use of NASA's Astrophysics Data System Bibliographic Services. This research made use of SciPy (Jones et al. 2001), NumPy (van der Walt et al. 2011), matplotlib (a Python library for publication quality graphics Hunter 2007) and Astropy (a community-developed core Python package for Astronomy Astropy Collaboration et al. 2013; The Astropy Collaboration et al. 2018). This research made use of ds9, a tool for data visualization supported by the Chandra X-ray Science Center (CXC) and the High Energy Astrophysics Science Archive Center (HEASARC) with support from the JWST Mission office at the Space Telescope Science Institute for 3D visualization. IRAF is distributed by the National Optical Astronomy Observatory, which is operated by the Association of Universities for Research in Astronomy (AURA) under cooperative agreement with the National Science Foundation (Tody 1993).

The Pan-STARRS1 Surveys (PS1) and the PS1 public science archive have been made possible through contributions by the Institute for Astronomy, the University of Hawaii, the Pan-STARRS Project Office, the Max-Planck Society and its participating institutes, the Max Planck Institute for Astronomy, Heidelberg and the Max Planck Institute for Extraterrestrial Physics, Garching, The Johns Hopkins University, Durham University, the University of Edinburgh, the Queen's University Belfast, the Harvard-Smithsonian Center for Astrophysics, the Las Cumbres Observatory Global Telescope Network Incorporated, the National Central University of Taiwan, the Space Telescope Science Institute, the National Aeronautics and Space Administration under Grant No. NNX08AR22G issued through the Planetary Science Division of the NASA Science Mission Directorate, the National Science Foundation Grant No. AST-1238877, the University of Maryland, Eotvos Lorand University (ELTE), the Los Alamos National Laboratory, and the Gordon and Betty Moore Foundation.

The acknowledgements were compiled in part using the Astronomy Acknowledgement Generator.

*Facilities:* Subaru (HSC), PS1

*Software:* Python (van Rossum & de Boer 1991), Matplotlib (Hunter 2007), NumPy (van der Walt et al. 2011), SciPy (Jones et al. 2001), TRIPPy (Fraser et al. 2016), Ureka (Hirst et al. 2014), IRAF (Tody 1993), Astropy (Astropy Collaboration et al. 2013; The Astropy Collaboration et al. 2018), SExtractor (Bertin & Arnouts 1996), ds9 Joye & Mandel (2003)

## REFERENCES

- Aihara, H., Arimoto, N., Armstrong, R., et al. 2018, PASJ, 70, S4
- Alexandersen, M., Gladman, B., Kavelaars, J. J., et al. 2016, AJ, 152, 111
- Astropy Collaboration, Robitaille, T. P., Tollerud, E. J., et al. 2013, A&A, 558, A33
- Bannister, M. T., Kavelaars, J. J., Petit, J.-M., et al. 2016, AJ, 152, 70
- Bannister, M. T., Schwamb, M. E., Fraser, W. C., et al. 2017, ApJL, 851, L38
- Bannister, M. T., Gladman, B. J., Kavelaars, J. J., et al. 2018, The Astrophysical Journal Supplement Series, 236, 18
- Batygin, K., Brown, M. E., & Fraser, W. C. 2011, ApJ, 738, 13
- Benechchi, S. D., & Sheppard, S. S. 2013, AJ, 145, 124
- Bertin, E., & Arnouts, S. 1996, A&AS, 117, 393
- Bianco, F. B., et al. 2009, AJ, 138, 568
- Bickerton, S. J., Kavelaars, J. J., & Welch, D. L. 2008, AJ, 135, 1039
- Bosch, J., Armstrong, R., Bickerton, S., et al. 2018, PASJ, 70, S5
- Buie, M. W., Zangari, A. M., Marchi, S., Levison, H. F., & Mottola, S. 2018, AJ, in press
- Castro-Chacón, J. H. 2018, in preparation
- Duffard, R., Ortiz, J. L., Thirouin, A., Santos-Sanz, P., & Morales, N. 2009, A&A, 505, 1283
- Fraser, W., Alexandersen, M., Schwamb, M. E., et al. 2016, AJ, 151, 158
- Fraser, W. C., & Brown, M. E. 2012, ApJ, 749, 33
- Fraser, W. C., Brown, M. E., Morbidelli, A., Parker, A., & Batygin, K. 2014, ApJ, 782, 100
- Gladman, B., Marsden, B. G., & Vanlaerhoven, C. 2008, Nomenclature in the Outer Solar System (The University of Arizona Press), 43–57
- Hahn, J. M., & Malhotra, R. 2005, AJ, 130, 2392
- Hirst, P., Slocum, C., Turner, J., et al. 2014, in Astronomical Society of the Pacific Conference Series, Vol. 485, Astronomical Data Analysis Software and Systems XXIII, ed. N. Manset & P. Forshay, 335

- Hunter, J. D. 2007, *Computing In Science & Engineering*, 9, 90
- Ivezic, Z., Tyson, J. A., Abel, B., et al. 2008, *ArXiv e-prints*, arXiv:0805.2366
- Jones, E., Oliphant, T., Peterson, P., & Others. 2001, *SciPy: Open source scientific tools for Python*, . . <http://www.scipy.org/>
- Joye, W. A., & Mandel, E. 2003, in *Astronomical Society of the Pacific Conference Series*, Vol. 295, *Astronomical Data Analysis Software and Systems XII*, ed. H. E. Payne, R. I. Jedrzejewski, & R. N. Hook, 489
- Kaula, W. M., & Newman, W. I. 1992, *Advances in Space Research*, 12, 3
- Kavelaars, J. J., Jones, R. L., Gladman, B. J., et al. 2009, *AJ*, 137, 4917
- Kortenkamp, S. J., Malhotra, R., & Michtchenko, T. 2004, *Icarus*, 167, 347
- Lacerda, P. 2011, *AJ*, 142, 90
- Lacerda, P., McNeill, A., & Peixinho, N. 2014, *MNRAS*, 437, 3824
- Lawler, S. M., Shankman, C., Kavelaars, J. J., et al. 2018, *AJ*, 155, 197
- Lehner, M. J., Wang, S.-Y., Reyes-Ruiz, M., et al. 2016, in *Proc. SPIE*, Vol. 9906, *Ground-based and Airborne Telescopes VI*, 99065M
- Levison, H. F., Morbidelli, A., Van Laerhoven, C., Gomes, R., & Tsiganis, K. 2008, *Icarus*, 196, 258
- Li, J., Zhou, L.-Y., & Sun, Y.-S. 2008, *ChA&A*, 32, 409
- Liu, C.-Y., et al. 2008, *MNRAS*, 388, L44
- LSST Science Collaboration, Abell, P. A., Allison, J., et al. 2009, *ArXiv e-prints*, arXiv:0912.0201
- Lupton, R., Gunn, J. E., Ivezić, Z., Knapp, G. R., & Kent, S. 2001, in *Astronomical Society of the Pacific Conference Series*, Vol. 238, *Astronomical Data Analysis Software and Systems X*, ed. F. R. Harnden, Jr., F. A. Primini, & H. E. Payne, 269
- Magnier, E. A., Schlafly, E., Finkbeiner, D., et al. 2013, *ApJS*, 205, 20
- Malhotra, R. 1993, *Nature*, 365, 819
- . 1995, *AJ*, 110, 420
- Miyazaki, S., Komiyama, Y., Kawanomoto, S., et al. 2018, *PASJ*, 70, S1
- Murray-Clay, R. A., & Chiang, E. I. 2005, *ApJ*, 619, 623
- Nihei, T. C., et al. 2007, *AJ*, 134, 1596
- Peixinho, N., Doressoundiram, A., Delsanti, A., et al. 2003, *A&A*, 410, L29
- Petit, J.-M., Kavelaars, J. J., Gladman, B. J., et al. 2011, *Astronomical Journal*, 142, 131
- Pike, R. E., Fraser, W. C., Schwamb, M. E., et al. 2017, *AJ*, 154, 101
- Romanishin, W., & Tegler, S. C. 1999, *Nature*, 398, 129
- Roques, F., Moncuquet, M., & Sicardy, B. 1987, *AJ*, 93, 1549
- Roques, F., et al. 2003, *ApJL*, 594, L63
- Ryan, E. L., Sharkey, B. N. L., & Woodward, C. E. 2017, *AJ*, 153, 116
- Schlafly, E. F., Finkbeiner, D. P., Jurić, M., et al. 2012, *ApJ*, 756, 158
- Schlichting, H. E., et al. 2012, *ApJ*, 761, 150
- Shankman, C., Gladman, B. J., Kaib, N., Kavelaars, J. J., & Petit, J. M. 2013, *Astrophysical Journal Letters*, 764, L2
- Sheppard, S. S. 2012, *AJ*, 144, 169
- Sheppard, S. S., & Jewitt, D. 2004, *AJ*, 127, 3023
- Sheppard, S. S., Lacerda, P., & Ortiz, J. L. 2008, *Photometric Lightcurves of Transneptunian Objects and Centaurs: Rotations, Shapes, and Densities*, ed. M. A. Barucci, H. Boehnhardt, D. P. Cruikshank, A. Morbidelli, & R. Dotson, 129–142
- Spearman, C. 1904, *The American Journal of Psychology*, 15, 72. <http://www.jstor.org/stable/1412159>
- Stellingwerf, R. F. 1978, *ApJ*, 224, 953
- Tegler, S. C., Romanishin, W., Consolmagno, G. J., & J., S. 2016, *AJ*, 152, 210
- Terai, T., Yoshida, F., Ohtsuki, K., et al. 2018, *PASJ*, 70, S40
- The Astropy Collaboration, Price-Whelan, A. M., Sipőcz, B. M., et al. 2018, *ArXiv e-prints*, arXiv:1801.02634
- Thirouin, A., Noll, K. S., Ortiz, J. L., & Morales, N. 2014, *A&A*, 569, A3
- Thirouin, A., Ortiz, J. L., Duffard, R., et al. 2010, *A&A*, 522, A93
- Thirouin, A., & Sheppard, S. S. 2017, *AJ*, 154, 241
- . 2018, *Astronomical Journal*, 155, 248
- Thirouin, A., Sheppard, S. S., & Noll, K. S. 2017, *ApJ*, 844, 135
- Thirouin, A., Sheppard, S. S., Noll, K. S., et al. 2016, *AJ*, 151, 148
- Thommes, E. W., Duncan, M. J., & Levison, H. F. 2002, *AJ*, 123, 2862
- Tody, D. 1993, in *Astronomical Society of the Pacific Conference Series*, Vol. 52, *Astronomical Data Analysis Software and Systems II*, ed. R. J. Hanisch, R. J. V. Brissenden, & J. Barnes, 173
- Tonry, J. L., Stubbs, C. W., Lykke, K. R., et al. 2012, *ApJ*, 750, 99
- Trujillo, C. A., & Brown, M. E. 2002, *ApJL*, 566, L125
- Tsiganis, K., Gomes, R., Morbidelli, A., & Levison, H. F. 2005, *Nature*, 435, 459
- van der Walt, S., Colbert, S. C., & Varoquaux, G. 2011, *Computing in Science Engineering*, 13, 22
- van Rossum, G., & de Boer, J. 1991, in *EurOpen. UNIX Distributed Open Systems in Perspective. Proceedings of the Spring 1991 EurOpen Conference*, Tromsø, Norway, May 20–24, 1991, ed. EurOpen (Buntingford, Herts, UK: EurOpen), 229–247
- Zhang, Z.-W., et al. 2013, *AJ*, 146, 14

APPENDIX

.1. *Supplementary materials*

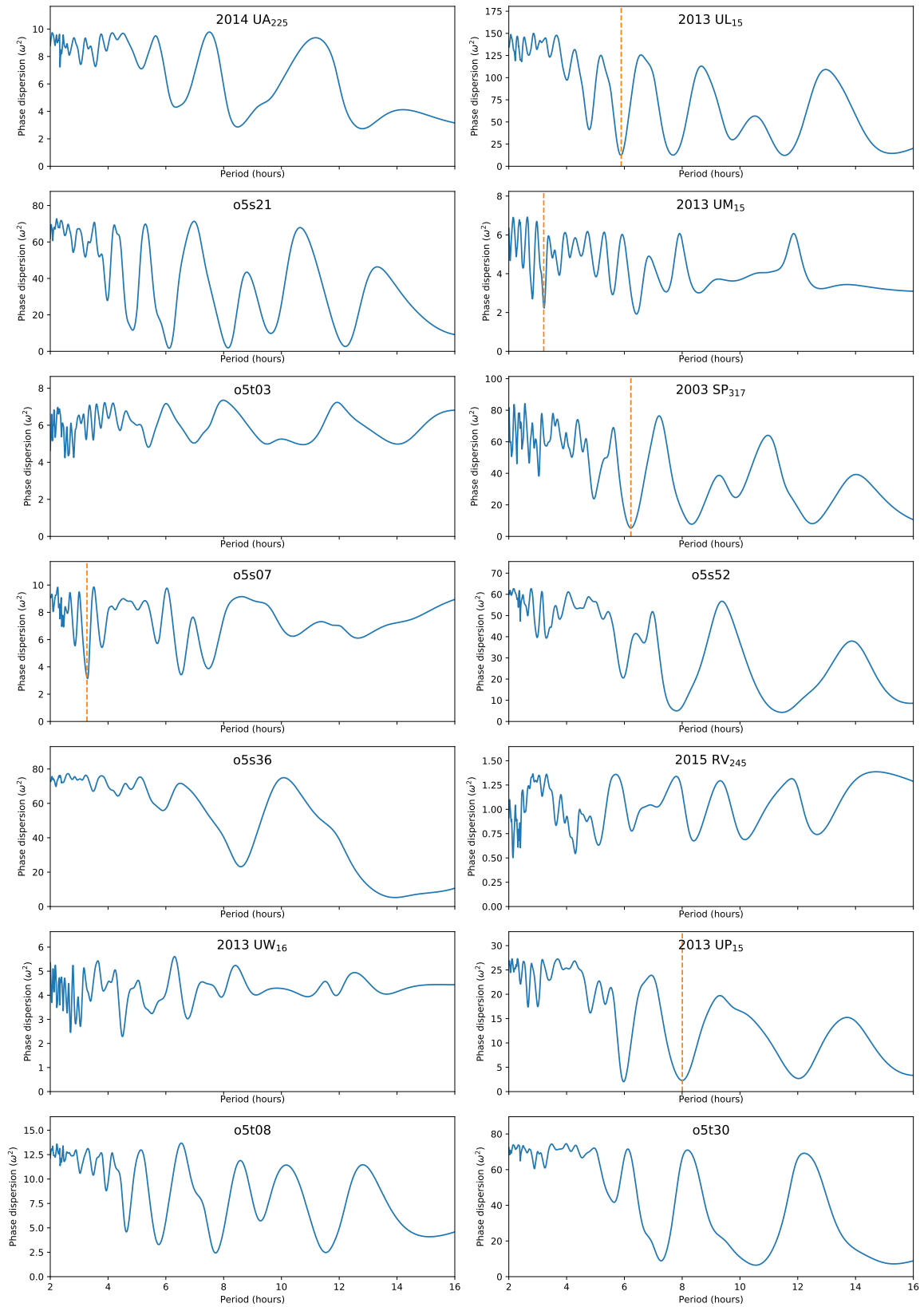


**Figure 10.** PDM plot from our period analysis. Vertical dashed orange lines show our favored single-peak period for the objects listed in Table 6 and shown in Figure 8. Objects 0–13, ordered by average magnitude.

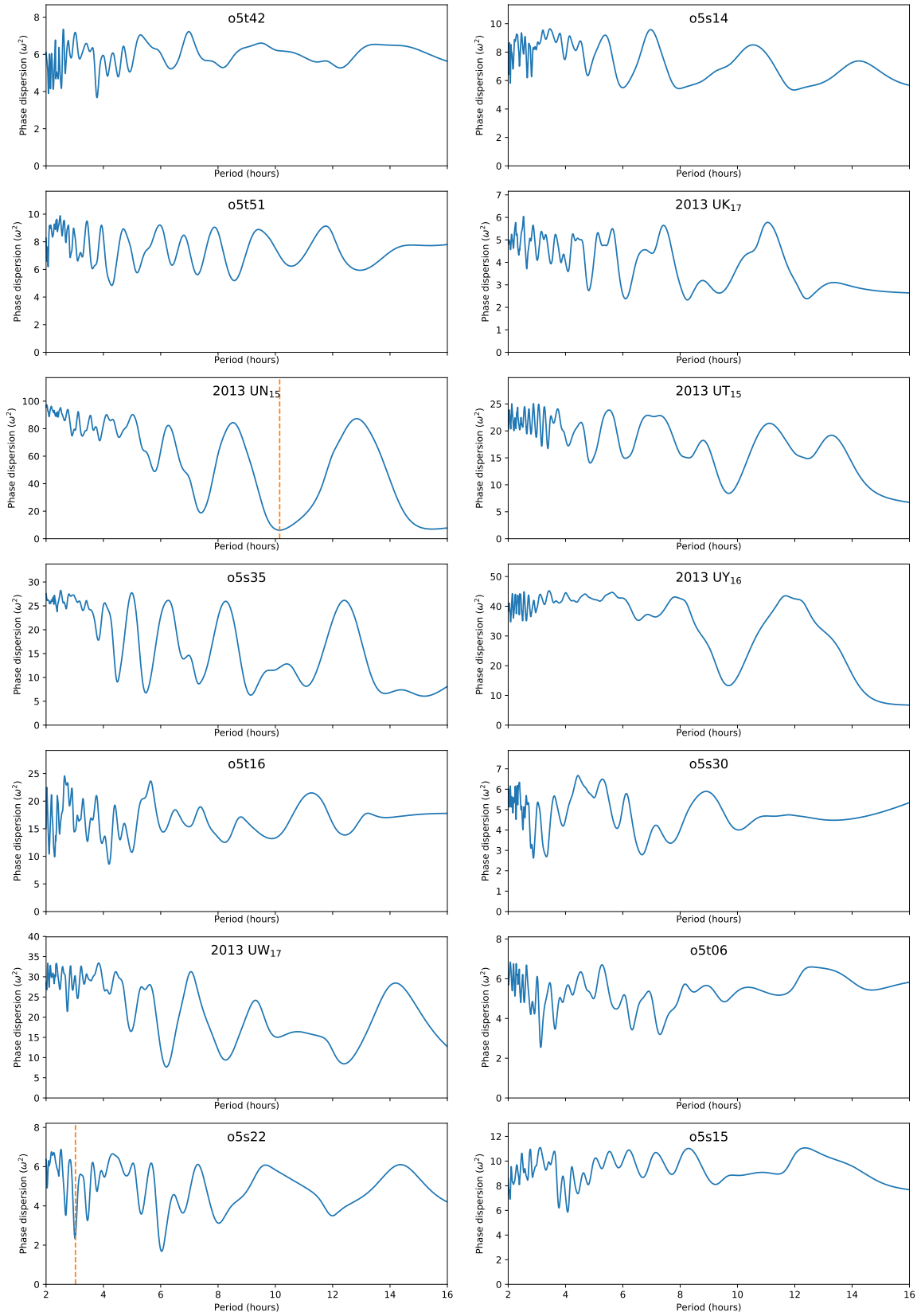


**Figure 11.** PDM plot from our period analysis. Vertical dashed orange lines show our favored single-peak period for the objects listed in Table 6 and shown in Figure 8. Objects 14–27, ordered by average magnitude.

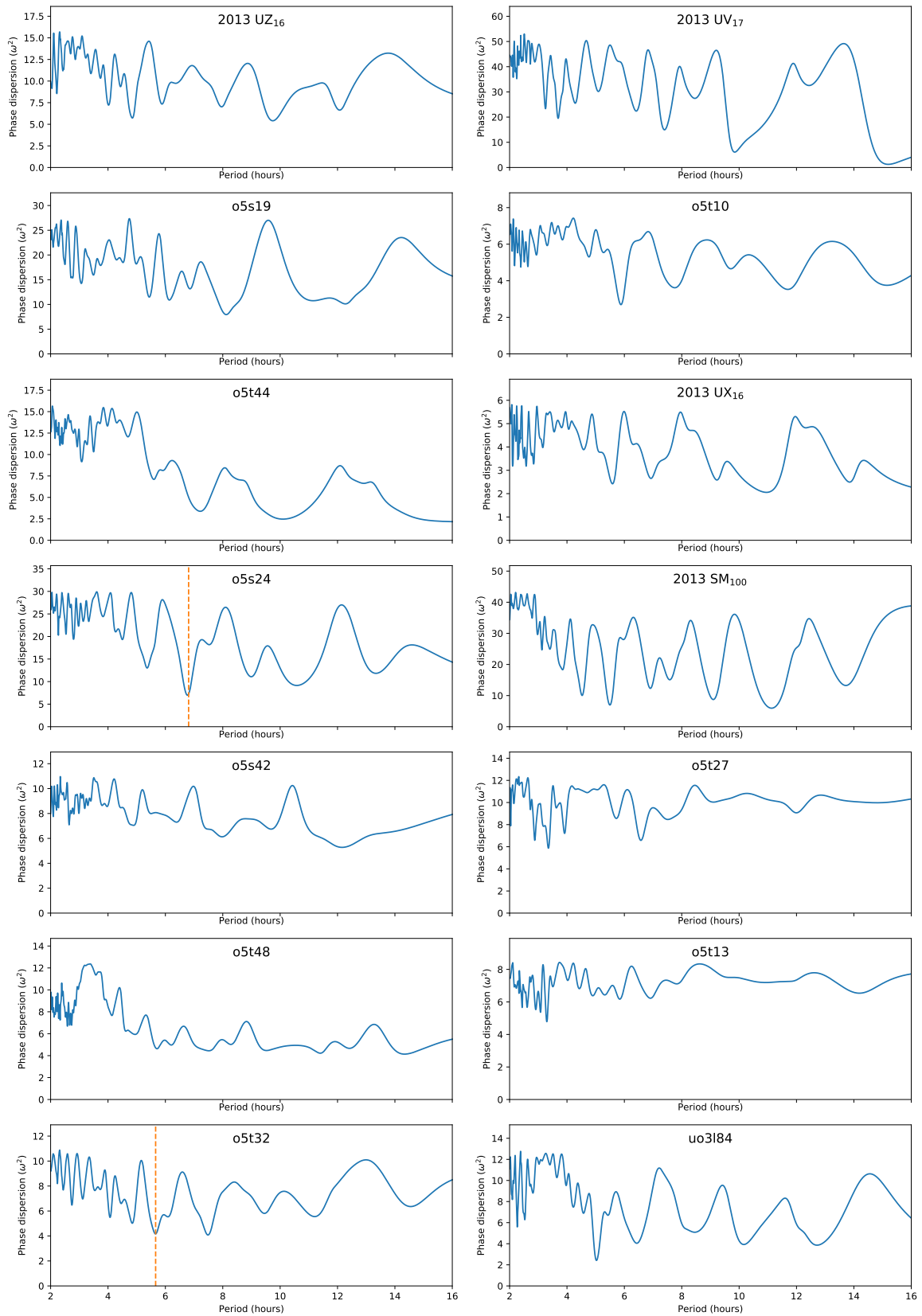


**Figure 12.** PDM plot from our period analysis. Vertical dashed orange lines show our favored single-peak period for the objects listed in Table 6 and shown in Figure 8. Objects 28–41, ordered by average magnitude.

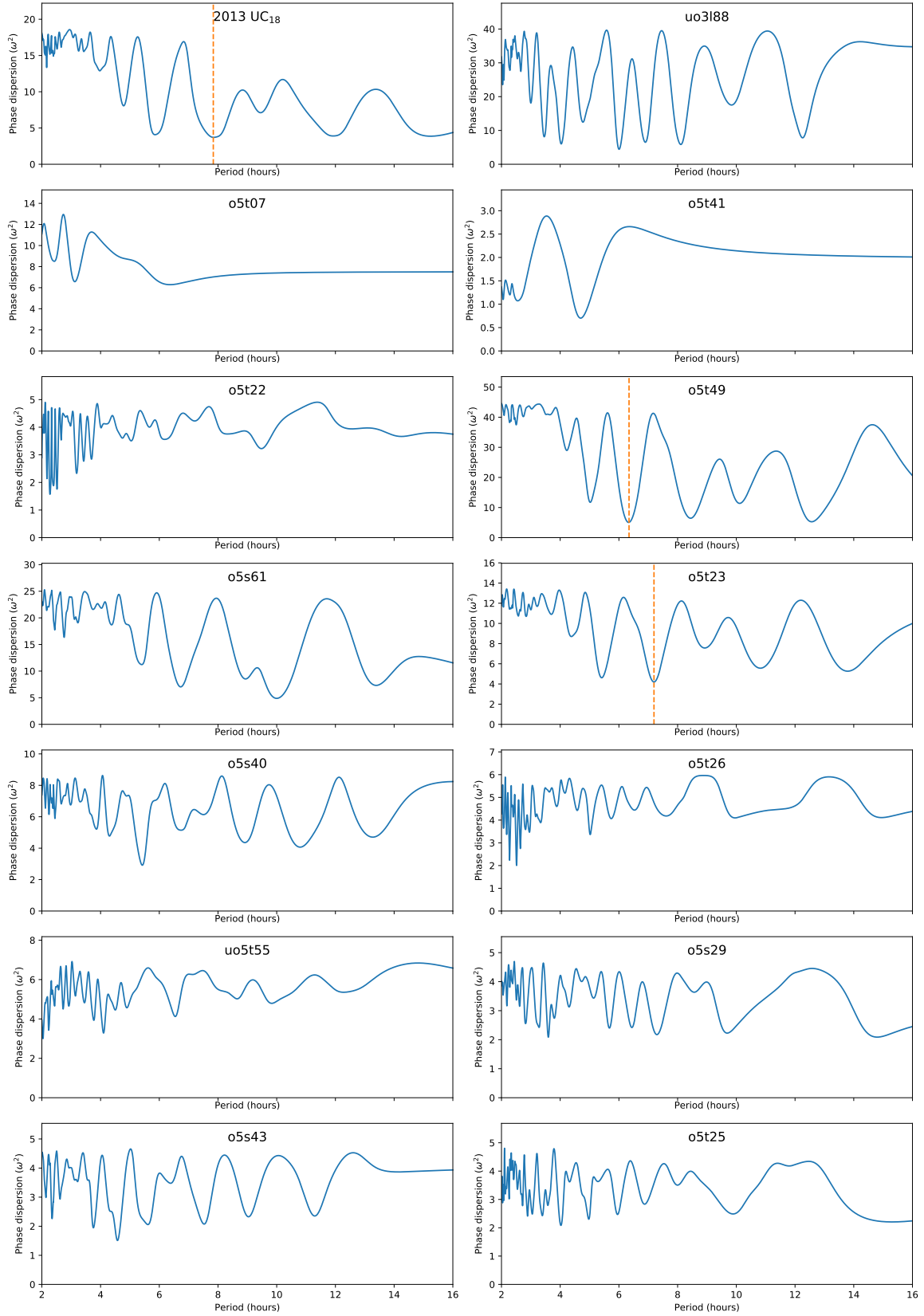


**Figure 13.** PDM plot from our period analysis. Vertical dashed orange lines show our favored single-peak period for the objects listed in Table 6 and shown in Figure 8. Objects 42–55, ordered by average magnitude.

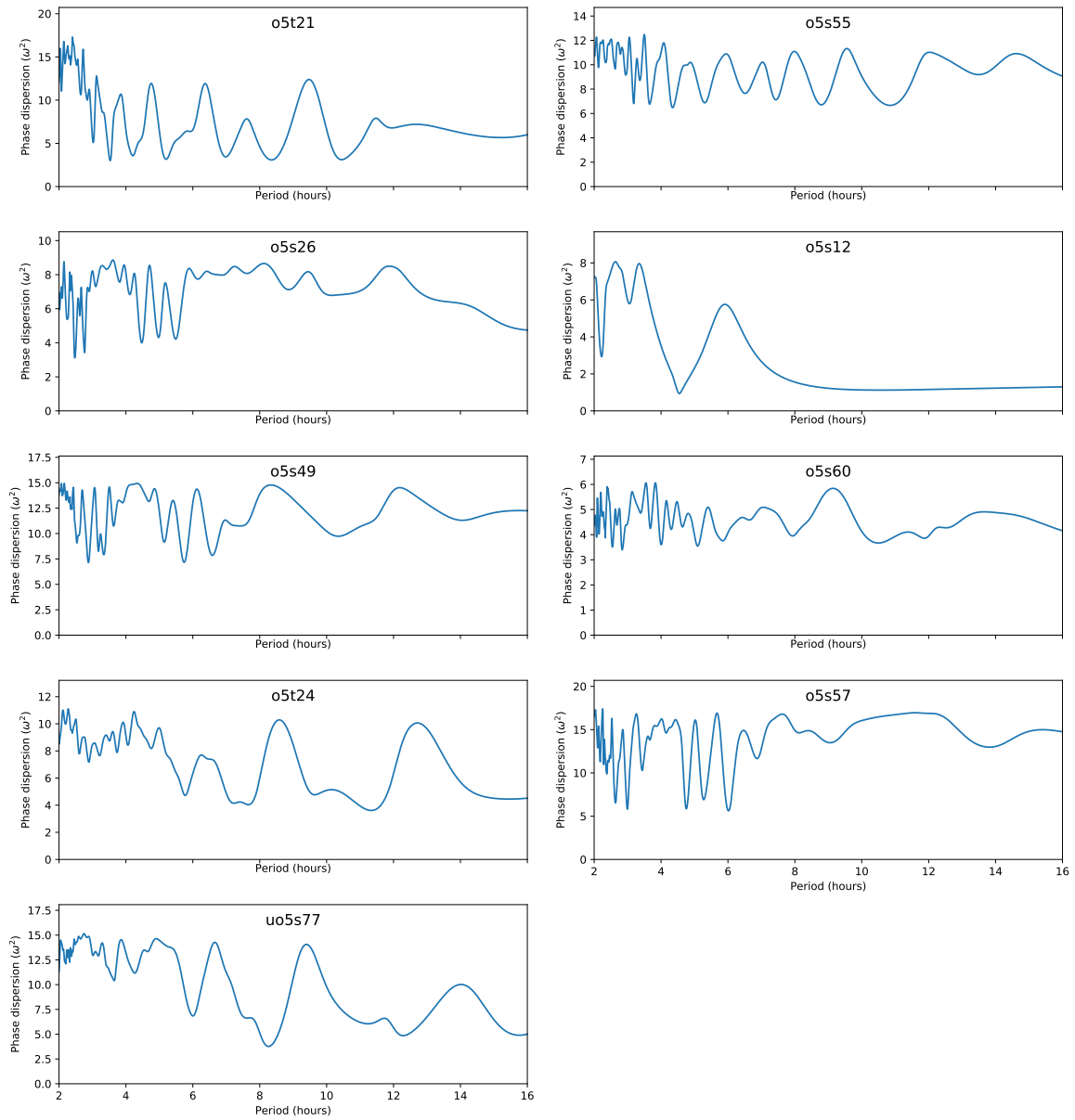


**Figure 14.** PDM plot from our period analysis. Objects 56–64, ordered by average magnitude.

**Table 7.** Photometry from HSC data.  $\sigma_{Rand}$  is the random uncertainty of the  $m_r$  magnitude measurement.  $Zp$  is the zero-point used.  $\sigma_{Sys}$  is the systematic uncertainty on the zero-point (and thus also on the measurement).

MJD-57620	$m_r \pm \sigma_{Rand}$	$Zp \pm \sigma_{Sys}$
o3119		
6.3913125	24.09 ± 0.03	26.995 ± 0.005
6.4154337	24.21 ± 0.02	27.012 ± 0.005
6.4393438	24.45 ± 0.02	27.022 ± 0.005
6.4634385	24.69 ± 0.04	27.058 ± 0.005
6.4876346	24.78 ± 0.03	27.047 ± 0.005
6.5123402	24.56 ± 0.03	27.039 ± 0.005
6.5375195	24.41 ± 0.03	27.043 ± 0.005
6.5628085	24.29 ± 0.03	27.045 ± 0.005
6.5875091	24.28 ± 0.02	27.038 ± 0.005
7.3876072	24.55 ± 0.03	26.978 ± 0.005
7.4114040	24.67 ± 0.03	27.002 ± 0.005
7.4353624	24.45 ± 0.02	26.885 ± 0.005
7.4595078	24.47 ± 0.02	26.869 ± 0.005
7.5081300	24.36 ± 0.03	26.497 ± 0.005
7.5584662	24.35 ± 0.02	27.019 ± 0.005
7.5830743	24.42 ± 0.02	27.004 ± 0.005
7.6079518	24.58 ± 0.02	26.994 ± 0.005
o3120		
6.3953584	24.07 ± 0.03	27.064 ± 0.005
6.4194196	23.90 ± 0.03	27.081 ± 0.005
6.5669337	24.13 ± 0.02	27.113 ± 0.005
6.5914968	24.31 ± 0.02	27.115 ± 0.005
6.6162295	24.34 ± 0.03	27.120 ± 0.005
7.3915762	24.38 ± 0.03	27.051 ± 0.005
7.4153740	24.38 ± 0.02	27.064 ± 0.005
7.4392927	24.32 ± 0.03	26.805 ± 0.005
7.4634533	24.41 ± 0.03	26.750 ± 0.005
7.5121937	24.57 ± 0.04	26.556 ± 0.005
7.5373777	24.57 ± 0.04	26.693 ± 0.005
7.5625508	24.52 ± 0.03	27.054 ± 0.005
7.5870985	24.43 ± 0.02	27.102 ± 0.005
7.6118595	24.36 ± 0.02	27.094 ± 0.005
o3143		
6.3913125	23.020 ± 0.013	26.968 ± 0.004
6.4154337	22.953 ± 0.009	26.986 ± 0.004
6.4393438	22.935 ± 0.008	27.001 ± 0.004
6.4634385	22.906 ± 0.012	27.028 ± 0.004
6.4876346	22.874 ± 0.009	27.022 ± 0.004
6.5123402	22.887 ± 0.010	27.015 ± 0.004
6.5375195	22.916 ± 0.010	27.023 ± 0.004
6.5628085	23.005 ± 0.009	27.015 ± 0.004
6.5875091	23.128 ± 0.010	27.019 ± 0.004
7.3876072	23.089 ± 0.010	26.956 ± 0.004
7.4114040	22.933 ± 0.008	26.968 ± 0.004
7.4353624	22.901 ± 0.010	26.858 ± 0.004

Table 7 continued on next page

**Table 7** (*continued*)

MJD=57620	$m_r \pm \sigma_{\text{Rand}}$	$Z_p \pm \sigma_{\text{Sys}}$
7.4595078	22.882 ± 0.009	26.848 ± 0.004
7.4835834	22.903 ± 0.011	26.542 ± 0.004
7.5081300	22.945 ± 0.013	26.485 ± 0.004
7.5584662	23.167 ± 0.010	26.986 ± 0.004
7.5830743	23.233 ± 0.009	26.980 ± 0.004
7.6079518	23.130 ± 0.010	26.977 ± 0.004
o3l44		
6.3953584	24.70 ± 0.05	26.975 ± 0.008
6.4194196	24.60 ± 0.03	26.997 ± 0.008
6.4433222	24.78 ± 0.04	27.019 ± 0.008
6.5416699	24.39 ± 0.04	27.027 ± 0.008
6.5669337	24.44 ± 0.02	27.025 ± 0.008
6.5914968	24.64 ± 0.03	27.031 ± 0.008
6.6162295	24.55 ± 0.03	27.037 ± 0.008
7.3915762	24.76 ± 0.03	26.960 ± 0.008
7.4153740	24.75 ± 0.04	26.972 ± 0.008
7.4392927	24.65 ± 0.03	26.717 ± 0.008
7.4634533	24.51 ± 0.03	26.658 ± 0.008
7.5121937	24.34 ± 0.03	26.472 ± 0.008
7.5373777	24.38 ± 0.04	26.604 ± 0.008
7.5625508	24.47 ± 0.02	26.961 ± 0.008
7.5870985	24.47 ± 0.02	27.020 ± 0.008
7.6118595	24.50 ± 0.03	27.017 ± 0.008
o3l46		
6.3953584	23.689 ± 0.023	27.004 ± 0.007
6.4194196	23.660 ± 0.014	27.017 ± 0.007
6.4433222	23.614 ± 0.017	27.048 ± 0.007
6.4674370	23.681 ± 0.020	27.077 ± 0.007
6.4916604	23.730 ± 0.018	27.055 ± 0.007
6.5163993	23.668 ± 0.013	27.055 ± 0.007
6.5416699	23.730 ± 0.021	27.060 ± 0.007
6.5669337	23.781 ± 0.015	27.055 ± 0.007
6.5914968	23.902 ± 0.021	27.059 ± 0.007
6.6162295	23.878 ± 0.020	27.079 ± 0.007
7.3915762	23.694 ± 0.016	26.986 ± 0.007
7.4153740	23.655 ± 0.015	26.995 ± 0.007
7.4392927	23.667 ± 0.018	26.745 ± 0.007
7.4634533	23.634 ± 0.019	26.701 ± 0.007
7.5121937	23.688 ± 0.019	26.498 ± 0.007
7.5373777	23.682 ± 0.021	26.613 ± 0.007
7.5625508	23.795 ± 0.014	26.981 ± 0.007
7.5870985	23.857 ± 0.018	27.036 ± 0.007
7.6118595	23.866 ± 0.017	27.035 ± 0.007
o3l55		
6.4154337	24.188 ± 0.024	27.047 ± 0.007
6.4393438	24.245 ± 0.018	27.060 ± 0.007
6.4634385	24.201 ± 0.025	27.085 ± 0.007
6.4876346	24.197 ± 0.023	27.075 ± 0.007
6.5123402	24.228 ± 0.025	27.078 ± 0.007
6.5375195	24.268 ± 0.020	27.086 ± 0.007
6.5628085	24.084 ± 0.018	27.075 ± 0.007
6.5875091	24.205 ± 0.022	27.075 ± 0.007
7.3876072	23.984 ± 0.015	27.015 ± 0.007
7.4114040	24.046 ± 0.018	27.040 ± 0.007
7.4353624	23.913 ± 0.014	26.920 ± 0.007

*Table 7 continued on next page*

Table 7 (continued)

MJD=57620	$m_r \pm \sigma_{Rand}$	$Z_p \pm \sigma_{Sys}$
7.4595078	23.997 ± 0.017	26.914 ± 0.007
7.4835834	23.976 ± 0.019	26.608 ± 0.007
7.5081300	23.910 ± 0.021	26.539 ± 0.007
7.5584662	23.993 ± 0.015	27.041 ± 0.007
7.5830743	24.028 ± 0.019	27.045 ± 0.007
7.6079518	23.995 ± 0.014	27.039 ± 0.007
o3l57		
6.3953584	23.332 ± 0.017	27.051 ± 0.009
6.4194196	23.366 ± 0.012	27.071 ± 0.009
6.4433222	23.313 ± 0.012	27.083 ± 0.009
6.4674370	23.261 ± 0.020	27.117 ± 0.009
6.4916604	23.332 ± 0.013	27.105 ± 0.009
6.5163993	23.316 ± 0.012	27.094 ± 0.009
6.5416699	23.300 ± 0.015	27.091 ± 0.009
6.5669337	23.294 ± 0.011	27.093 ± 0.009
6.5914968	23.262 ± 0.014	27.097 ± 0.009
6.6162295	23.285 ± 0.012	27.092 ± 0.009
7.3915762	23.246 ± 0.012	27.036 ± 0.009
7.4153740	23.255 ± 0.012	27.049 ± 0.009
7.4392927	23.305 ± 0.015	26.796 ± 0.009
7.4634533	23.313 ± 0.013	26.723 ± 0.009
7.5121937	23.299 ± 0.017	26.540 ± 0.009
7.5373777	23.271 ± 0.014	26.664 ± 0.009
o3l62		
6.3913125	24.24 ± 0.04	27.04 ± 0.02
6.4154337	24.36 ± 0.03	27.06 ± 0.02
6.4393438	24.36 ± 0.03	27.06 ± 0.02
7.3876072	24.47 ± 0.02	27.02 ± 0.02
7.4114040	24.47 ± 0.02	27.03 ± 0.02
7.4353624	24.47 ± 0.02	26.92 ± 0.02
7.4595078	24.44 ± 0.03	26.91 ± 0.02
7.4835834	24.43 ± 0.03	26.61 ± 0.02
7.5081300	24.50 ± 0.04	26.53 ± 0.02
7.5584662	24.43 ± 0.03	27.05 ± 0.02
7.5830743	24.35 ± 0.03	27.05 ± 0.02
7.6079518	24.47 ± 0.03	27.04 ± 0.02
o3l63		
6.3953584	23.878 ± 0.024	27.056 ± 0.008
6.4194196	24.044 ± 0.018	27.069 ± 0.008
6.4433222	24.071 ± 0.020	27.088 ± 0.008
6.4674370	24.061 ± 0.031	27.121 ± 0.008
6.4916604	24.195 ± 0.023	27.111 ± 0.008
6.5163993	24.163 ± 0.020	27.098 ± 0.008
6.5416699	24.253 ± 0.027	27.095 ± 0.008
6.5669337	24.140 ± 0.017	27.097 ± 0.008
6.5914968	24.076 ± 0.024	27.100 ± 0.008
6.6162295	23.919 ± 0.017	27.090 ± 0.008
7.3915762	24.136 ± 0.022	27.043 ± 0.008
7.4153740	23.978 ± 0.020	27.054 ± 0.008
7.4392927	24.020 ± 0.023	26.801 ± 0.008
7.4634533	23.930 ± 0.019	26.728 ± 0.008
7.5121937	23.852 ± 0.023	26.545 ± 0.008
7.5373777	23.846 ± 0.023	26.672 ± 0.008
7.5625508	23.762 ± 0.015	27.039 ± 0.008
7.5870985	23.716 ± 0.013	27.077 ± 0.008

Table 7 continued on next page

**Table 7** (*continued*)

MJD=57620	$m_r \pm \sigma_{Rand}$	$Zp \pm \sigma_{Sys}$
7.6118595	23.690 ± 0.012	27.068 ± 0.008
	o3l64	
6.4154337	23.665 ± 0.019	27.044 ± 0.007
6.4393438	23.695 ± 0.014	27.045 ± 0.007
6.4634385	23.714 ± 0.021	27.081 ± 0.007
6.4876346	23.724 ± 0.016	27.071 ± 0.007
6.5123402	23.764 ± 0.016	27.067 ± 0.007
6.5375195	23.733 ± 0.020	27.071 ± 0.007
6.5628085	23.749 ± 0.015	27.063 ± 0.007
6.5875091	23.690 ± 0.015	27.065 ± 0.007
7.3876072	23.762 ± 0.014	27.005 ± 0.007
7.4114040	23.756 ± 0.013	27.029 ± 0.007
7.4353624	23.696 ± 0.014	26.906 ± 0.007
7.4595078	23.764 ± 0.016	26.897 ± 0.007
7.4835834	23.762 ± 0.017	26.594 ± 0.007
7.5081300	23.770 ± 0.019	26.524 ± 0.007
7.5584662	23.668 ± 0.014	27.035 ± 0.007
7.5830743	23.762 ± 0.017	27.029 ± 0.007
7.6079518	23.720 ± 0.014	27.024 ± 0.007
	o3l65	
6.3913125	24.43 ± 0.04	27.109 ± 0.008
6.4154337	24.46 ± 0.03	27.128 ± 0.008
6.4393438	24.31 ± 0.02	27.133 ± 0.008
6.4634385	24.36 ± 0.04	27.166 ± 0.008
6.4876346	24.23 ± 0.03	27.167 ± 0.008
6.5123402	24.29 ± 0.02	27.157 ± 0.008
6.5375195	24.14 ± 0.02	27.161 ± 0.008
6.5628085	24.11 ± 0.02	27.157 ± 0.008
6.5875091	24.26 ± 0.02	27.155 ± 0.008
7.3876072	24.19 ± 0.02	27.092 ± 0.008
7.4114040	24.24 ± 0.02	27.119 ± 0.008
7.4353624	24.35 ± 0.02	27.002 ± 0.008
7.4595078	24.32 ± 0.02	26.987 ± 0.008
7.4835834	24.22 ± 0.03	26.704 ± 0.008
7.5081300	24.23 ± 0.03	26.613 ± 0.008
7.5584662	24.15 ± 0.02	27.119 ± 0.008
7.5830743	24.29 ± 0.02	27.121 ± 0.008
7.6079518	24.30 ± 0.02	27.118 ± 0.008
	o3l71	
6.3953584	24.03 ± 0.03	27.055 ± 0.008
6.4194196	24.06 ± 0.02	27.074 ± 0.008
6.4433222	24.17 ± 0.02	27.090 ± 0.008
6.4674370	24.05 ± 0.03	27.119 ± 0.008
6.4916604	24.07 ± 0.02	27.107 ± 0.008
6.5163993	24.29 ± 0.02	27.099 ± 0.008
6.5416699	24.14 ± 0.03	27.096 ± 0.008
6.5669337	24.32 ± 0.02	27.096 ± 0.008
6.5914968	24.41 ± 0.03	27.099 ± 0.008
6.6162295	24.15 ± 0.02	27.105 ± 0.008
7.3915762	24.16 ± 0.02	27.039 ± 0.008
7.4153740	24.14 ± 0.02	27.053 ± 0.008
7.4392927	24.08 ± 0.02	26.796 ± 0.008
7.4634533	24.03 ± 0.02	26.727 ± 0.008
7.5121937	24.10 ± 0.03	26.544 ± 0.008
7.5373777	24.13 ± 0.03	26.672 ± 0.008

*Table 7 continued on next page*

Table 7 (continued)

MJD=57620	$m_r \pm \sigma_{Rand}$	$Z_p \pm \sigma_{Sys}$
7.5625508	24.28 ± 0.02	27.037 ± 0.008
7.5870985	24.34 ± 0.02	27.076 ± 0.008
7.6118595	24.43 ± 0.02	27.067 ± 0.008
o3182		
6.4876346	23.98 ± 0.02	27.138 ± 0.005
6.5123402	23.99 ± 0.02	27.137 ± 0.005
6.5375195	23.96 ± 0.03	27.127 ± 0.005
6.5628085	23.94 ± 0.02	27.124 ± 0.005
6.5875091	23.99 ± 0.02	27.132 ± 0.005
7.3876072	23.93 ± 0.02	27.056 ± 0.005
7.4114040	23.90 ± 0.02	27.094 ± 0.005
7.4353624	23.86 ± 0.02	26.963 ± 0.005
7.4595078	23.93 ± 0.02	26.964 ± 0.005
7.4835834	23.88 ± 0.02	26.658 ± 0.005
7.5081300	23.98 ± 0.02	26.614 ± 0.005
7.5584662	23.91 ± 0.02	27.110 ± 0.005
7.6079518	23.93 ± 0.02	27.080 ± 0.005
o3183		
6.3913125	24.04 ± 0.03	27.140 ± 0.008
6.4154337	23.95 ± 0.02	27.152 ± 0.008
6.4393438	24.16 ± 0.02	27.165 ± 0.008
6.4634385	24.04 ± 0.03	27.188 ± 0.008
6.4876346	24.14 ± 0.02	27.183 ± 0.008
6.5123402	24.17 ± 0.02	27.182 ± 0.008
6.5375195	24.10 ± 0.03	27.181 ± 0.008
6.5628085	24.02 ± 0.02	27.180 ± 0.008
6.5875091	23.98 ± 0.02	27.171 ± 0.008
7.3876072	23.90 ± 0.02	27.122 ± 0.008
7.4114040	23.86 ± 0.02	27.143 ± 0.008
7.4353624	23.97 ± 0.02	27.032 ± 0.008
7.4595078	23.91 ± 0.02	27.013 ± 0.008
7.4835834	24.03 ± 0.02	26.729 ± 0.008
7.5081300	23.96 ± 0.02	26.632 ± 0.008
7.5584662	24.02 ± 0.02	27.149 ± 0.008
7.5830743	23.86 ± 0.02	27.135 ± 0.008
7.6079518	23.90 ± 0.02	27.138 ± 0.008
o5s05		
6.3707916	23.613 ± 0.028	27.102 ± 0.006
6.4352162	23.651 ± 0.018	27.146 ± 0.006
6.4592812	23.633 ± 0.021	27.168 ± 0.006
6.4836121	23.693 ± 0.022	27.168 ± 0.006
6.5081487	23.635 ± 0.016	27.141 ± 0.006
6.5331158	23.642 ± 0.018	27.145 ± 0.006
6.5584302	23.623 ± 0.013	27.122 ± 0.006
6.6074840	23.636 ± 0.016	27.143 ± 0.006
6.6324802	23.650 ± 0.028	27.127 ± 0.006
7.3671196	23.630 ± 0.016	27.095 ± 0.006
7.3828990	23.657 ± 0.014	27.097 ± 0.006
7.4312212	23.611 ± 0.014	26.964 ± 0.006
7.4553161	23.633 ± 0.014	26.904 ± 0.006
7.4795908	23.661 ± 0.014	26.975 ± 0.006
7.5540967	23.654 ± 0.012	27.100 ± 0.006
7.5788737	23.651 ± 0.016	27.126 ± 0.006
7.6030791	23.629 ± 0.013	27.120 ± 0.006
7.6279949	23.625 ± 0.015	27.100 ± 0.006

Table 7 continued on next page

**Table 7** (*continued*)

MJD=57620	$m_r \pm \sigma_{Rand}$	$Z_p \pm \sigma_{Sys}$
o5s07		
6.3629552	23.618 ± 0.028	27.085 ± 0.007
6.3787089	23.603 ± 0.014	27.090 ± 0.007
6.4035606	23.588 ± 0.013	27.106 ± 0.007
6.4274177	23.597 ± 0.017	27.124 ± 0.007
6.4514017	23.616 ± 0.016	27.137 ± 0.007
6.4756753	23.664 ± 0.020	27.147 ± 0.007
6.5002049	23.644 ± 0.015	27.139 ± 0.007
6.5253136	23.577 ± 0.017	27.107 ± 0.007
6.5506281	23.561 ± 0.015	27.130 ± 0.007
6.5754235	23.611 ± 0.013	27.123 ± 0.007
6.5996149	23.667 ± 0.015	27.119 ± 0.007
6.6246785	23.735 ± 0.017	27.118 ± 0.007
7.3592398	23.517 ± 0.014	27.066 ± 0.007
7.3750037	23.564 ± 0.016	27.077 ± 0.007
7.3995302	23.622 ± 0.013	27.085 ± 0.007
7.4233746	23.607 ± 0.014	27.051 ± 0.007
7.4473473	23.636 ± 0.014	26.861 ± 0.007
7.4716900	23.592 ± 0.013	26.615 ± 0.007
7.5463287	23.668 ± 0.016	27.021 ± 0.007
7.5710852	23.624 ± 0.013	27.097 ± 0.007
7.5952966	23.649 ± 0.014	27.102 ± 0.007
7.6201860	23.562 ± 0.014	27.100 ± 0.007
o5s12		
7.3671196	24.98 ± 0.03	27.005 ± 0.015
7.4073685	25.15 ± 0.04	27.020 ± 0.015
7.4312212	25.13 ± 0.04	26.870 ± 0.015
7.4553161	25.22 ± 0.04	26.810 ± 0.015
7.4795908	25.02 ± 0.04	26.875 ± 0.015
7.5540967	24.94 ± 0.03	27.015 ± 0.015
7.6030791	25.18 ± 0.04	27.043 ± 0.015
7.6279949	25.33 ± 0.07	27.033 ± 0.015
o5s14		
6.3590364	23.878 ± 0.032	27.057 ± 0.005
6.3747757	23.996 ± 0.021	27.064 ± 0.005
6.3994429	23.886 ± 0.021	27.079 ± 0.005
6.4234893	23.963 ± 0.015	27.090 ± 0.005
6.4474580	23.962 ± 0.017	27.098 ± 0.005
6.4716710	23.871 ± 0.029	27.117 ± 0.005
6.4961375	23.936 ± 0.018	27.097 ± 0.005
6.5212088	23.798 ± 0.019	27.120 ± 0.005
6.5465833	23.927 ± 0.017	27.097 ± 0.005
6.5714735	23.806 ± 0.015	27.002 ± 0.005
6.5957299	23.864 ± 0.015	27.085 ± 0.005
6.6207267	23.920 ± 0.017	27.083 ± 0.005
7.3552420	23.901 ± 0.016	27.036 ± 0.005
7.3711027	23.928 ± 0.015	27.053 ± 0.005
7.3956323	23.929 ± 0.017	27.056 ± 0.005
7.4194678	23.922 ± 0.014	27.065 ± 0.005
7.4434311	24.007 ± 0.017	26.843 ± 0.005
7.4676871	23.936 ± 0.017	26.731 ± 0.005
7.5423084	23.939 ± 0.024	26.881 ± 0.005
7.5671285	23.857 ± 0.014	27.065 ± 0.005
7.5913265	23.901 ± 0.014	27.060 ± 0.005
7.6163059	23.919 ± 0.019	27.069 ± 0.005

*Table 7 continued on next page*

Table 7 (continued)

MJD=57620	$m_r \pm \sigma_{Rand}$	$Zp \pm \sigma_{Sys}$
o5s15		
6.3590364	24.25 ± 0.05	27.029 ± 0.005
6.3747757	24.12 ± 0.03	27.041 ± 0.005
6.3994429	24.07 ± 0.02	27.061 ± 0.005
6.4234893	24.34 ± 0.03	27.066 ± 0.005
6.4474580	24.32 ± 0.03	27.077 ± 0.005
6.4716710	24.08 ± 0.03	27.105 ± 0.005
6.4961375	24.17 ± 0.02	27.085 ± 0.005
6.5212088	24.23 ± 0.03	27.087 ± 0.005
6.5465833	24.26 ± 0.02	27.085 ± 0.005
6.5714735	24.17 ± 0.02	26.996 ± 0.005
6.5957299	24.32 ± 0.02	27.078 ± 0.005
6.6207267	24.25 ± 0.03	27.076 ± 0.005
7.3552420	24.20 ± 0.03	27.011 ± 0.005
7.3711027	24.32 ± 0.03	27.027 ± 0.005
7.3956323	24.30 ± 0.02	27.036 ± 0.005
7.4194678	24.31 ± 0.02	27.043 ± 0.005
7.4434311	24.32 ± 0.02	26.829 ± 0.005
7.4676871	24.25 ± 0.03	26.725 ± 0.005
7.5423084	24.36 ± 0.03	26.843 ± 0.005
7.5671285	24.24 ± 0.02	27.060 ± 0.005
7.5913265	24.25 ± 0.02	27.055 ± 0.005
7.6163059	24.29 ± 0.03	27.053 ± 0.005
o5s19		
6.3865586	24.44 ± 0.03	27.022 ± 0.006
6.4114120	24.54 ± 0.02	27.034 ± 0.006
6.4352162	24.40 ± 0.02	27.050 ± 0.006
6.4592812	24.47 ± 0.03	27.069 ± 0.006
6.4836121	24.39 ± 0.04	27.077 ± 0.006
6.5081487	24.36 ± 0.02	27.053 ± 0.006
6.5331158	24.38 ± 0.02	27.053 ± 0.006
6.5584302	24.23 ± 0.02	27.040 ± 0.006
6.5833062	24.22 ± 0.02	27.052 ± 0.006
7.3671196	24.39 ± 0.02	26.997 ± 0.006
7.4073685	24.45 ± 0.02	27.012 ± 0.006
7.4312212	24.36 ± 0.02	26.864 ± 0.006
7.4553161	24.32 ± 0.02	26.805 ± 0.006
7.4795908	24.29 ± 0.02	26.870 ± 0.006
7.5540967	24.48 ± 0.02	27.017 ± 0.006
7.5788737	24.36 ± 0.02	27.044 ± 0.006
7.6030791	24.16 ± 0.02	27.033 ± 0.006
7.6279949	24.18 ± 0.03	27.025 ± 0.006
o5s21		
6.3707916	23.142 ± 0.021	27.037 ± 0.004
6.3865586	23.183 ± 0.013	27.044 ± 0.004
6.4114120	23.227 ± 0.011	27.066 ± 0.004
6.4836121	23.459 ± 0.017	27.105 ± 0.004
6.5081487	23.381 ± 0.013	27.090 ± 0.004
6.5331158	23.303 ± 0.013	27.086 ± 0.004
6.5584302	23.191 ± 0.009	27.060 ± 0.004
6.5833062	23.157 ± 0.011	27.085 ± 0.004
6.6074840	23.105 ± 0.013	27.086 ± 0.004
6.6324802	23.135 ± 0.018	27.077 ± 0.004
7.3671196	23.126 ± 0.012	27.022 ± 0.004
7.3828990	23.124 ± 0.009	27.027 ± 0.004

Table 7 continued on next page

**Table 7** (*continued*)

MJD=57620	$m_r \pm \sigma_{Rand}$	$Z_p \pm \sigma_{Sys}$
7.4073685	23.179 ± 0.011	27.046 ± 0.004
7.4312212	23.238 ± 0.012	26.895 ± 0.004
7.4553161	23.331 ± 0.014	26.837 ± 0.004
7.4795908	23.442 ± 0.011	26.912 ± 0.004
7.5540967	23.269 ± 0.011	27.042 ± 0.004
7.5788737	23.233 ± 0.011	27.070 ± 0.004
7.6030791	23.130 ± 0.012	27.064 ± 0.004
7.6279949	23.138 ± 0.014	27.062 ± 0.004
o5s22		
6.3707916	24.19 ± 0.04	27.168 ± 0.004
6.3865586	24.17 ± 0.02	27.180 ± 0.004
6.4114120	24.11 ± 0.02	27.201 ± 0.004
6.4352162	24.19 ± 0.02	27.205 ± 0.004
6.4592812	24.18 ± 0.03	27.217 ± 0.004
6.4836121	24.22 ± 0.03	27.224 ± 0.004
6.5081487	24.27 ± 0.02	27.213 ± 0.004
6.5331158	24.16 ± 0.02	27.213 ± 0.004
6.5584302	24.23 ± 0.02	27.195 ± 0.004
6.5833062	24.27 ± 0.02	27.199 ± 0.004
6.6074840	24.25 ± 0.03	27.203 ± 0.004
6.6324802	24.14 ± 0.04	27.194 ± 0.004
7.3671196	24.27 ± 0.02	27.164 ± 0.004
7.3828990	24.18 ± 0.02	27.163 ± 0.004
7.4073685	24.11 ± 0.02	27.177 ± 0.004
7.4312212	24.14 ± 0.02	27.036 ± 0.004
7.4553161	24.26 ± 0.02	26.966 ± 0.004
7.4795908	24.22 ± 0.02	27.035 ± 0.004
7.5540967	24.18 ± 0.02	27.168 ± 0.004
7.5788737	24.28 ± 0.03	27.179 ± 0.004
7.6030791	24.27 ± 0.02	27.186 ± 0.004
7.6279949	24.27 ± 0.03	27.167 ± 0.004
o5s24		
6.3707916	24.23 ± 0.05	27.042 ± 0.008
6.3865586	24.09 ± 0.03	27.061 ± 0.008
6.4114120	24.24 ± 0.03	27.078 ± 0.008
6.4352162	24.31 ± 0.02	27.084 ± 0.008
6.5081487	24.42 ± 0.03	27.088 ± 0.008
6.5331158	24.53 ± 0.03	27.087 ± 0.008
6.5584302	24.66 ± 0.04	27.071 ± 0.008
6.5833062	24.60 ± 0.04	27.087 ± 0.008
6.6074840	24.49 ± 0.03	27.084 ± 0.008
6.6324802	24.37 ± 0.06	27.072 ± 0.008
7.3671196	24.34 ± 0.04	27.028 ± 0.008
7.3828990	24.55 ± 0.03	27.036 ± 0.008
7.4073685	24.63 ± 0.03	27.054 ± 0.008
7.4312212	24.49 ± 0.03	26.898 ± 0.008
7.4553161	24.51 ± 0.03	26.837 ± 0.008
7.4795908	24.43 ± 0.02	26.911 ± 0.008
7.5540967	24.31 ± 0.02	27.048 ± 0.008
7.5788737	24.60 ± 0.03	27.074 ± 0.008
7.6030791	24.49 ± 0.02	27.059 ± 0.008
o5s26		
6.3668707	25.20 ± 0.11	27.148 ± 0.008
6.3826668	25.18 ± 0.07	27.149 ± 0.008
6.4075038	25.32 ± 0.05	27.160 ± 0.008

*Table 7 continued on next page*

Table 7 (continued)

MJD=57620	$m_r \pm \sigma_{Rand}$	$Z_p \pm \sigma_{Sys}$
6.4796213	25.08 ± 0.07	27.198 ± 0.008
6.5041451	25.27 ± 0.06	27.191 ± 0.008
6.5291947	25.15 ± 0.06	27.150 ± 0.008
6.5545235	25.02 ± 0.05	27.164 ± 0.008
6.5793264	25.35 ± 0.06	27.163 ± 0.008
6.6035457	25.24 ± 0.05	27.162 ± 0.008
6.6285747	25.20 ± 0.08	27.166 ± 0.008
7.3631959	24.91 ± 0.04	27.112 ± 0.008
7.3789568	25.07 ± 0.05	27.121 ± 0.008
7.4034703	25.00 ± 0.03	27.143 ± 0.008
7.4272957	25.07 ± 0.06	26.945 ± 0.008
7.4513626	25.11 ± 0.06	26.770 ± 0.008
7.4756250	24.85 ± 0.04	26.764 ± 0.008
7.5502231	25.29 ± 0.08	27.145 ± 0.008
7.5750150	24.90 ± 0.04	27.153 ± 0.008
7.5992025	25.00 ± 0.04	27.144 ± 0.008
7.6240933	25.01 ± 0.05	27.133 ± 0.008
o5s29		
6.3590364	25.05 ± 0.09	27.016 ± 0.006
6.3747757	25.02 ± 0.07	27.023 ± 0.006
6.3994429	25.15 ± 0.04	27.035 ± 0.006
6.4234893	24.93 ± 0.03	27.047 ± 0.006
6.4474580	24.94 ± 0.04	27.061 ± 0.006
6.5212088	24.88 ± 0.06	27.068 ± 0.006
6.5465833	24.98 ± 0.04	27.059 ± 0.006
6.5714735	24.93 ± 0.04	26.969 ± 0.006
6.5957299	24.91 ± 0.04	27.046 ± 0.006
6.6207267	25.09 ± 0.05	27.038 ± 0.006
7.3552420	25.04 ± 0.04	27.003 ± 0.006
7.4194678	24.98 ± 0.04	27.030 ± 0.006
7.4434311	25.12 ± 0.04	26.810 ± 0.006
7.4676871	24.98 ± 0.04	26.690 ± 0.006
7.5423084	25.13 ± 0.07	26.827 ± 0.006
7.5671285	25.13 ± 0.04	27.027 ± 0.006
7.5913265	25.15 ± 0.04	27.029 ± 0.006
7.6163059	25.01 ± 0.04	27.020 ± 0.006
o5s30		
6.5465833	24.13 ± 0.03	27.176 ± 0.004
6.5714735	24.14 ± 0.02	27.080 ± 0.004
6.5957299	24.19 ± 0.02	27.156 ± 0.004
6.6207267	24.21 ± 0.02	27.152 ± 0.004
7.3552420	24.14 ± 0.02	27.113 ± 0.004
7.3711027	24.04 ± 0.02	27.124 ± 0.004
7.3956323	24.15 ± 0.02	27.132 ± 0.004
7.4194678	24.13 ± 0.02	27.143 ± 0.004
7.4434311	24.30 ± 0.03	26.929 ± 0.004
7.4676871	24.16 ± 0.02	26.797 ± 0.004
7.5423084	24.14 ± 0.03	26.950 ± 0.004
7.5671285	24.22 ± 0.02	27.147 ± 0.004
7.5913265	24.20 ± 0.02	27.133 ± 0.004
7.6163059	24.17 ± 0.02	27.141 ± 0.004
o5s35		
6.3668707	23.94 ± 0.03	27.001 ± 0.007
6.3826668	24.00 ± 0.02	27.004 ± 0.007
6.4075038	23.91 ± 0.02	27.020 ± 0.007

Table 7 continued on next page

Table 7 (continued)

MJD=57620	$m_r \pm \sigma_{Rand}$	$Z_p \pm \sigma_{Sys}$
6.4313154	23.98 ± 0.02	27.032 ± 0.007
6.4553362	24.03 ± 0.02	27.051 ± 0.007
6.4796213	23.95 ± 0.02	27.051 ± 0.007
6.5041451	24.09 ± 0.02	27.060 ± 0.007
6.5291947	24.19 ± 0.02	27.034 ± 0.007
6.5545235	24.12 ± 0.02	27.028 ± 0.007
6.5793264	24.02 ± 0.02	27.040 ± 0.007
7.3631959	23.98 ± 0.02	26.991 ± 0.007
7.3789568	24.01 ± 0.02	26.989 ± 0.007
7.4034703	24.11 ± 0.02	27.006 ± 0.007
7.4272957	24.20 ± 0.02	26.818 ± 0.007
7.4513626	24.27 ± 0.02	26.619 ± 0.007
7.4756250	24.25 ± 0.02	26.637 ± 0.007
7.5992025	24.03 ± 0.02	27.041 ± 0.007
7.6240933	24.10 ± 0.02	27.020 ± 0.007
o5s36		
6.3668707	23.694 ± 0.026	27.091 ± 0.004
6.3826668	23.651 ± 0.017	27.107 ± 0.004
6.4075038	23.657 ± 0.012	27.119 ± 0.004
6.4313154	23.623 ± 0.014	27.129 ± 0.004
6.4553362	23.648 ± 0.015	27.139 ± 0.004
6.4796213	23.497 ± 0.016	27.151 ± 0.004
6.5041451	23.506 ± 0.015	27.148 ± 0.004
6.5291947	23.519 ± 0.014	27.119 ± 0.004
6.5545235	23.503 ± 0.012	27.125 ± 0.004
6.5793264	23.487 ± 0.012	27.136 ± 0.004
6.6035457	23.431 ± 0.012	27.130 ± 0.004
6.6285747	23.445 ± 0.015	27.132 ± 0.004
7.3631959	23.771 ± 0.018	27.078 ± 0.004
7.3789568	23.849 ± 0.016	27.086 ± 0.004
7.4034703	23.803 ± 0.016	27.098 ± 0.004
7.4272957	23.842 ± 0.022	26.914 ± 0.004
7.4513626	23.799 ± 0.017	26.731 ± 0.004
7.4756250	23.715 ± 0.016	26.737 ± 0.004
7.5502231	23.748 ± 0.017	27.092 ± 0.004
7.5750150	23.651 ± 0.015	27.123 ± 0.004
7.5992025	23.600 ± 0.011	27.110 ± 0.004
7.6240933	23.592 ± 0.015	27.108 ± 0.004
o5s40		
6.4313154	25.12 ± 0.04	27.052 ± 0.008
6.4553362	25.02 ± 0.04	27.066 ± 0.008
6.4796213	25.05 ± 0.06	27.072 ± 0.008
6.5041451	24.85 ± 0.04	27.064 ± 0.008
6.5291947	24.98 ± 0.05	27.022 ± 0.008
6.5545235	24.91 ± 0.04	27.050 ± 0.008
6.5793264	24.92 ± 0.03	27.058 ± 0.008
6.6035457	24.97 ± 0.03	27.059 ± 0.008
6.6285747	25.09 ± 0.06	27.053 ± 0.008
7.3631959	25.11 ± 0.04	27.003 ± 0.008
7.3789568	24.80 ± 0.03	27.008 ± 0.008
7.4034703	24.94 ± 0.03	27.027 ± 0.008
7.4272957	24.94 ± 0.04	26.841 ± 0.008
7.4513626	24.86 ± 0.04	26.648 ± 0.008
7.4756250	24.82 ± 0.04	26.651 ± 0.008
7.5502231	25.15 ± 0.05	27.013 ± 0.008

Table 7 continued on next page

**Table 7** (*continued*)

MJD=57620	$m_r \pm \sigma_{Rand}$	$Zp \pm \sigma_{Sys}$
7.5750150	25.08 ± 0.04	27.044 ± 0.008
7.5992025	24.96 ± 0.03	27.038 ± 0.008
7.6240933	24.78 ± 0.04	27.036 ± 0.008
o5s42		
6.3707916	24.42 ± 0.04	27.008 ± 0.007
6.3865586	24.47 ± 0.03	27.015 ± 0.007
6.4114120	24.56 ± 0.02	27.036 ± 0.007
6.4352162	24.36 ± 0.02	27.046 ± 0.007
6.4592812	24.59 ± 0.03	27.059 ± 0.007
6.4836121	24.32 ± 0.03	27.061 ± 0.007
6.5081487	24.42 ± 0.02	27.053 ± 0.007
6.5331158	24.42 ± 0.02	27.049 ± 0.007
6.5584302	24.39 ± 0.02	27.034 ± 0.007
6.5833062	24.51 ± 0.02	27.041 ± 0.007
6.6074840	24.69 ± 0.04	27.046 ± 0.007
6.6324802	24.66 ± 0.05	27.031 ± 0.007
7.3671196	24.46 ± 0.03	26.999 ± 0.007
7.3828990	24.48 ± 0.02	27.001 ± 0.007
7.4073685	24.51 ± 0.02	27.014 ± 0.007
7.4795908	24.44 ± 0.02	26.874 ± 0.007
o5s43		
6.4961375	24.98 ± 0.03	27.063 ± 0.006
6.5212088	25.05 ± 0.06	27.079 ± 0.006
6.5465833	25.17 ± 0.05	27.075 ± 0.006
6.5714735	25.39 ± 0.07	26.985 ± 0.006
6.5957299	24.98 ± 0.04	27.062 ± 0.006
6.6207267	24.94 ± 0.04	27.061 ± 0.006
7.3552420	25.06 ± 0.05	27.013 ± 0.006
7.3711027	25.02 ± 0.04	27.021 ± 0.006
7.3956323	24.95 ± 0.03	27.028 ± 0.006
7.4194678	24.97 ± 0.04	27.044 ± 0.006
7.4434311	25.14 ± 0.06	26.817 ± 0.006
7.4676871	25.05 ± 0.05	26.708 ± 0.006
7.5423084	25.07 ± 0.06	26.839 ± 0.006
7.5671285	24.95 ± 0.03	27.046 ± 0.006
7.5913265	25.00 ± 0.03	27.046 ± 0.006
7.6163059	24.98 ± 0.03	27.039 ± 0.006
o5s49		
6.3994429	25.11 ± 0.05	27.036 ± 0.004
6.4234893	24.97 ± 0.04	27.048 ± 0.004
6.4474580	25.21 ± 0.04	27.058 ± 0.004
6.4716710	24.96 ± 0.07	27.072 ± 0.004
6.4961375	25.18 ± 0.04	27.064 ± 0.004
6.5212088	25.15 ± 0.07	27.073 ± 0.004
6.5465833	25.05 ± 0.04	27.064 ± 0.004
6.5714735	25.14 ± 0.04	26.966 ± 0.004
6.5957299	25.84 ± 0.08	27.053 ± 0.004
6.6207267	25.28 ± 0.07	27.046 ± 0.004
7.3552420	25.07 ± 0.04	26.990 ± 0.004
7.3711027	25.17 ± 0.06	27.007 ± 0.004
7.3956323	25.01 ± 0.04	27.018 ± 0.004
7.4194678	25.32 ± 0.05	27.023 ± 0.004
7.4434311	25.57 ± 0.05	26.800 ± 0.004
7.4676871	25.13 ± 0.05	26.689 ± 0.004
7.5671285	25.27 ± 0.05	27.033 ± 0.004

*Table 7 continued on next page*

**Table 7** (*continued*)

MJD=57620	$m_r \pm \sigma_{Rand}$	$Zp \pm \sigma_{Sys}$
7.5913265	25.12 ± 0.04	27.031 ± 0.004
7.6163059	24.84 ± 0.05	27.035 ± 0.004
o5s52		
6.4114120	23.453 ± 0.011	27.038 ± 0.005
6.4352162	23.506 ± 0.012	27.047 ± 0.005
6.4836121	23.559 ± 0.018	27.078 ± 0.005
6.5081487	23.630 ± 0.012	27.053 ± 0.005
6.5331158	23.657 ± 0.013	27.057 ± 0.005
6.5584302	23.648 ± 0.013	27.037 ± 0.005
6.5833062	23.754 ± 0.014	27.048 ± 0.005
6.6074840	23.687 ± 0.015	27.054 ± 0.005
6.6324802	23.616 ± 0.028	27.052 ± 0.005
7.3671196	23.463 ± 0.012	26.998 ± 0.005
7.3828990	23.505 ± 0.012	27.002 ± 0.005
7.4073685	23.522 ± 0.011	27.012 ± 0.005
7.4312212	23.554 ± 0.012	26.866 ± 0.005
7.4553161	23.634 ± 0.013	26.802 ± 0.005
7.4795908	23.633 ± 0.014	26.870 ± 0.005
7.5540967	23.671 ± 0.012	27.012 ± 0.005
7.5788737	23.747 ± 0.015	27.036 ± 0.005
7.6030791	23.754 ± 0.012	27.029 ± 0.005
7.6279949	23.707 ± 0.019	27.028 ± 0.005
o5s55		
6.3668707	25.12 ± 0.08	27.003 ± 0.008
6.3826668	24.85 ± 0.03	27.008 ± 0.008
6.4075038	24.88 ± 0.03	27.024 ± 0.008
6.4313154	25.19 ± 0.05	27.035 ± 0.008
6.4553362	24.95 ± 0.04	27.043 ± 0.008
6.4796213	25.42 ± 0.07	27.056 ± 0.008
6.5041451	25.32 ± 0.06	27.048 ± 0.008
6.5291947	25.11 ± 0.05	27.019 ± 0.008
6.5545235	25.15 ± 0.04	27.022 ± 0.008
6.5793264	24.98 ± 0.04	27.035 ± 0.008
6.6035457	24.99 ± 0.04	27.033 ± 0.008
6.6285747	25.08 ± 0.06	27.028 ± 0.008
7.3631959	25.10 ± 0.04	26.982 ± 0.008
7.3789568	24.99 ± 0.03	26.987 ± 0.008
7.4034703	25.26 ± 0.03	27.002 ± 0.008
7.4272957	25.22 ± 0.04	26.818 ± 0.008
7.4513626	25.05 ± 0.03	26.625 ± 0.008
7.4756250	25.02 ± 0.04	26.637 ± 0.008
7.5502231	25.32 ± 0.06	26.996 ± 0.008
7.5750150	25.13 ± 0.03	27.031 ± 0.008
7.5992025	25.12 ± 0.04	27.019 ± 0.008
7.6240933	25.10 ± 0.04	27.014 ± 0.008
o5s57		
6.3590364	25.56 ± 0.15	27.050 ± 0.006
6.3747757	25.29 ± 0.09	27.066 ± 0.006
6.3994429	25.17 ± 0.05	27.087 ± 0.006
6.4234893	25.39 ± 0.06	27.093 ± 0.006
6.4474580	25.45 ± 0.05	27.100 ± 0.006
6.4716710	25.36 ± 0.11	27.110 ± 0.006
6.4961375	24.94 ± 0.05	27.101 ± 0.006
6.5212088	24.79 ± 0.04	27.118 ± 0.006
6.5465833	25.26 ± 0.06	27.111 ± 0.006

*Table 7 continued on next page*

**Table 7** (*continued*)

MJD=57620	$m_r \pm \sigma_{Rand}$	$Z_p \pm \sigma_{Sys}$
6.5714735	25.44 ± 0.09	27.009 ± 0.006
6.5957299	25.16 ± 0.05	27.098 ± 0.006
6.6207267	24.96 ± 0.05	27.090 ± 0.006
7.3552420	25.52 ± 0.06	27.037 ± 0.006
7.3956323	24.99 ± 0.04	27.067 ± 0.006
7.4194678	25.50 ± 0.05	27.065 ± 0.006
7.4676871	25.45 ± 0.06	26.732 ± 0.006
7.5423084	25.55 ± 0.10	26.868 ± 0.006
7.5671285	25.33 ± 0.05	27.079 ± 0.006
7.5913265	25.28 ± 0.04	27.071 ± 0.006
7.6163059	25.12 ± 0.04	27.070 ± 0.006
o5s60		
6.3707916	25.01 ± 0.09	27.017 ± 0.003
6.3865586	25.10 ± 0.05	27.034 ± 0.003
6.4114120	25.21 ± 0.04	27.048 ± 0.003
6.4352162	25.22 ± 0.04	27.054 ± 0.003
6.4592812	25.11 ± 0.07	27.071 ± 0.003
6.4836121	25.31 ± 0.08	27.069 ± 0.003
6.5081487	25.32 ± 0.05	27.057 ± 0.003
6.5331158	25.25 ± 0.05	27.068 ± 0.003
6.5584302	25.05 ± 0.04	27.046 ± 0.003
6.5833062	25.40 ± 0.05	27.055 ± 0.003
6.6074840	25.33 ± 0.06	27.057 ± 0.003
6.6324802	25.16 ± 0.10	27.059 ± 0.003
7.3828990	25.07 ± 0.03	27.015 ± 0.003
7.4073685	25.06 ± 0.03	27.036 ± 0.003
7.4312212	25.21 ± 0.04	26.888 ± 0.003
7.4553161	25.21 ± 0.05	26.815 ± 0.003
7.4795908	25.26 ± 0.04	26.875 ± 0.003
7.5540967	25.19 ± 0.04	27.020 ± 0.003
7.5788737	25.23 ± 0.06	27.043 ± 0.003
7.6030791	25.16 ± 0.04	27.038 ± 0.003
7.6279949	24.92 ± 0.04	27.035 ± 0.003
o5s61		
6.3707916	24.69 ± 0.06	27.019 ± 0.006
6.3865586	24.67 ± 0.04	27.033 ± 0.006
6.4352162	24.77 ± 0.04	27.062 ± 0.006
6.4592812	24.83 ± 0.05	27.069 ± 0.006
6.4836121	24.76 ± 0.03	27.073 ± 0.006
6.5081487	24.61 ± 0.03	27.061 ± 0.006
6.5331158	24.70 ± 0.03	27.061 ± 0.006
6.5584302	24.55 ± 0.03	27.043 ± 0.006
6.5833062	24.49 ± 0.03	27.050 ± 0.006
6.6074840	24.41 ± 0.04	27.056 ± 0.006
6.6324802	24.91 ± 0.06	27.052 ± 0.006
7.3671196	24.59 ± 0.03	27.015 ± 0.006
7.3828990	24.59 ± 0.03	27.012 ± 0.006
7.4073685	24.45 ± 0.03	27.031 ± 0.006
7.5540967	25.05 ± 0.04	27.025 ± 0.006
7.5788737	25.02 ± 0.04	27.036 ± 0.006
7.6030791	24.71 ± 0.03	27.041 ± 0.006
7.6279949	24.74 ± 0.04	27.028 ± 0.006
o5t03		
6.3668707	23.454 ± 0.027	27.028 ± 0.004
6.3826668	23.348 ± 0.013	27.034 ± 0.004

*Table 7 continued on next page*

Table 7 (continued)

MJD=57620	$m_r \pm \sigma_{Rand}$	$Z_p \pm \sigma_{Sys}$
6.4075038	23.408 ± 0.013	27.045 ± 0.004
6.4313154	23.334 ± 0.012	27.052 ± 0.004
6.4553362	23.359 ± 0.013	27.069 ± 0.004
6.4796213	23.408 ± 0.018	27.084 ± 0.004
6.5041451	23.313 ± 0.013	27.067 ± 0.004
6.5291947	23.404 ± 0.015	27.032 ± 0.004
6.6035457	23.374 ± 0.014	27.058 ± 0.004
6.6285747	23.433 ± 0.017	27.053 ± 0.004
7.3631959	23.386 ± 0.012	27.004 ± 0.004
7.3789568	23.338 ± 0.013	27.006 ± 0.004
7.4034703	23.368 ± 0.012	27.025 ± 0.004
7.4272957	23.378 ± 0.013	26.845 ± 0.004
7.4513626	23.417 ± 0.015	26.649 ± 0.004
7.4756250	23.416 ± 0.016	26.659 ± 0.004
7.5502231	23.417 ± 0.017	27.036 ± 0.004
7.5750150	23.380 ± 0.015	27.060 ± 0.004
7.5992025	23.313 ± 0.014	27.046 ± 0.004
7.6240933	23.347 ± 0.014	27.042 ± 0.004
o5t06		
6.3629552	24.21 ± 0.06	27.055 ± 0.007
6.3787089	24.10 ± 0.03	27.057 ± 0.007
6.4035606	24.16 ± 0.02	27.085 ± 0.007
6.4274177	24.24 ± 0.04	27.091 ± 0.007
6.4514017	24.30 ± 0.03	27.109 ± 0.007
6.4756753	24.29 ± 0.04	27.106 ± 0.007
6.5002049	24.19 ± 0.02	27.102 ± 0.007
6.5253136	24.09 ± 0.02	27.066 ± 0.007
6.5506281	24.17 ± 0.03	27.103 ± 0.007
6.5754235	24.19 ± 0.02	27.085 ± 0.007
6.5996149	24.30 ± 0.02	27.088 ± 0.007
6.6246785	24.10 ± 0.03	27.094 ± 0.007
7.3995302	24.24 ± 0.02	27.060 ± 0.007
7.4233746	24.18 ± 0.02	27.046 ± 0.007
7.4473473	24.18 ± 0.03	26.830 ± 0.007
7.4716900	24.16 ± 0.03	26.571 ± 0.007
7.5463287	24.10 ± 0.02	26.999 ± 0.007
7.5710852	24.18 ± 0.02	27.077 ± 0.007
7.5952966	24.12 ± 0.02	27.073 ± 0.007
7.6201860	24.16 ± 0.03	27.072 ± 0.007
o5t07		
6.3590364	24.81 ± 0.08	27.022 ± 0.005
6.3747757	24.66 ± 0.04	27.046 ± 0.005
6.4234893	24.83 ± 0.04	27.080 ± 0.005
6.4474580	24.57 ± 0.04	27.085 ± 0.005
6.4716710	24.65 ± 0.06	27.098 ± 0.005
6.4961375	24.50 ± 0.03	27.087 ± 0.005
6.5212088	24.38 ± 0.04	27.091 ± 0.005
6.5465833	24.53 ± 0.03	27.084 ± 0.005
6.5714735	24.64 ± 0.03	27.000 ± 0.005
6.5957299	24.44 ± 0.03	27.073 ± 0.005
6.6207267	24.71 ± 0.05	27.072 ± 0.005
o5t08		
6.3629552	23.784 ± 0.029	27.044 ± 0.007
6.3787089	23.726 ± 0.018	27.042 ± 0.007
6.4035606	23.766 ± 0.014	27.058 ± 0.007

Table 7 continued on next page

Table 7 (continued)

MJD=57620	$m_r \pm \sigma_{Rand}$	$Z_p \pm \sigma_{Sys}$
6.4274177	23.739 ± 0.014	27.077 ± 0.007
6.4514017	23.717 ± 0.019	27.090 ± 0.007
6.4756753	23.735 ± 0.025	27.091 ± 0.007
6.5002049	23.834 ± 0.015	27.078 ± 0.007
6.5253136	23.858 ± 0.016	27.052 ± 0.007
6.5506281	23.847 ± 0.017	27.085 ± 0.007
6.5754235	23.831 ± 0.016	27.076 ± 0.007
6.5996149	23.770 ± 0.015	27.073 ± 0.007
6.6246785	23.674 ± 0.018	27.077 ± 0.007
7.3592398	23.681 ± 0.017	27.029 ± 0.007
7.3750037	23.711 ± 0.012	27.037 ± 0.007
7.3995302	23.738 ± 0.014	27.043 ± 0.007
7.4233746	23.729 ± 0.014	27.006 ± 0.007
7.4473473	23.761 ± 0.013	26.811 ± 0.007
7.5463287	23.770 ± 0.016	26.984 ± 0.007
7.5710852	23.728 ± 0.013	27.056 ± 0.007
7.5952966	23.712 ± 0.015	27.063 ± 0.007
7.6201860	23.656 ± 0.013	27.053 ± 0.007
o5t09		
6.3668707	22.648 ± 0.013	27.093 ± 0.011
6.3826668	22.638 ± 0.008	27.091 ± 0.011
6.4075038	22.657 ± 0.009	27.104 ± 0.011
6.4313154	22.645 ± 0.007	27.119 ± 0.011
6.4553362	22.656 ± 0.009	27.128 ± 0.011
6.4796213	22.633 ± 0.008	27.133 ± 0.011
6.5041451	22.657 ± 0.009	27.136 ± 0.011
6.5291947	22.622 ± 0.008	27.107 ± 0.011
6.5545235	22.626 ± 0.007	27.105 ± 0.011
6.5793264	22.617 ± 0.008	27.124 ± 0.011
6.6035457	22.589 ± 0.009	27.118 ± 0.011
6.6285747	22.574 ± 0.010	27.115 ± 0.011
7.3631959	22.585 ± 0.009	27.066 ± 0.011
7.3789568	22.598 ± 0.007	27.078 ± 0.011
7.4034703	22.628 ± 0.007	27.089 ± 0.011
7.4272957	22.605 ± 0.007	26.904 ± 0.011
7.4513626	22.632 ± 0.009	26.703 ± 0.011
7.4756250	22.630 ± 0.008	26.719 ± 0.011
7.5502231	22.683 ± 0.009	27.082 ± 0.011
7.5750150	22.637 ± 0.007	27.103 ± 0.011
7.5992025	22.617 ± 0.007	27.101 ± 0.011
7.6240933	22.609 ± 0.007	27.094 ± 0.011
o5t10		
6.3590364	24.52 ± 0.06	27.008 ± 0.005
6.3747757	24.31 ± 0.03	27.014 ± 0.005
6.3994429	24.51 ± 0.03	27.030 ± 0.005
6.4234893	24.41 ± 0.02	27.038 ± 0.005
6.4474580	24.43 ± 0.02	27.051 ± 0.005
6.4716710	24.26 ± 0.04	27.074 ± 0.005
6.4961375	24.38 ± 0.03	27.051 ± 0.005
6.5212088	24.29 ± 0.03	27.066 ± 0.005
6.5465833	24.34 ± 0.02	27.064 ± 0.005
6.5714735	24.32 ± 0.03	26.966 ± 0.005
6.5957299	24.34 ± 0.03	27.055 ± 0.005
6.6207267	24.36 ± 0.03	27.043 ± 0.005
7.3552420	24.38 ± 0.03	26.995 ± 0.005

Table 7 continued on next page

**Table 7** (*continued*)

MJD=57620	$m_r \pm \sigma_{\text{Rand}}$	$Z_p \pm \sigma_{\text{Sys}}$
7.3711027	24.45 ± 0.03	27.008 ± 0.005
7.3956323	24.52 ± 0.03	27.011 ± 0.005
7.4434311	24.38 ± 0.02	26.804 ± 0.005
7.4676871	24.27 ± 0.03	26.683 ± 0.005
7.5423084	24.32 ± 0.03	26.826 ± 0.005
7.5671285	24.29 ± 0.02	27.029 ± 0.005
7.5913265	24.37 ± 0.02	27.019 ± 0.005
7.6163059	24.41 ± 0.03	27.024 ± 0.005
o5t13		
6.3629552	24.28 ± 0.05	27.027 ± 0.006
6.3787089	24.55 ± 0.03	27.037 ± 0.006
6.4035606	24.52 ± 0.02	27.050 ± 0.006
6.4274177	24.54 ± 0.03	27.062 ± 0.006
6.4514017	24.67 ± 0.04	27.077 ± 0.006
6.4756753	24.43 ± 0.04	27.078 ± 0.006
6.5002049	24.64 ± 0.03	27.071 ± 0.006
6.5253136	24.61 ± 0.04	27.039 ± 0.006
6.5506281	24.55 ± 0.03	27.072 ± 0.006
6.5754235	24.53 ± 0.03	27.067 ± 0.006
6.5996149	24.57 ± 0.03	27.064 ± 0.006
6.6246785	24.33 ± 0.03	27.065 ± 0.006
7.3592398	24.61 ± 0.04	27.021 ± 0.006
7.3750037	24.46 ± 0.02	27.029 ± 0.006
7.3995302	24.59 ± 0.02	27.034 ± 0.006
7.4233746	24.66 ± 0.03	26.995 ± 0.006
7.4473473	24.49 ± 0.03	26.805 ± 0.006
7.4716900	24.47 ± 0.03	26.557 ± 0.006
7.5463287	24.64 ± 0.04	26.970 ± 0.006
7.5710852	24.48 ± 0.02	27.042 ± 0.006
7.5952966	24.51 ± 0.02	27.045 ± 0.006
7.6201860	24.54 ± 0.03	27.040 ± 0.006
o5t16		
6.3629552	23.98 ± 0.04	26.978 ± 0.007
6.3787089	24.17 ± 0.03	26.987 ± 0.007
6.4035606	24.16 ± 0.02	27.007 ± 0.007
6.4274177	24.19 ± 0.02	27.020 ± 0.007
6.4514017	24.12 ± 0.03	27.026 ± 0.007
6.4756753	24.21 ± 0.03	27.039 ± 0.007
6.5002049	24.33 ± 0.02	27.033 ± 0.007
6.5253136	24.19 ± 0.03	26.998 ± 0.007
7.3592398	24.21 ± 0.02	26.960 ± 0.007
7.3750037	24.24 ± 0.02	26.974 ± 0.007
7.3995302	24.07 ± 0.02	26.983 ± 0.007
7.4233746	24.09 ± 0.02	26.952 ± 0.007
7.4473473	24.06 ± 0.02	26.758 ± 0.007
7.4716900	24.14 ± 0.03	26.505 ± 0.007
7.5463287	24.27 ± 0.02	26.930 ± 0.007
7.5710852	24.23 ± 0.02	27.007 ± 0.007
7.5952966	23.98 ± 0.02	27.003 ± 0.007
7.6201860	24.21 ± 0.02	27.003 ± 0.007
o5t21		
6.4035606	25.26 ± 0.05	27.091 ± 0.007
6.4274177	25.10 ± 0.05	27.105 ± 0.007
6.4514017	25.13 ± 0.06	27.120 ± 0.007
6.4756753	24.98 ± 0.05	27.125 ± 0.007

*Table 7 continued on next page*

Table 7 (continued)

MJD=57620	$m_r \pm \sigma_{Rand}$	$Z_p \pm \sigma_{Sys}$
6.5002049	24.83 ± 0.03	27.111 ± 0.007
6.5253136	25.12 ± 0.06	27.079 ± 0.007
6.5506281	25.12 ± 0.05	27.116 ± 0.007
6.5754235	25.33 ± 0.04	27.103 ± 0.007
6.5996149	25.42 ± 0.06	27.098 ± 0.007
6.6246785	25.07 ± 0.06	27.101 ± 0.007
7.3592398	25.06 ± 0.05	27.049 ± 0.007
7.3750037	24.86 ± 0.03	27.059 ± 0.007
7.3995302	25.06 ± 0.04	27.071 ± 0.007
o5t22		
6.3629552	24.60 ± 0.07	27.040 ± 0.004
6.3787089	24.73 ± 0.04	27.048 ± 0.004
6.4035606	24.63 ± 0.04	27.062 ± 0.004
6.4274177	24.66 ± 0.03	27.072 ± 0.004
6.4514017	24.55 ± 0.03	27.101 ± 0.004
6.5506281	24.56 ± 0.03	27.089 ± 0.004
6.5754235	24.73 ± 0.03	27.082 ± 0.004
6.5996149	24.63 ± 0.03	27.069 ± 0.004
6.6246785	24.67 ± 0.04	27.077 ± 0.004
7.3592398	24.66 ± 0.04	27.014 ± 0.004
7.3750037	24.73 ± 0.03	27.029 ± 0.004
7.3995302	24.64 ± 0.03	27.033 ± 0.004
7.4233746	24.78 ± 0.03	27.007 ± 0.004
7.4473473	24.71 ± 0.04	26.833 ± 0.004
7.4716900	24.64 ± 0.04	26.556 ± 0.004
7.5463287	24.61 ± 0.03	26.980 ± 0.004
7.5710852	24.79 ± 0.04	27.053 ± 0.004
7.5952966	24.63 ± 0.03	27.053 ± 0.004
o5t23		
6.3629552	24.66 ± 0.07	27.084 ± 0.009
6.3787089	24.75 ± 0.04	27.084 ± 0.009
6.4035606	24.69 ± 0.03	27.101 ± 0.009
6.4274177	24.63 ± 0.04	27.122 ± 0.009
6.4514017	24.74 ± 0.04	27.132 ± 0.009
6.4756753	24.79 ± 0.05	27.133 ± 0.009
6.5002049	25.15 ± 0.06	27.130 ± 0.009
6.5506281	25.26 ± 0.07	27.123 ± 0.009
6.5754235	24.86 ± 0.03	27.112 ± 0.009
6.5996149	24.70 ± 0.03	27.108 ± 0.009
6.6246785	24.70 ± 0.05	27.115 ± 0.009
7.3592398	24.65 ± 0.04	27.062 ± 0.009
7.3750037	24.84 ± 0.04	27.068 ± 0.009
7.3995302	24.88 ± 0.03	27.082 ± 0.009
7.4233746	24.96 ± 0.03	27.047 ± 0.009
7.4473473	25.13 ± 0.05	26.856 ± 0.009
7.4716900	24.72 ± 0.03	26.612 ± 0.009
7.5463287	24.73 ± 0.03	27.011 ± 0.009
7.5710852	24.75 ± 0.03	27.092 ± 0.009
7.5952966	24.71 ± 0.04	27.095 ± 0.009
7.6201860	24.77 ± 0.04	27.089 ± 0.009
o5t24		
6.3668707	25.12 ± 0.11	27.025 ± 0.003
6.3826668	25.16 ± 0.06	27.033 ± 0.003
6.4075038	25.10 ± 0.05	27.055 ± 0.003
6.4313154	25.09 ± 0.05	27.062 ± 0.003

Table 7 continued on next page

Table 7 (continued)

MJD=57620	$m_r \pm \sigma_{Rand}$	$Zp \pm \sigma_{Sys}$
6.4553362	25.16 ± 0.06	27.079 ± 0.003
6.4796213	25.62 ± 0.10	27.074 ± 0.003
6.5041451	25.18 ± 0.06	27.083 ± 0.003
6.5291947	25.56 ± 0.11	27.043 ± 0.003
6.5545235	25.37 ± 0.05	27.044 ± 0.003
6.5793264	25.31 ± 0.06	27.067 ± 0.003
6.6035457	25.20 ± 0.05	27.057 ± 0.003
6.6285747	25.47 ± 0.11	27.061 ± 0.003
7.3631959	25.12 ± 0.05	27.007 ± 0.003
7.3789568	25.11 ± 0.04	27.014 ± 0.003
7.4034703	25.34 ± 0.05	27.029 ± 0.003
7.4272957	25.34 ± 0.05	26.863 ± 0.003
7.4513626	25.34 ± 0.06	26.654 ± 0.003
7.4756250	25.38 ± 0.08	26.673 ± 0.003
7.5502231	25.64 ± 0.09	27.017 ± 0.003
7.5750150	25.19 ± 0.06	27.062 ± 0.003
7.5992025	24.93 ± 0.04	27.042 ± 0.003
7.6240933	24.91 ± 0.04	27.044 ± 0.003
o5t25		
6.5002049	24.84 ± 0.04	27.073 ± 0.006
6.5253136	25.18 ± 0.08	27.036 ± 0.006
6.5506281	24.97 ± 0.04	27.064 ± 0.006
6.5754235	25.08 ± 0.05	27.063 ± 0.006
6.5996149	25.22 ± 0.05	27.066 ± 0.006
6.6246785	25.07 ± 0.06	27.072 ± 0.006
7.3592398	25.11 ± 0.05	27.004 ± 0.006
7.3750037	25.06 ± 0.05	27.009 ± 0.006
7.3995302	25.00 ± 0.03	27.029 ± 0.006
7.4233746	25.12 ± 0.04	27.001 ± 0.006
7.4473473	25.16 ± 0.04	26.817 ± 0.006
7.4716900	25.11 ± 0.05	26.554 ± 0.006
7.5463287	25.12 ± 0.05	26.960 ± 0.006
7.5710852	25.10 ± 0.04	27.041 ± 0.006
7.5952966	25.13 ± 0.05	27.047 ± 0.006
7.6201860	25.06 ± 0.05	27.045 ± 0.006
o5t26		
6.3668707	24.88 ± 0.08	27.045 ± 0.007
6.3826668	24.95 ± 0.05	27.049 ± 0.007
6.4075038	25.16 ± 0.05	27.064 ± 0.007
6.4313154	24.80 ± 0.03	27.073 ± 0.007
6.5291947	24.90 ± 0.06	27.073 ± 0.007
6.5545235	24.88 ± 0.03	27.068 ± 0.007
6.5793264	24.94 ± 0.04	27.082 ± 0.007
6.6035457	25.03 ± 0.04	27.080 ± 0.007
6.6285747	25.07 ± 0.07	27.074 ± 0.007
7.3631959	24.99 ± 0.05	27.020 ± 0.007
7.3789568	24.85 ± 0.04	27.036 ± 0.007
7.4034703	24.94 ± 0.04	27.048 ± 0.007
7.4272957	24.88 ± 0.04	26.866 ± 0.007
7.4513626	25.15 ± 0.05	26.659 ± 0.007
7.4756250	24.86 ± 0.05	26.681 ± 0.007
7.5502231	25.12 ± 0.13	27.029 ± 0.007
7.5750150	25.02 ± 0.04	27.060 ± 0.007
7.5992025	25.03 ± 0.04	27.057 ± 0.007
7.6240933	25.06 ± 0.05	27.058 ± 0.007

Table 7 continued on next page

Table 7 (continued)

MJD=57620	$m_r \pm \sigma_{Rand}$	$Zp \pm \sigma_{Sys}$
o5t27		
6.3629552	24.44 ± 0.06	27.067 ± 0.005
6.3787089	24.39 ± 0.04	27.080 ± 0.005
6.4035606	24.69 ± 0.03	27.094 ± 0.005
6.4274177	24.59 ± 0.04	27.109 ± 0.005
6.4514017	24.47 ± 0.03	27.121 ± 0.005
6.4756753	24.61 ± 0.04	27.130 ± 0.005
6.5002049	24.36 ± 0.02	27.114 ± 0.005
6.5253136	24.39 ± 0.03	27.081 ± 0.005
6.5506281	24.59 ± 0.03	27.120 ± 0.005
6.5754235	24.45 ± 0.02	27.108 ± 0.005
6.5996149	24.45 ± 0.03	27.105 ± 0.005
6.6246785	24.27 ± 0.03	27.108 ± 0.005
7.3592398	24.45 ± 0.03	27.051 ± 0.005
7.3750037	24.64 ± 0.03	27.064 ± 0.005
7.3995302	24.52 ± 0.02	27.074 ± 0.005
7.4233746	24.45 ± 0.02	27.034 ± 0.005
7.4473473	24.46 ± 0.03	26.839 ± 0.005
7.4716900	24.48 ± 0.03	26.600 ± 0.005
7.5463287	24.59 ± 0.03	27.020 ± 0.005
7.5710852	24.46 ± 0.02	27.088 ± 0.005
7.5952966	24.53 ± 0.03	27.095 ± 0.005
7.6201860	24.50 ± 0.03	27.086 ± 0.005
o5t30		
6.3629552	24.049 ± 0.045	26.996 ± 0.005
6.3787089	23.964 ± 0.029	27.001 ± 0.005
6.4035606	24.145 ± 0.020	27.029 ± 0.005
6.4274177	24.026 ± 0.028	27.044 ± 0.005
6.4514017	23.872 ± 0.020	27.061 ± 0.005
6.4756753	23.917 ± 0.024	27.081 ± 0.005
6.5002049	23.728 ± 0.014	27.045 ± 0.005
6.5253136	23.689 ± 0.016	27.019 ± 0.005
6.5506281	23.634 ± 0.015	27.045 ± 0.005
6.5754235	23.627 ± 0.015	27.056 ± 0.005
6.5996149	23.666 ± 0.013	27.048 ± 0.005
6.6246785	23.591 ± 0.015	27.051 ± 0.005
7.3592398	23.871 ± 0.019	26.985 ± 0.005
7.3750037	23.756 ± 0.017	26.996 ± 0.005
7.3995302	23.719 ± 0.014	27.007 ± 0.005
7.4233746	23.673 ± 0.015	26.979 ± 0.005
7.4473473	23.662 ± 0.015	26.788 ± 0.005
7.4716900	23.707 ± 0.018	26.540 ± 0.005
7.5710852	23.814 ± 0.017	27.031 ± 0.005
7.5952966	23.929 ± 0.016	27.028 ± 0.005
7.6201860	23.991 ± 0.018	27.026 ± 0.005
o5t32		
6.3629552	24.72 ± 0.08	27.070 ± 0.009
6.3787089	24.56 ± 0.04	27.087 ± 0.009
6.4035606	24.55 ± 0.03	27.089 ± 0.009
6.4274177	24.59 ± 0.04	27.099 ± 0.009
6.4514017	24.48 ± 0.03	27.118 ± 0.009
6.4756753	24.31 ± 0.03	27.134 ± 0.009
6.5002049	24.33 ± 0.03	27.111 ± 0.009
6.5253136	24.60 ± 0.04	27.076 ± 0.009
6.5506281	24.70 ± 0.04	27.110 ± 0.009

Table 7 continued on next page

Table 7 (continued)

MJD=57620	$m_r \pm \sigma_{Rand}$	$Z_p \pm \sigma_{Sys}$
6.6246785	24.49 ± 0.03	27.096 ± 0.009
7.3592398	24.54 ± 0.04	27.042 ± 0.009
7.3750037	24.44 ± 0.03	27.055 ± 0.009
7.3995302	24.47 ± 0.02	27.055 ± 0.009
7.4233746	24.42 ± 0.03	27.032 ± 0.009
7.4473473	24.57 ± 0.03	26.844 ± 0.009
7.4716900	24.56 ± 0.04	26.580 ± 0.009
7.5463287	24.75 ± 0.05	27.020 ± 0.009
7.5710852	24.60 ± 0.03	27.070 ± 0.009
7.5952966	24.52 ± 0.02	27.065 ± 0.009
7.6201860	24.55 ± 0.03	27.077 ± 0.009
o5t34		
6.3994429	23.413 ± 0.025	27.095 ± 0.007
6.4234893	23.343 ± 0.014	27.122 ± 0.007
6.4474580	23.291 ± 0.010	27.135 ± 0.007
6.4716710	23.360 ± 0.049	27.184 ± 0.007
6.4961375	23.397 ± 0.016	27.125 ± 0.007
6.5212088	23.484 ± 0.024	27.154 ± 0.007
6.5465833	23.572 ± 0.014	27.136 ± 0.007
6.5714735	23.699 ± 0.024	27.028 ± 0.007
6.5957299	23.733 ± 0.024	27.111 ± 0.007
7.3552420	23.721 ± 0.020	27.068 ± 0.007
7.3711027	23.790 ± 0.027	27.071 ± 0.007
7.3956323	23.676 ± 0.038	27.276 ± 0.007
7.4194678	23.486 ± 0.037	27.074 ± 0.007
7.4434311	23.291 ± 0.026	27.029 ± 0.007
7.4676871	23.241 ± 0.041	26.976 ± 0.007
7.5423084	23.481 ± 0.021	26.907 ± 0.007
7.5671285	23.366 ± 0.016	27.248 ± 0.007
7.5913265	23.610 ± 0.034	27.086 ± 0.007
7.6163059	23.767 ± 0.019	27.098 ± 0.007
o5t41		
7.3592398	24.72 ± 0.04	27.053 ± 0.006
7.3750037	24.65 ± 0.03	27.062 ± 0.006
7.3995302	24.59 ± 0.03	27.085 ± 0.006
7.4233746	24.57 ± 0.04	27.054 ± 0.006
7.4473473	24.78 ± 0.04	26.870 ± 0.006
7.4716900	24.69 ± 0.03	26.602 ± 0.006
7.5463287	24.64 ± 0.04	27.022 ± 0.006
7.5710852	24.68 ± 0.03	27.085 ± 0.006
7.5952966	24.60 ± 0.03	27.094 ± 0.006
7.6201860	24.66 ± 0.04	27.090 ± 0.006
o5t42		
6.3747757	23.758 ± 0.020	27.037 ± 0.011
6.3994429	23.804 ± 0.014	27.042 ± 0.011
6.4234893	23.832 ± 0.015	27.061 ± 0.011
6.4474580	23.858 ± 0.013	27.072 ± 0.011
6.4716710	23.798 ± 0.022	27.084 ± 0.011
6.4961375	23.912 ± 0.015	27.062 ± 0.011
6.5212088	23.883 ± 0.023	27.080 ± 0.011
6.5465833	23.807 ± 0.018	27.078 ± 0.011
6.5714735	23.793 ± 0.015	26.984 ± 0.011
6.5957299	23.899 ± 0.015	27.066 ± 0.011
6.6207267	23.806 ± 0.018	27.064 ± 0.011
7.3552420	23.800 ± 0.014	27.003 ± 0.011

Table 7 continued on next page

**Table 7** (*continued*)

MJD=57620	$m_r \pm \sigma_{Rand}$	$Z_p \pm \sigma_{Sys}$
7.4194678	23.807 ± 0.013	27.031 ± 0.011
7.4434311	23.876 ± 0.015	26.824 ± 0.011
7.4676871	23.794 ± 0.015	26.701 ± 0.011
7.5423084	23.896 ± 0.022	26.847 ± 0.011
7.5671285	23.846 ± 0.014	27.041 ± 0.011
7.5913265	23.823 ± 0.013	27.033 ± 0.011
7.6163059	23.828 ± 0.015	27.043 ± 0.011
o5t44		
6.3787089	24.35 ± 0.03	27.047 ± 0.009
6.4035606	24.32 ± 0.02	27.064 ± 0.009
6.4274177	24.39 ± 0.03	27.078 ± 0.009
6.4514017	24.36 ± 0.02	27.087 ± 0.009
6.4756753	24.36 ± 0.03	27.096 ± 0.009
6.5002049	24.49 ± 0.03	27.093 ± 0.009
6.5253136	24.46 ± 0.03	27.056 ± 0.009
7.3995302	24.54 ± 0.02	27.061 ± 0.007
7.4233746	24.44 ± 0.02	27.027 ± 0.007
7.4473473	24.50 ± 0.02	26.832 ± 0.007
7.4716900	24.37 ± 0.02	26.592 ± 0.007
7.5463287	24.30 ± 0.03	27.001 ± 0.007
7.5710852	24.28 ± 0.02	27.071 ± 0.007
7.5952966	24.33 ± 0.03	27.084 ± 0.007
7.6201860	24.27 ± 0.02	27.078 ± 0.007
o5t48		
6.3590364	24.48 ± 0.06	27.093 ± 0.007
6.3747757	24.55 ± 0.04	27.102 ± 0.007
6.3994429	24.63 ± 0.03	27.116 ± 0.007
6.4234893	24.53 ± 0.03	27.136 ± 0.007
6.4474580	24.77 ± 0.03	27.143 ± 0.007
6.4716710	24.55 ± 0.05	27.170 ± 0.007
6.4961375	24.62 ± 0.03	27.137 ± 0.007
6.5212088	24.42 ± 0.04	27.144 ± 0.007
6.5465833	24.51 ± 0.03	27.142 ± 0.007
6.5714735	24.36 ± 0.03	27.043 ± 0.007
6.5957299	24.40 ± 0.02	27.115 ± 0.007
6.6207267	24.57 ± 0.04	27.113 ± 0.007
7.5423084	24.46 ± 0.05	26.916 ± 0.007
7.5671285	24.51 ± 0.03	27.115 ± 0.007
o5t49		
6.3629552	24.47 ± 0.05	27.007 ± 0.007
6.3787089	24.42 ± 0.03	27.015 ± 0.007
6.4035606	24.40 ± 0.03	27.032 ± 0.007
6.4274177	24.43 ± 0.02	27.047 ± 0.007
6.4514017	24.64 ± 0.04	27.068 ± 0.007
6.4756753	24.81 ± 0.05	27.072 ± 0.007
6.5002049	24.79 ± 0.03	27.058 ± 0.007
6.5253136	24.99 ± 0.04	27.031 ± 0.007
6.5506281	24.91 ± 0.03	27.062 ± 0.007
6.5754235	24.64 ± 0.03	27.056 ± 0.007
6.5996149	24.60 ± 0.03	27.051 ± 0.007
7.3592398	24.94 ± 0.05	26.999 ± 0.007
7.3750037	24.59 ± 0.03	27.006 ± 0.007
7.3995302	24.64 ± 0.03	27.017 ± 0.007
7.4233746	24.46 ± 0.03	26.981 ± 0.007
7.4473473	24.46 ± 0.02	26.789 ± 0.007

*Table 7 continued on next page*

Table 7 (continued)

MJD=57620	$m_r \pm \sigma_{Rand}$	$Z_p \pm \sigma_{Sys}$
7.4716900	24.50 ± 0.03	26.543 ± 0.007
7.5463287	24.76 ± 0.03	26.963 ± 0.007
7.5710852	25.01 ± 0.04	27.036 ± 0.007
7.5952966	24.97 ± 0.03	27.040 ± 0.007
7.6201860	24.69 ± 0.03	27.031 ± 0.007
o5t51		
6.3629552	23.91 ± 0.04	27.007 ± 0.004
6.3787089	23.91 ± 0.02	27.016 ± 0.004
6.4035606	23.99 ± 0.02	27.029 ± 0.004
6.4274177	23.78 ± 0.02	27.049 ± 0.004
6.4514017	23.92 ± 0.02	27.066 ± 0.004
6.4756753	23.96 ± 0.03	27.081 ± 0.004
6.5002049	23.96 ± 0.02	27.060 ± 0.004
6.5253136	24.02 ± 0.02	27.023 ± 0.004
6.5506281	23.91 ± 0.02	27.062 ± 0.004
6.5754235	23.93 ± 0.02	27.053 ± 0.004
6.5996149	23.87 ± 0.02	27.046 ± 0.004
6.6246785	23.85 ± 0.02	27.052 ± 0.004
7.3592398	23.99 ± 0.02	26.991 ± 0.004
7.3750037	23.92 ± 0.02	26.997 ± 0.004
7.3995302	23.94 ± 0.02	27.010 ± 0.004
7.4233746	23.99 ± 0.02	26.974 ± 0.004
7.4473473	23.95 ± 0.02	26.788 ± 0.004
7.4716900	23.95 ± 0.02	26.540 ± 0.004
7.5463287	23.93 ± 0.02	26.958 ± 0.004
7.5710852	23.98 ± 0.02	27.026 ± 0.004
7.5952966	23.98 ± 0.02	27.025 ± 0.004
7.6201860	23.95 ± 0.02	27.034 ± 0.004
uo3184		
6.3913125	24.78 ± 0.06	27.092 ± 0.014
6.4154337	24.71 ± 0.04	27.115 ± 0.014
6.5123402	24.59 ± 0.03	27.136 ± 0.014
6.5375195	24.34 ± 0.04	27.137 ± 0.014
6.5628085	24.47 ± 0.03	27.136 ± 0.014
6.5875091	24.60 ± 0.03	27.125 ± 0.014
7.3876072	24.46 ± 0.02	27.077 ± 0.014
7.4114040	24.56 ± 0.03	27.091 ± 0.014
7.4353624	24.61 ± 0.03	26.977 ± 0.014
7.4595078	24.65 ± 0.03	26.969 ± 0.014
7.4835834	24.59 ± 0.03	26.669 ± 0.014
7.5081300	24.51 ± 0.04	26.595 ± 0.014
7.5584662	24.49 ± 0.03	27.100 ± 0.014
7.5830743	24.44 ± 0.03	27.091 ± 0.014
7.6079518	24.40 ± 0.02	27.085 ± 0.014
uo3188		
6.3913125	24.44 ± 0.04	27.027 ± 0.017
6.4154337	24.49 ± 0.03	27.047 ± 0.017
6.4393438	24.75 ± 0.03	27.055 ± 0.017
6.4634385	24.74 ± 0.05	27.083 ± 0.017
6.4876346	24.80 ± 0.04	27.077 ± 0.017
6.5123402	24.41 ± 0.02	27.076 ± 0.017
6.5375195	24.30 ± 0.03	27.090 ± 0.017
6.5628085	24.41 ± 0.02	27.067 ± 0.017
6.5875091	24.72 ± 0.03	27.065 ± 0.017
7.3876072	24.38 ± 0.02	27.011 ± 0.017

Table 7 continued on next page

**Table 7** (*continued*)

MJD=57620	$m_r \pm \sigma_{\text{Rand}}$	$Z_p \pm \sigma_{\text{Sys}}$
7.4114040	24.39 ± 0.02	27.029 ± 0.017
7.4353624	24.71 ± 0.03	26.913 ± 0.017
7.4595078	24.80 ± 0.03	26.906 ± 0.017
7.5584662	24.43 ± 0.02	27.038 ± 0.017
7.5830743	24.51 ± 0.03	27.035 ± 0.017
7.6079518	24.64 ± 0.03	27.036 ± 0.017
uo5s77		
6.3668707	25.97 ± 0.19	27.044 ± 0.005
6.3826668	25.47 ± 0.06	27.051 ± 0.005
6.4075038	25.42 ± 0.04	27.064 ± 0.005
6.4313154	25.52 ± 0.06	27.080 ± 0.005
6.4553362	25.32 ± 0.06	27.088 ± 0.005
6.4796213	25.31 ± 0.06	27.093 ± 0.005
6.5291947	25.60 ± 0.09	27.057 ± 0.005
6.5545235	25.92 ± 0.10	27.065 ± 0.005
6.5793264	26.18 ± 0.10	27.079 ± 0.005
6.6035457	25.59 ± 0.05	27.072 ± 0.005
6.6285747	25.56 ± 0.10	27.071 ± 0.005
7.3631959	25.28 ± 0.05	27.025 ± 0.005
7.3789568	25.31 ± 0.04	27.035 ± 0.005
7.4034703	25.29 ± 0.03	27.046 ± 0.005
7.4272957	25.67 ± 0.06	26.859 ± 0.005
7.4513626	25.33 ± 0.06	26.670 ± 0.005
7.4756250	25.43 ± 0.06	26.679 ± 0.005
7.5750150	26.10 ± 0.09	27.070 ± 0.005
7.5992025	25.95 ± 0.09	27.059 ± 0.005
7.6240933	25.85 ± 0.08	27.053 ± 0.005
uo5t55		
6.3787089	24.91 ± 0.05	27.081 ± 0.006
6.4514017	25.06 ± 0.07	27.123 ± 0.006
6.4756753	25.11 ± 0.06	27.131 ± 0.006
6.5002049	24.94 ± 0.03	27.115 ± 0.006
6.5253136	25.17 ± 0.06	27.083 ± 0.006
6.5506281	25.06 ± 0.05	27.118 ± 0.006
6.5754235	24.90 ± 0.03	27.110 ± 0.006
6.5996149	25.06 ± 0.04	27.107 ± 0.006
6.6246785	24.86 ± 0.05	27.106 ± 0.006
7.3592398	24.99 ± 0.05	27.053 ± 0.006
7.3750037	25.04 ± 0.04	27.065 ± 0.006
7.3995302	25.02 ± 0.03	27.076 ± 0.006
7.4233746	24.83 ± 0.03	27.036 ± 0.006
7.4473473	24.99 ± 0.04	26.841 ± 0.006
7.4716900	25.06 ± 0.05	26.601 ± 0.006
7.5463287	25.35 ± 0.07	27.027 ± 0.006
7.5710852	25.04 ± 0.04	27.089 ± 0.006
7.5952966	24.89 ± 0.04	27.097 ± 0.006